Filtering of Transient and Low-Level Mitochondrial Damage Signals by the PINK1:Parkin Mitophagy Pathway

by

J. Logan Bowling

A Dissertation Submitted in Partial Fulfillment of the Requirements for the Degree of Doctorate of Science in Molecular Bioscience

Middle Tennessee State University

May 2020

Dissertation Committee:

Dr. David E. Nelson, Chair

Dr. Mary Farone

Dr. Matthew Elrod-Erickson

Dr. Anthony L. Farone

Dr. Jason Jessen

To my parents for offering guidance and my precious daughter for being herself.

ACKNOWLEDGEMENTS

I wish to thank my family, friends, and lab mates for their continued support, oft-needed laughter, and help in the lab. If not for their presence, I very much doubt I would have made it this far. I would also like to thank Maggie, the wonderful mother of our daughter, for her help that made it possible for me to achieve one of my highest goals. To my committee members and Dr. Lynn Boyd, I am eternally grateful for your insights, technical expertise, and willingness to aid in shaping me into the scientist I am today. Finally, I want to specifically thank my chair, Dr. David Nelson, who gave me an opportunity, along with so much of his time, and always pushed me to be the best I could be. You all have played an important role in my journey and deserve every bit of gratitude I could possibly offer.

ABSTRACT

Mitophagy describes a collection of pathways that direct the selective autophagic removal of damaged or superfluous mitochondria within eukaryotic cells. Of these, the PINK1 (PTEN-induced putative kinase 1):Parkin mitophagy pathway is perhaps the best known and is responsible for marking depolarized mitochondria for destruction. PINK1 continuously surveils mitochondrial membrane potential (MMP), an indicator of mitochondrial health, and is stabilized at mitochondria that exhibit a significant loss in MMP, and recruits cytosolic Parkin. Together PINK1 and Parkin assemble phospho-polyubiquitin (ppUb) chains on outer mitochondrial membrane (OMM) substrates, thereby tagging those mitochondria for removal by autophagy. This is accomplished through the binding of autophagy receptors, such as optineurin (OPTN), to ppUb chains which facilitates the recruitment of the autophagosome and subsequent degradation of the mitochondrion. The topology of the PINK1:Parkin pathway is complex and contains several feedback loops, including a coherent feed-forward loop between PINK1, Parkin, and ppUb. It is believed that this network motif may create a delay in ppUb chain assembly, such that only mitochondria which demonstrate a near-complete and continuous loss in MMP are successfully autophagized. However, mitochondria are likely to experience a range of insults and stresses *in vivo*, particularly in aged cells, and it is unclear how the PINK1:Parkin pathway might interpret the resultant time-varying changes in MMP. In this study we investigate this in detail by carefully manipulating MMP in live cells through titration of the reversible protonophore carbonyl cyanide *m*-chlorophenyl hydrazine (CCCP), and measuring the dynamics of PINK1 and Parkin mitochondrial recruitment and loss by fluorescence microscopy. These data show that PINK1 is highly sensitive to fluctuations in MMP and rapidly dissociates when MMP is even partially restored. Conversely, Parkin dissociation and ppUb chain disassembly from repolarized mitochondria is comparatively slow and thus allows pulses of mitochondrial PINK1 to drive a step-wise accumulation of Parkin and ppUb. This nuanced view of the pathway proposes a model whereby mitochondria that do not exhibit large and persistent losses in MMP, but still pose a threat to overall cellular health, can be removed by PINK1 and Parkin activity.

TABLE OF CONTENTS

LIST OF FIGURES

LIST OF TABLES

LIST OF ABBREVIATIONS

CCCP	carbonyl cyanide m-cholorophenyl hydrazine
IMM	inner mitochondrial membrane
LC3	microtubule-associated protein 1A/1B-light chain 3
MMP	mitochondrial membrane potential
MPP	mitochondrial processing peptidase
MTS	mitochondrial targeting sequence
NDP52	nuclear dot protein 52
NF-κB	nuclear factor kappa-B
OMM	outer mitochondrial membrane
OPTN	optineurin
PARL	PINK1/PGAM-5 associated rhomboid-like
PD	Parkinson's disease
PINK1	PTEN (phosphatase and tensin homolog) induced putative kinase 1
ppUb	phosphopolyubiquitin
RBR	RING-between-RING

ROS	reactive oxygen species
S.E.M.	standard error of the mean
TIM	translocase of inner mitochondrial membrane
TMD	transmembrane domain
TMRM	tetramethylrhodamine methyl ester
TOM	translocase of outer mitochondrial membrane

CHAPTER ONE: INTRODUCTION

1.1 Parkinson's disease and mitochondria

1.1.1 Genetic forms of PD and Parkinsonian syndromes

Parkinson's disease (PD) is a neurodegenerative disorder characterized by the loss of dopaminergic neurons in the area of the brain known as the *substantia nigra pars compacta*, resulting in tremors and other motor deficits. The etiology of PD still remains largely enigmatic although early genomic studies identified commonly occurring mutations in familial PD patients (Hattori et al., 1998; Kitada et al., 1998; Lücking et al., 1998; Matsumine et al., 1997) . Many of these mutations are associated with early-onset forms of the disease, while even more are still being characterized today (Chai and Lim, 2013; Mehta et al., 2016; Olgiati et al., 2016; Yi et al., 2019). In total, PD-associated mutations have been identified in at least 18 gene loci and are referred to as *PARK* genes (Klein and Westenberger, 2012). Mutations in PARK1, for example, which encodes α-synuclein can cause autosomal dominant forms of PD, whereas mutations in PARK2 and 6, encoding Parkin and PINK1, respectively, are associated with autosomal recessive forms of the disease. Collectively, mutation in PARK family genes are thought to account for only 5-10% of all PD occurrences, lending credence to the notion that most sporadic cases are caused by more complex and as yet unrecognized genetic interactions, environmental factors, or some

combination of the two (Thomas and Beal, 2007). Despite this, study of familial cases and the PARK genes may yet provide insights into the underlying cellular processes that are involved in the development of PD. One of the best examples of this concerns mitochondrial quality control.

It has long been recognized that dopaminergic neurons in sporadic PD patients exhibit mitochondrial abnormalities (Thomas and Beal, 2007; Whitworth and Pallanck, 2009). Interestingly, several of the PARK genes encode proteins that localize to and affect mitochondrial function. The best characterized of which are PINK1 and Parkin. Although these were first linked to familial PD in the late 1990s, it was not until roughly ten years later that it was discovered that both proteins operated together to regulate mitochondrial quality control (Narendra et al., 2010b; Vives-Bauza et al., 2010; Whitworth and Pallanck, 2009). More specifically, Whitworth and Pollanck used a Drosophila model to demonstrate a genetic interaction between the PINK1 and Parkin gene by showing that they operate within a common pathway to direct the removal of dysfunctional mitochondria. This early work was fundamental in establishing a clear connection between mitochondria, PINK1:Parkin signaling, and PD.

1.2 The PINK1:Parkin axis in mitophagy

1.2.1 Overview

While mitochondria participate in a variety of essential cellular processes, their primary function is unquestionably the production of adenosine triphosphate (ATP) via oxidative phosphorylation. Even at 'normal' mitochondria this process will generate dangerous byproducts, such as reactive oxygen species (ROS), that could potentially be detrimental to mitochondrial networks and the cell itself (Murphy, 2009). Therefore, the cell requires mechanisms to identify, mark, and remove mitochondria that pose a threat to overall cellular health. Indeed, if mitochondria reach a critical electrostatic state, cytochrome C is released from cardiolipin in the inner mitochondrial membrane (IMM) and is solubilized such that it can diffuse into the cytosol to initiate apoptosis and the death of the entire cell (Ott et al., 2002). In metazoans, this mitochondrial surveillance and removal process is regulated by the PINK1:Parkin mitophagy pathway.

PINK1 is a nuclear-encoded serine/threonine kinase that functions as the primary sensor of mitochondrial depolarization for the mitophagy pathway. At functional mitochondria, where MMP remains intact, PINK1 is constitutively imported through the outer mitochondrial membrane (OMM) with its N-terminus also passing through the inner mitochondrial membrane (IMM) and reaching the

mitochondrial matrix. Here it is cleaved, and then degraded by cytosolic proteasomes (Yamano and Youle, 2013). The processing of PINK1 prior to its complete proteolysis is, at least, a two-step process involving the matrix-localized proteases mitochondrial processing peptidase (MPP) and PINK1/PGAM-5 associated rhomboid-like (PARL) protease (Liu et al., 2017). Both of these proteases remove a substantial portion of the PINK1 N-terminus, including the mitochondrial targeting sequence (MTS). The mechanism by which this processed form of PINK1 is degraded remains controversial (see *section 1.2.3*), but either involves the degradation of cytosolic PINK1 following the N-end rule or the ubiquitination and proteasomal degradation of cleaved OMM-tethered PINK1 (Liu et al., 2017; Yamano and Youle, 2013). Regardless, PINK1 is maintained at exceedingly low levels in cells with healthy mitochondrial networks.

When MMP is lost, PINK1 can no longer be imported across the IMM and remains associated with translocase of the outer mitochondrial membrane (TOM) transporters, embedded in the OMM in its full-length form and rapidly accumulates. Mitochondrial-bound PINK1 has long been thought of as the signal that activates Parkin and is responsible for its recruitment from the cytosol to the OMM of dysfunctional mitochondria (Narendra et al., 2008). Yet more recent

work has demonstrated that this model may not be the most accurate representation of Parkin translocation and activation. A more complex view argues that there is a step-wise activation of Parkin where the efficiency or ability of Parkin to ubiquitinate OMM proteins is directly affected by Parkin phosphorylation and the presence of phosphorylated Ub species at the OMM.

Critical to this is the ability of PINK1 to phosphorylate ubiquitin moieties and the N-terminal ubiquitin-like domain (Ubl) of Parkin at Ser65 (Kazlauskaite et al., 2014; Okatsu et al., 2018). It has been demonstrated that PINK1 phosphorylation in the Ubl domain of Parkin is insufficient for its translocation to the OMM (Gladkova et al., 2018). Gladkova *et al*. showed that Parkin is more likely recruited by pre-existing Ser65 pUb established through the action of other E3 ligases and PINK1 activity, and once Parkin is at the OMM it is then that PINK1-dependent phosphorylation of the Parkin Ubl occurs, releasing Parkin from an auto-inhibitory state, allowing for E2 recruitment in the RING1 domain and exposing the catalytically-active cysteine within the C-terminal RING2 domain (Tang et al., 2017). It is thought that both these events are required for full activation of Parkin. Then, Parkin is able to polyubiquitinate a plethora of substrates at the OMM (Martinez et al., 2017; Sarraf et al., 2013), and these chains are also phosphorylated by PINK1. This sets up a coherent feedforward loop

where yet more Parkin is recruited and activated at the OMM, leading to the production of a coat of phospho-polyubiquitin (ppUb) at affected mitochondria to which autophagy receptors such as OPTN and NDP52, can be efficiently recruited, followed shortly thereafter by microtubule-associated protein 1A/1B-light chain 3 (LC3) and autophagosome formation with the whole processes taking roughly 60-90 minutes (Heo et al., 2015; Wong and Holzbaur, 2015a). The final destruction of mitochondria isolated within autophagosomes occurs many hours later (usually within 24 h) when lysosomes are eventually recruited and fuse to produce autophagolysosomes. Overall, this work indicates how quick the PINK1:Parkin response is to identify and isolate depolarized mitochondria, separating them from the rest of the mitochondrial network for later degradation.

1.2.2 PINK1:Parkin independent mitophagy

While the PINK1:Parkin pathway is not the sole mitophagy pathway, it is, by and large, the most prominent regulator of mitophagy in response to a loss of MMP. However, hypoxia, loss of iron, calcium flux, and externalization of the IMM phospholipid, cardiolipin, to the OMM have all been shown to induce mitophagy and, in many reports, are entirely PINK1/Parkin-independent (Allen et al., 2013; Chu et al., 2013; von Stockum et al., 2018). Some of the research

suggests that the initial signaling steps, such as ubiquitination of OMM proteins by E3 ligases other than Parkin, occur without PINK1 or Parkin activity (von Stockum et al., 2018), but it is unclear if Parkin is recruited later to existing ubiquitin chains generated via the activity of these other E3s such as MUL1, which has been demonstrated to operate in parallel with the PINK1:Parkin axis and can even rescue mitophagy in PINK1:Parkin deficient cell lines (Yun et al., 2014). This suggests that the pathways do operate independently, but recent studies of the Parkin recruitment and activation mechanism indicate that pre-established ubiquitin chains could be used to promote PINK1:Parkin mitophagy (see *section 1.2.5*) (Gladkova et al., 2018; Tang et al., 2017; Wauer et al., 2015a).

In late 2018, a group of researchers examined the E3 ligase HECT, UBA and WWE domain-containing protein 1 (HUWE1) for potential roles in PINK1:Parkin-independent mitophagy (Di Rita et al., 2018). The lab had previously demonstrated that autophagy and beclin 1 regulator 1 (AMBRA1) participated in mitophagy by binding and recruiting LC3 and concluded that this interaction was critical for both Parkin-dependent and –independent mitophagy (Strappazzon et al., 2015). The latter finding, however, begins to paint a more complete picture whereby HUWE1 regulates AMBRA1-mediated mitophagy through an unknown mechanism involving inhibitor kappa B kinase alpha

(IKKα) phosphorylation of AMBRA1 at S104. This phosphorylation event is required for mitophagy by AMBRA1 and establishes a novel function for IKKα outside of the context of the nuclear-factor kappa B (NF-κB) pathway. Furthermore, the group noted that AMBRA-mediated mitophagy occurs independently of the main mitophagy receptors, OPTN and NDP52, and is initiated in response to ischemia through HUWE1-targeted ubiquitination of MFN2.

1.2.3 Other purposes for mitophagy

BCL2 and adenovirus E1B 19-kDa-interacting protein 3 (BNIP3) has been widely studied, mostly for its duality in promoting both autophagy and non-apoptotic cell death (Daido et al., 2004; Vande Velde et al., 2000; Zhang and Ney, 2009). In response to hypoxic conditions, BNIP3 induces mitophagy by promoting stabilization of PINK1 at the OMM (Zhang et al., 2016). While there is no direct evidence to suggest that subsequent PINK1:Parkin signaling would promote cell death, it is possible that these two powerful mitophagic regulators alter the OMM landscape such that cell death is permitted to occur through a "necrosis-like" manner. Indeed, *Vande Velde et al.* show that though the exact mechanism by which BNIP3 induces cell death remains unclear – lacking caspase activation and cytochrome C release – cells transfected with BNIP3 do exhibit mitophagy,

extensive cytoplasmic vacuolization, and the increased plasma membrane permeability that is typically associated with necrosis and credit this to the opening of the mitochondrial permeability transition pore. There is ample evidence for BNIP3 involvement in both cell death and autophagic functions (Peng et al., 2019; Zhang et al., 2019a, 2019b) but whether cell death is the result of excessive autophagy or other causes has yet to be determined. If nothing else, this body of work demonstrates the ability of the PINK1:Parkin axis to respond to a variety of mitochondrial insults and highlights its overall importance in reacting to physiological stress at the cellular level.

As a result of studying BNIP3, researchers discovered the protein BNIP3-like protein X, or NIX, and soon began to question whether it had similar intracellular functions as its namesake (Matsushima et al., 1998). On the heels of its discovery, *Imazu et al*. showed that, similar to BNIP3, NIX was capable of localizing to the mitochondria, increasing membrane permeability, and promoting cell death (Imazu et al., 1999). The group did not discuss a potential role for NIX during mitophagy and only implicated the protein being targeted to mitochondria in order to induce apoptosis. However, they did demonstrate that a loss of MMP precedes cytochrome C release and apoptosis, suggesting there is the potential for mitophagy to occur. In fact, a well-defined role for NIX-

dependent elimination of mitochondria is seen in erythroid differentiation (Kundu et al., 2008; Schweers et al., 2007). During this process, it is thought that NIX causes depolarization of the mitochondria and that this can initiate the mitophagic response (Sandoval et al., 2008). Furthermore, it has been demonstrated that NIX is transcriptionally upregulated during the later parts of erythroid maturation and that NIX knockout mice show deficits in mitochondrial clearance (Aerbajinai et al., 2003; Diwan et al., 2007).

1.2.4 PINK1 structure and function

X-ray crystallography, in addition to other structural analysis studies, have identified various functional domains within PINK1 and Parkin and pinpoint the sites responsible for the activity, regulation, and processing of these two mitophagic regulators (Okatsu et al., 2018; Schubert et al., 2017; Trempe et al., 2013). Full-length human PINK1 contains 581 amino acids. Like many nuclear-encoded mitochondrial proteins, PINK1 contains a N-terminal MTS at 1-34 aa, which is responsible for the protein being directed to the mitochondria. Here, it is imported through the TOM/translocase of the inner mitochondrial membrane (TIM) complex. Subunit TOM20 recognizes the MTS and passes PINK1 into the TOM40 channel to TIM23, where it is believed that the positive charge of the MTS essentially electrophoreses or drives it across the polarized inner

mitochondrial membrane (IMM) (Sekine and Youle, 2018). After the PINK1 N-terminus passes through the TIM complex, it reaches the mitochondrial matrix and is cleaved by MPP. While the the exact site of cleavage unknown, it is thought that only a small portion of the PINK1 N-terminus is removed as a consequence of MPP activity (Greene et al., 2012). Further processing involves cleavage between Ala103 and Phe104 in the transmembrane domain (TMD) by the PARL protease (Deas et al., 2011). This event is pivotal as it yields the mature 52 kDa form of PINK1 that is retrotranslocated to the cytosol and ubiquitinated for degradation possibly via the N-end rule proteasome pathway (Yamano and Youle, 2013) . This observation was based on the premise that F104 of PINK1 is facing the cytosol, where the E3 ligases responsible for N-end rule degradation reside. However, this was never confirmed and additional investigation demonstrated that F104 did not, in fact, face the cytosol and would be unavailable for recognition by the N-end rule pathway, leaving open questions as to the true mechanism for PINK1 degradation (Liu et al., 2017).

While the N-terminus of PINK1 is essential for the targeting of the proteins to the mitochondria and regulating its stability, the larger C-terminal domain (156-509 aa) is responsible for the kinase activity of the protein, and within this region over 60 PD-associated mutations have been discovered (Figure 1 A). An

important early discovery found that the C-terminal kinase domain of PINK1 faces the cytosol at depolarized mitochondria once the unprocessed N-terminus of PINK1 is embedded in the OMM and that this orientation is unaffected by the A217D, T313M, or L347P mutations (Zhou et al., 2008). These results suggest that mutations within the kinase domain of PINK1, while common amongst PD individuals, affect activity but not the localization of PINK1. However, Zhou *et al*. noted that deletion of the TMD segment did interfere with this topology, foreshadowing the important future discovery of PARL-mediated cleavage between amino acids 103 and 104 of the TMD and its role in PINK1 localization, orientation, and signaling. Further adding to the complexity of PINK1 function was the finding that autophosphorylation sites within the kinase domain at Ser228 and Ser402 are critical in substrate recognition of Parkin and ubiquitin and has implications affecting the coherent feed-forward loop of the PINK1:Parkin axis (Rasool et al., 2018).

1.2.5 Parkin structure and function

The human Parkin protein contains 6 domains: Ubl (aa 1-76); really interesting new gene 0 (RING0; aa 141-225); RING1 (aa 225-327); in-between RING (IBR; aa 327-378), repressor element of Parkin (REP; aa 391-403) and RING2 (aa 410-465) (Figure 1 B). It belongs to a group of proteins called E3 ligases, of which there are

three types: ring-between-ring, HECT, and hybrid ligases. The types of E3 ligases vary in mechanism but all serve to transfer ubiquitin onto substrate proteins. Parkin is classified as a hybrid type E3 ubiquitin ligase. This means it retains properties of both HECT and RBR E3s because it contains a catalytic cysteine residue, C431, that aids in ubiquitin transfer from the E2, in addition to possessing a RBR domain. Notably, this residue is mutated in some PD patients, fully ablating the activity of the protein (Seirafi et al., 2015)

Parkin exists largely in an auto-inhibited state within the cytosol and will selectively translocate to impaired or depolarized mitochondria to become activated (Narendra et al., 2010b). The auto-inhibitory state adopted by Parkin is the result of several stable interactions between its domains (Tang et al., 2017). Chief among these inhibitory interactions are is the REP:RING1 association that blocks the binding of E2 enzymes to RING1, the Ubl:RING1 interaction that prevents phosphorylation at Ser65 by PINK1, and the RING0:RING2 interaction that occludes the catalytic cysteine. *Tang et al.* demonstrate that Parkin is activated in a step-wise fashion consisting of first binding PINK1-generated phosphoubiquitin, stimulating a rearrangement of the Parkin structure that permits phosphorylation in the Ubl domain by PINK1. This is followed by dissociation of the REP domain from RING1, resulting in full ligase activity.

Furthermore, the group showed that mutations designed to ablate either the RING0:RING2 interface or REP binding to RING1 enhanced Parkin activity and mitophagy by increasing the rate at which Parkin is able to assemble ubiquitin chains and was also sufficient to rescue some Parkin mutants, including the phosphorylation-deficient S65A. While these effects are noteworthy, other data has shown that differences between translocation kinetics of WT-Parkin and hyperactive mutants may not be profound at the single-cell level (Ordureau et al., 2014). Overall, the main regulatory step in Parkin activation is conformational change upon binding pUb that exposes S65 for phosphorylation and C431 for ubiquitin transfer.

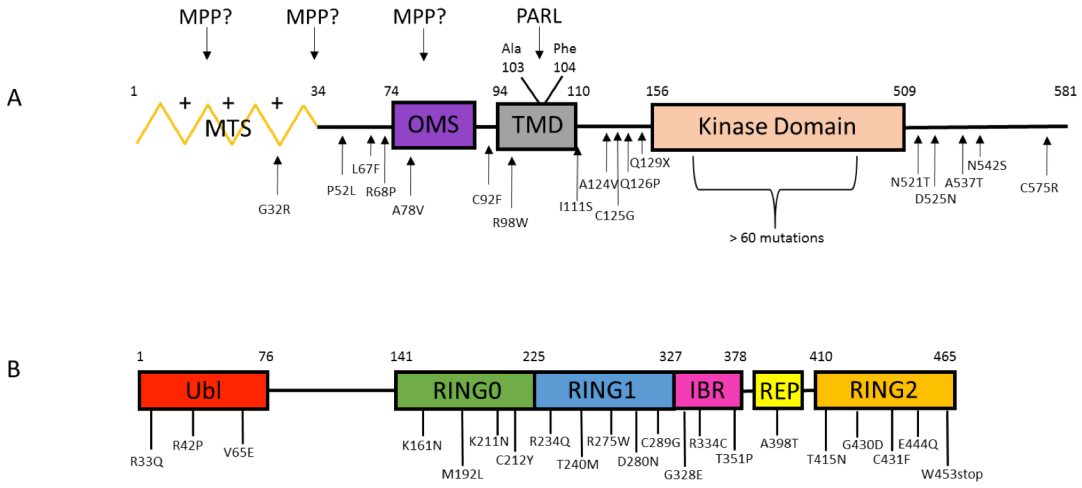

Figure 1: **Structural domains and PD-associated mutations within human PINK1 and Parkin**. Sites of proteolytic processing for PINK1 by MPP and PARL are indicated above the structure. The exact cleavage site of PINK1 by MPP is unknown. Several PD-associated mutations in PINK1 (A) and Parkin (B) are depicted below the domain maps.

**Adapted from Sekine & Youle, 2017 and Seirafi et al. 2015*

1.2.6 Role of ubiquitination in PINK1:Parkin mitophagy

Ubiquitination is vitally important in numerous well characterized cellular signaling pathways, including NF-κB, p53, and many others. It also plays a role in the regulation of endocytosis, receptor desensitization and DNA damage repair amongst other fundamental cellular processes. The ubiquitination of a protein can take many forms – the conjugation of individual or chains of ubiquitin to a substrate – and can have a variety of consequences, from a change in activity or relocalization to proteasomal destruction. Within the context of the PINK1:Parkin pathway however, it serves multiple roles; the recruitment and activation of Parkin and serving as an assembly scaffold for the autophagy machinery around damaged mitochondria. As mentioned previously, Parkin is the principle E3 ubiquitin ligase in the pathway, although other mitochondrial E3 ligases may play minor roles. The process of ubiquitination typically requires the sequential action of three enzymes: an E1 ubiquitin-activating enzyme, an E2 ubiquitin-conjugating enzyme, and an E3 ubiquitin-ligase enzyme. As a RING-HECT hybrid E3 ligase, Parkin receives ubiquitin moieties from E2 enzymes, which are transferred to the catalytic cysteine residue, forming a thioester intermediate. Unlike standard RBR ligases, it may then also participate in catalysis, transferring the ubiquitin to the substrate.

Substrates of Parkin are commonly labeled with polyubiquitin chains of various linkages at different lysine residues. Parkin is capable of building at least four types of ubiquitin chain linkages, K6, K11, K48, and K63 (Ordureau et al., 2014). K48 and K63 chains are the most prominent, with K48 targeting polyubiquitinated substrates to the proteasome and K6 and K63 linkages serving to recruit autophagic machinery (Akutsu et al., 2016). Surprisingly, Parkin does not display a high degree of substrate specificity and will ubiquitinate hundreds of OMM proteins, including mitofusins, voltage-dependent anion channel (VDAC), components of the translocase machinery TOM20 and TOM70, autophagy receptors p62 and calcium-binding and coiled-coil domain-containing protein 2 (CALCOCO2), supporting a strong role for Parkin in modification of the mitochondrial proteome landscape as well as or as a part of the mitophagy process (Sarraf et al., 2013)

At healthy, polarized mitochondria, ubiquitination still plays a minor role in PINK1:Parkin regulation. As described mentioned (section 1.2.1), the ubiquitination of PINK1 at polarized mitochondria regulates its turnover after it is processed at the mitochondrial membrane. Yet, the mechanism regulating PINK1 degradation has yet to be fully resolved and there are two conflicting mechanisms 1) N-end rule (Yamano and Youle, 2013) and 2) polyubiquitination

followed by proteasome recruitment (Liu et al., 2017) . The theory proposed by *Liu et al.* argues that full-length 63-kDa PINK1 is rapidly imported into mitochondria, processed into the mature 52-kDa form and is polyubiquitinated at K137 at the OMM. It is subsequently degraded by the proteasome. Importantly, the group demonstrated that Ub-PINK1 is a characteristic of healthy mammalian mitochondria and that proteasome inhibition caused a more profound increase in 52-kDa PINK1 than the full-length form, indicating that these two PINK1 species interact with the proteasome differently.

It is worth noting that the ubiquitination mechanism for PINK1 degradation is incompatible with the previously suggested N-end rule mechanism. The first evidence for this was the finding that the purportedly exposed F104 of mitochondrially-anchored PINK1, which should induce N-end rule degradation, does not face the cytosol but instead is contained within the OMM (Liu et al., 2017). Further support for this model was recently published showing that the submitochondrial localization of PINK1 is near the mitochondrial-endoplasmic reticulum interface and that here the ERAD-associated E3 ligases gp78 and synoviolin 1 (SYNV1 – also known as HRD1) are capable of catalyzing PINK1 ubiquitination (Guardia-Laguarta et al., 2019).

Another important and unique role ubiquitin plays in mitophagic signaling involves its arrangement into phospho-polyubiquitin chains (ppUb) through the combined actions of PINK1 and Parkin (Harper et al., 2018). More importantly, the PINK1:Parkin axis senses and responds to ppUb differently than monomeric, non-phosphorylated ubiquitin. As chains grow, PINK1 phosphorylates ubiquitin at Ser65, which serves as an even more efficient docking site for Parkin to bind and continue extending the ubiquitin chain (Kazlauskaite et al., 2014; Okatsu et al., 2015). Although phosphorylated ubiquitin species have been implicated in other biological processes, the phospho-S65 modification of polyubiquitin chains so far appears to be exclusive to mitophagy (Okatsu et al., 2015, 2018; Wauer et al., 2015b). While the binding of Parkin to ppUb represents an important step in Parkin activation (Gladkova et al., 2018; Sauvé et al., 2018) and constitutes a coherent feedforward loop in the PINK1:Parkin axis, it serves a dual function by also facilitating the recruitment of autophagy receptors, optineurin (OPTN) and nuclear dot-protein 52 (NDP52), which link PINK1:Parkin activity to the autophagy system (Heo et al., 2015; Tang et al., 2017).

1.2.7 Feedback loops and negative regulators within the PINK1:Parkin pathway

The PINK1:Parkin mitophagy pathway consists of two interlocking coherent feed-forward loops. In brief, a coherent feedforward loop within cellular

signaling systems arises when two activators co-regulate an output, and one activator is capable of activating the other (Alon, 2007). In the context of the PINK1:Parkin axis, both PINK1 and Parkin work together as activators in order to establish ppUb chains at the OMM with PINK1 also serving to activate Parkin (Figure 2*).* If the current model is correct, PINK1 activates Parkin in two ways: one indirectly and the other directly (Tang et al., 2017). Initially, Parkin translocation to the mitochondria is triggered by the presence of phosphoubiquitin moieties conjugated to OMM proteins that were established by other E3s and phosphorylated by mitochondrial-bound PINK1, and thus highlights the indirect activation of Parkin by PINK1. After Parkin is present at the OMM, it is thought that PINK1 can directly phosphorylate Parkin within the N-terminal domain at S65 to allow for its full catalytic activity in extending the polyubiquitin chain, which in turn is phosphorylated by PINK1 and recruits even more Parkin.

The ability of the PINK1:Parkin axis to assess the degree to which mitochondria are depolarized and initiate a proper response is not without the action of other proteins that are involved with surveillance of mitochondrial health and modifications to the OMM. Phosphatase and tensin homolog-long (PTEN-L) and ubiquitin carboxy-terminal hydrolase 30 (USP30) represent two recently

identified negative regulators of PINK1:Parkin mitophagy (Bingol et al., 2014; Marcassa et al., 2019; Wang et al., 2018a, 2018b). USP30 is tethered to the OMM (Wauer et al., 2015b), while PTEN-L is largely cytosolic (Wang et al., 2018a). As its name implies, PTEN-L is a phosphatase involved in removing the phosphorylation at Ser65 of ubiquitin, while USP30 operates as a deubiquitinase enzyme capable of removing ubiquitin and effectively shortening the ubiquitin chain. At this time, it is unclear whether PTEN-L activity is required in order for USP30 to remove ubiquitin from OMM-tagged substrates. However, there is some evidence that S65 modification of polyubiquitin decreases the ability of USP30 to dissemble polyubiquitin chains (Wauer et al., 2015b). This suggests a scenario in which PTEN-L-dependent removal of the phosphoryl group must occur before USP30 can remove ubiquitin from growing chains. These negative regulators demonstrate a type of balancing act in mitophagy where PINK1 and Parkin must establish ppUb chains faster than PTEN-L/USP30 can remove them. In fact, it has been shown that overexpression of USP30 or PTEN-L can halt Parkin-dependent mitophagy and that knockout of either of these proteins is sufficient to rescue mitophagic deficits caused by some pathogenic mutations in PINK1 and Parkin (Bingol et al., 2014; Miller and Muqit, 2019). Furthering the complexity of this signaling is the observation that USP30 is itself a target of

Parkin-dependent ubiquitination (Cunningham et al., 2015), thereby generating an additional feedback loop between Parkin, USP30, and OMM ubiquitin chains.

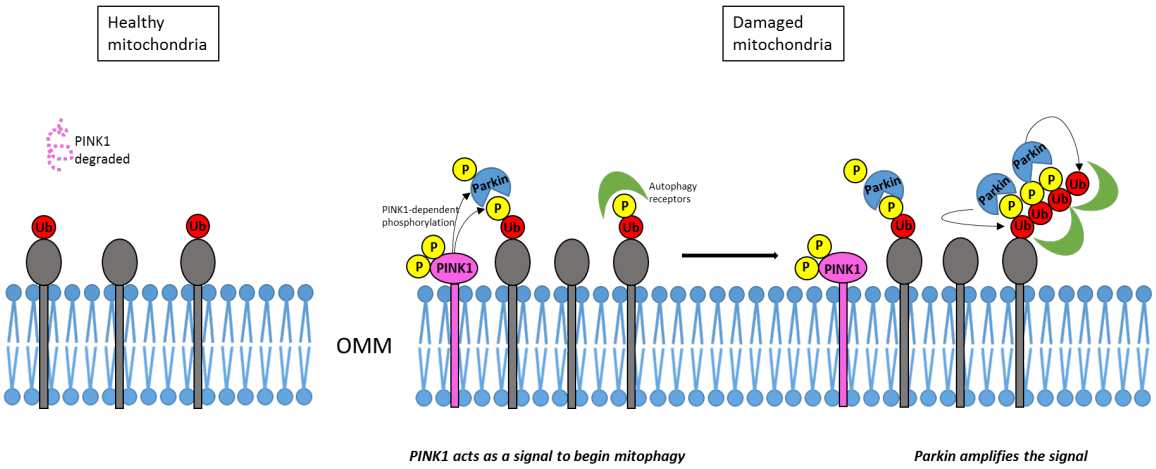

Figure 2: **The PINK1:Parkin axis in mitophagy signaling.** In healthy mitochondria, PINK1 is constitutively imported, processed, and released into the cytosol for degradation. When mitochondria become damaged – via ROS or depolarization – PINK1 is stabilized at the OMM to recruit/activate Parkin and helps establish ppUb chains that are thought to recruit autophagy receptors that initiate formation of the autophagosome.

**Adapted from Sekine & Youle, 2017*

1.2.8 Autophagy receptors associated with Parkin-dependent mitophagy

The ppUb chains established at depolarized mitochondria by PINK1 and Parkin are not sufficient to recruit the general autophagy machinery alone. Cargo adaptor proteins, capable of binding both ppUb and LC3 via LC3-interacting region (LIR) domains, are also required. These bivalent proteins are referred to as autophagy receptors and essentially connect the PINK1:Parkin axis to the autophagic apparatus. The search for 'the' genuine autophagy receptor for mitophagy has been and continues to be a highly active and competitive area of research that has yielded several candidate proteins including SQSTM1 (p62), TAX1BP1, OPTN, and NDP52. Of these, p62 was the first to be identified but its role in mitophagy remains controversial (Narendra et al., 2010a; Okatsu et al., 2010; Rojansky et al., 2016; Zhong et al., 2016) . Live cell imaging studies have demonstrated that while it can be recruited to depolarized mitochondria, it preferentially associates at interface between mitochondrial fragments rather than coating them entirely (Narendra et al., 2010a; Seibenhener et al., 2013). Furthermore, p62 appears largely dispensable for the autophagic clearance of damaged mitochondria. Together, these observations suggest that p62 plays a role in the aggregation of damaged mitochondria rather than functioning as a

canonical autophagy receptor and its overall importance in this context appears questionable.

Currently, the weight of evidence suggests that OPTN and NDP52 are most likely to be genuine autophagy receptors for Parkin-dependent mitophagy (Heo et al., 2015; Wong and Holzbaur, 2015a) (Figure 3). Both proteins are recruited to depolarized mitochondria in a Parkin-dependent manner and can functionally compensate for the loss of the other, although OPTN appears to be the more important of the two and has been shown to be rate-limiting for the Parkin-dependent sequestration of depolarized mitochondria into autophagosomes (Moore and Holzbaur, 2016a). Furthermore, inactivating mutations in the *OPTN* gene have been associated with amyotrophic lateral sclerosis (ALS). In *in vitro* experiments, the E478G *OPTN* mutation, which is causative for ALS, has been shown to impair recruitment of the autophagosome to damaged mitochondria (Wong and Holzbaur, 2015a). Mutation of the *OPTN* gene has additionally been linked to frontotemporal dementia (Ferrari et al., 2016). While these disorders differ from PD, the connection to genetic neurodegenerative disorders provides further evidence for the importance of mitophagy in the maintenance of neurons within the central nervous system.

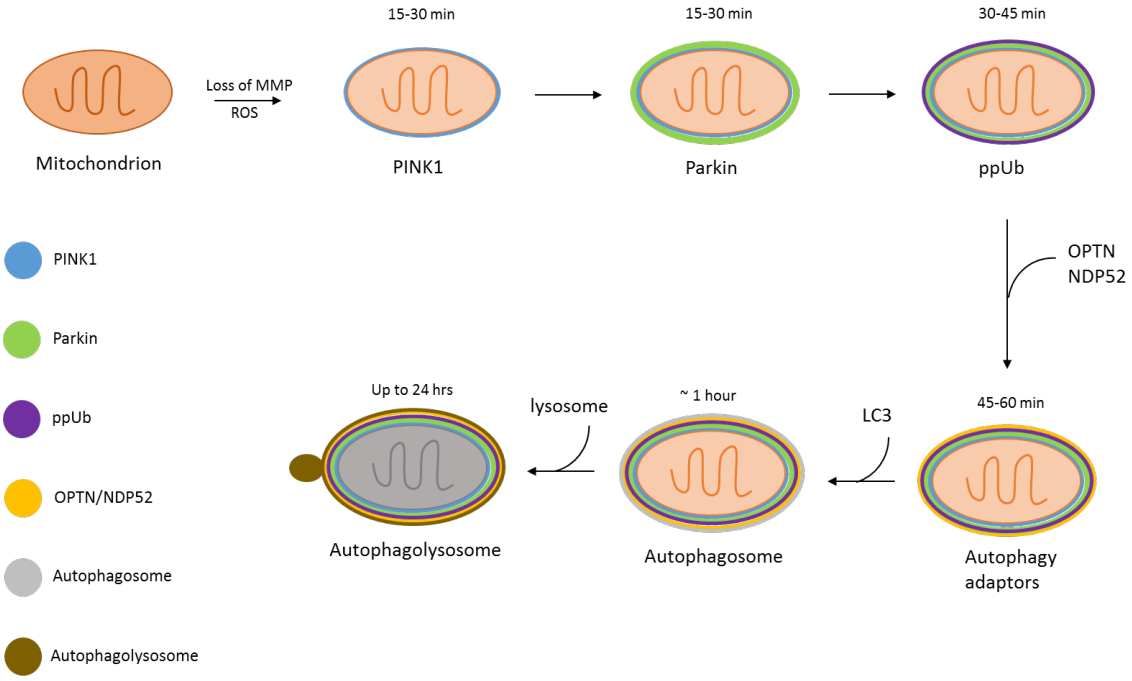

Figure 3: **PINK1:Parkin-dependent labelling of a mitochondrion for autophagic clearance.** Upon a loss of MMP or ROS production, PINK1 is rapidly stabilized at the OMM to recruit Parkin. Shortly thereafter the establishment of ppUb chains facilitate the binding of autophagy adaptor proteins that initiate formation of the autophagosome. These events happen quickly, but it may take ~24 hours before the mitochondrion is degraded within the autophagolysosome.

**Adapted from Wong & Holzbaur, 2014 and Skolfield thesis, 2019*

1.2.9 Regulation of OPTN during mitophagy

Like Parkin, OPTN is also regulated by phosphorylation during mitophagy but seemingly not by PINK1. *Bansal et al.* demonstrated that S177 phosphorylation of OPTN was required for formation of the autophagosome but was not necessary for recruitment of OPTN to the phagophore (Bansal et al., 2018). The Harper lab has further shown that tank-binding kinase 1 (TBK1) is also recruited to depolarized mitochondria where it is capable of phosphorylating OPTN at S473 (Heo et al., 2015). This event increases binding affinity between pUb and OPTN, which likely aids OPTN retention at the OMM (Harper et al., 2018; Richter et al., 2016).

Live imaging studies have shown that OPTN is initially recruited as puncta to depolarized mitochondrial fragments (Wong and Holzbaur, 2015a). These eventually spread and surround the mitochondrion, promoting LC3 recruitment and autophagosome formation, marking an irreversible step in the mitophagic process. Once isolated within the autophagosome, the mitochondrion is degraded by acid hydrolases delivered by the lysosome. As OPTN is a critical mediator of this event, it is important to understand the processes that regulate OPTN recruitment and retention and how the dynamics of this might differ in response to differing mitochondrial stresses.

1.2.10 Relationship between mitophagy and autophagy

As a specific mitochondrial form of autophagy, mitophagy ultimately ends with degradation of mitochondria within the autophagolysosome. Therefore, it is not surprising that mitophagy shares some common features with previously established autophagy signaling – p62 and LC3 recruitment amongst others. After OPTN recruits LC3, an isolation membrane begins to form and develop into an autophagosome, which fuses with lysosomes to acidfy and degrade substrates within the vesicle compartment. However, it has been shown that mitophagy occurs with two distinct phases 1) association of the mitochondrion at the site of autophagosome formation and 2) incorporation of the mitochondrion into the autophagosome. Interestingly, the first step occurs independently of LC3 but is required for engulfment into the autophagosome (Yoshii and Mizushima, 2015). This data supports the hypothesis that ppUb tagging of mitochondria is dynamic, reversible, and must reach a critical threshold to ensure LC3 recruitment and mitochondrial degradation.

Packaging of the mitochondrion into the autophagosome also requires the actions of canonical signaling from the large family of autophagy-related (ATG) proteins. While these proteins were originally discovered in yeast (Tsukada and Ohsumi, 1993), the mammalian homolog of ATG32, Bcl2-L-13, has been

implicated in mitochondrial fission and mitophagy and highlights the highly conserved mechanism for sequestration of mitochondria within the autophagolysosome (Murakawa et al., 2015). Initially, the ULK1 complex and ATG9A are involved in recognition of damaged mitochondria and help determine the site of autophagosome formation (Itakura et al., 2012). This is followed quickly thereafter by incorporation of mitochondria into a LC3-positive membrane thought to be facilitated by the adaptor protein OPTN. The complete enclosure of the isolation membrane around the mitochondrion requires the OMM protein Fis1 and its Rab-GTPAse activating protein, TBC1D15/17 (Shen et al., 2014; Yamano et al., 2014). These findings suggest a step-wise clearance of mitochondria via the PINK1:Parkin axis and offer mechanistic insights into its regulation.

1.2.11 Using live cell imaging to study mitophagy

The ability to peer inside the machine and see how its parts work together provides insights as to how that machine operates as a whole. Molecular and cellular biologists are not immune to this axiom and regularly ask ourselves how our cells (machines) operate through the combined actions of its parts (signaling proteins). Live cell imaging represents a very powerful tool for the scientist interested in addressing questions on how the dynamic behaviors of proteins

affect cellular actions and fate. Using genetically encoded tags, including green fluorescent protein (GFP) that can be visualized using microscopy, allows for investigations concerning changes in the expression and localization of a protein in living cells over time. One strong advantage this holds over many biochemical techniques, which generally report averages in expression or localization across large cell populations, is that it allows for experimentation to be performed at the single-cell level. This is important as 'average' cell behaviors may not accurately reflect the true behavior of individual cells (Levsky and Singer, 2003). In fact, single cell western blots of frog oocytes demonstrate that mitogen-activated protein kinase (MAPK) is phosphorylated in an 'all-or-none' cascade that ensures the cells arrest in certain meiotic stages (Ferrell and Machleder, 1998). Furthermore, live-cell microscopy provides a way for the scientist to follow biological processes with high temporal resolution, on the order of seconds or minutes, over many hours. This enables observation of subtle changes in signaling dynamics, such as those associated with pathogenic mutations, which may otherwise go undetected using other approaches.

The literature published from the field's leading labs relies heavily on the use of live cell microscopy and fluorescent protein tagging of mitophagic regulators such as Parkin, PINK1, LC3 and the mitochondrial autophagy adaptor proteins

OPTN and NDP52 (Heo et al., 2015; Narendra et al., 2010b; Yamano and Youle, 2013). Using live cell microscopy, the Youle lab was able to demonstrate that Parkin affinity for mitochondria is increased upon loss of MMP (Narendra et al., 2008). This is noteworthy because the live cell imaging approach was necessary for the observation. By utilizing the inherent properties of a fluorescent protein to photobleach, or lose its fluorescent capability due to prolonged exposure of high intensity and specific wavelength light, the authors used the technique fluorescence loss in photobleaching (FLIP) to show that mitochondrial-localized YFP-Parkin is depleted more slowly than cytosolic YFP-Parkin, which suggests a driving force for retention of Parkin at depolarized mitochondria.

Similarly, the Holzbaur lab has demonstrated that recruitment of OPTN to depolarized mitochondria occurs much slower for the ALS-associated E478G OPTN mutant than for the wild-type protein. Again, this finding was made possible through the use of a live cell microscopy approach that allowed the investigators to track the cells by taking images several times per minute (Moore and Holzbaur, 2016a). Another interesting tool available to the live cell microscopist is the mitochondrially-targeted genetically encoded photosensitizer KillerRed-dMito (mt-KR) which is capable of generating local, acute bursts of ROS at a specific subset of mitochondria upon photobleaching (Wang et al., 2012)

and can induce Parkin recruitment to mitochondria (Yang and Yang, 2013). While these results were exciting, the use of mt-KR in the study presented here was not consistently reproducible and, for this reason, research questions were not investigated using this approach (see section 3.1) (Figure 10).

One potential drawback of using FP-tagged fusions to study mitophagy is that reports have claimed N-terminal tagging of Parkin can increase its activity and autoubiquitination ability (Burchell et al., 2012). The issue of N-terminally tagging Parkin arises from the observation that the Ubl domain, in cooperation with REP, at the N-terminus play a regulatory function in structurally occluding the E2 binding site and may result in an increase in basal levels of Parkin autocatalytic activity (Chaugule et al., 2011). This means that tagging Parkin at the N-terminus may disrupt its auto inhibition. These findings were taken into account when designing the study presented here, but fusions were tested by transient transfection and sequenced to determine proper expression and localization.

1.2.12 Aims and dissertation statement

This study is designed to determine how PINK1 and Parkin respond to different durations and magnitudes of mitochondrial depolarization by CCCP and how this affects the cell's ability to degrade mitochondria. The hypothesis for this

investigation is that the way in which the PINK1:Parkin axis works to establish and alter the identity of ubiquitin chains at the OMM enables the cell to recognize mitochondria that have been partially or transiently depolarized, rather than only mitochondria that have been completely or persistently depolarized. Fundamentally, this mechanism imparts biological memory at the level of ppUb, enabling the cell to recognize mitochondria that have experienced a prior insult or depolarization event and have not had adequate time to recover or "reset". In this manner, the presence or absence of ppUb appears to be the deciding factor in whether or not the cell will commit to mitophagy.

Proposed here is that the nature of this signaling has evolved such that it allows the cell to filter out natural, stochastic fluctuations in MMP and only commit to mitophagy in circumstances where mitochondria are either completely depolarized for long periods of time or are exposed to repeated rounds of intermediate mitochondrial depolarization and repolarization with high temporal frequency. This hypothesis was investigated utilizing primarily fluorescence microscopy approaches to measure the mitochondrial dynamics of PINK1, Parkin, OPTN, and MMP. Mitochondrial mass was also quantified to determine how the actions of PINK1, Parkin, and OPTN are incorporated by the cell and translate to the downstream degradation of mitochondria. Taken

together, the data suggest a novel process for temporal integration of mitochondrial stress signals by the PINK1:Parkin mitophagy pathway.

CHAPTER TWO: MATERIALS & METHODS

2.1 Molecular biology

2.1.1 Bacterial transformation

The cells used for bacterial transformation were Subcloning Efficiency DH5α Competent Cells (ThermoScientifc, Hampton, NH, USA). For transformation of newly ligated plasmids containing an ampicillin resistance gene, 5 μL of the ligation mixture was added to 50 μL DH5α in a 1.5 mL microcentrifuge tube and incubated on ice for 30 minutes. The cells were heat-shocked at 42°C for 30 seconds and allowed to recovered on ice for 2 minutes before being plated on ampicillin-containing (100 μg/mL) LB agar plates and incubated overnight (~16 hours) at 37°C. For plasmids containing a kanamycin resistance gene, an hour-long outgrowth step was performed before plating by adding 1 mL of LB broth to the competent cells and shaking with 250 RPM at 37°C. Following the outgrowth step, the competent cells were pelleted by centrifugation at 3,000 RPM for 5 minutes and resuspended in roughly 100 μL of LB broth, then plated on kanamycin-containing (100 μg/mL) LB agar plates for overnight incubation.

Retransformation of closed plasmids was performed using the procedure described above, however 100 ng of plasmid DNA was added to the competent cells and incubated on ice for only 10 minutes prior to heat-shocking.

2.1.2 Purification and small scale amplification of plasmid DNA (miniprep)

Miniprep purification of plasmid DNA was performed using the Omega Bio-tek (Norcross, GA USA) E.Z.N.A. Plasmid DNA Mini Kit II and spin-method protocol. After transformation of competent cells, a single colony was isolated from a freshly streaked selective plate. This colony was used to inoculate a 5 mL culture of lysogeny broth (LB) medium containing the appropriate selective antibiotic (either ampicillin or kanamycin 100 μg/μL). The culture was incubated for ~16 hours at 37°C and shaken at 250 RPM in a culture flask 4 times the volume of the culture itself.

At the end of the incubation, the culture was collected, centrifuged at 5,000 x g for 10 minutes at room temperature to pellet bacterial cells, and the supernatant was decanted. The pellet was resuspended to homogeneity in 500 μL Solution I containing RNase A by vortex, ensuring complete resuspension of bacterial cell pellet. The suspension was transferred into a new 2 mL microcentrifuge tube and the bacteria were lysed by adding 500 μL Solution II, an alkaline lysis buffer. The tube was inverted and gently rotated several times and incubated for 2 to 3-minute to allow the reaction to complete. The incubation was not allowed to exceed 5 minutes as this can result in genomic DNA contamination of the plasmid prep. The lysis reaction was ended by adding 700 μL Solution III, a

neutralization buffer, and immediately inverting the tube several times until a white precipitate formed. The solution was centrifuged at maximum speed (>13,000 x g) for 10 minutes at room temperature to form a compact white pellet.

A HiBind DNA Mini Column was inserted into a 2 mL collection tube. The column was equilibrated for optimal plasmid yields by adding 100 μL of 3 M NaOH to the HiBind DNA Mini Column and centrifuged at maximum speed for 30-60 seconds. 700 μL of cleared lysate was transferred from the microcentrifuge tube to the HiBind DNA Column, taking care to not disturb the pellet so that no cellular debris was transferred to the column. The column was centrifuged at maximum speed for 1 minute, the filtrate was discarded, and the collection tube was reused. This process was repeated until all the cleared supernatant had been passed through the column.

The column was washed by adding 500 μL of isopropanol-containing HBC buffer to the column and centrifuging for 1 minute at maximum speed. The filtrate was discarded and the collection tube reused. Then 700 μL of ethanol-containing DNA Wash Buffer was added to the column and centrifuged at maximum speed for 1 minute, followed by decanting of the filtrate. This step was repeated and then residual ethanol was removed from the column matrix by centrifuging the column again in an empty collection tube for 2 minutes at maximum speed. The

HiBind DNA mini column was transferred to a sterile, DNase-free 1.5 mL microcentrifuge tube, 50 μL elution buffer added directly to the center of the column membrane, and left to sit at room temperature for 1 minute. The column was centrifuged at max speed for 1 minute. Eluate was placed back onto column and centrifuged again at maximum speed for 1 minute to recover additional bound DNA. The concentration of recovered DNA was quantified using a Nanodrop (see section *2.1.4*), and stored at -20°C.

2.1.3 Purification and medium scale amplification of plasmid DNA (midiprep)

Midiprep purification of plasmid DNA was performed using the Omega Bio-tek E.Z.N.A. Plasmid DNA Midi Kit Centrifugation protocol. However, the protocol was heavily modified to accommodate the equipment available to perform the midiprep. Following transformation of competent cells on a freshly streaked selective plate, a single colony was isolated and used to inoculate a 50 mL culture of LB medium in a 250 mL Erlen-Meyer flask. This was shaken at 250 RPM for ~16 hours at 37°C. The culture was transferred to a 50 mL centrifuge tube. The culture was then spun at 4,000x g for 10 min to pellet bacterial cells. The culture medium was decanted and any residue was removed using a sterile pipette. The pellet was resuspended completely by vortexing in 2.25 mL of RNase A-containing Solution I. The cell suspension was divided into 4 equal 563 μL

aliquots in sterile 2 mL microcentrifuge tubes and the bacteria lysed by adding 563 μL Solution II to each tube and inverted or gently rotated 8-10 times to obtain a cleared lysate. The alkaline lysis buffer was neutralized by adding 800 μL Solution III to each tube and repeatedly inverting them until a white precipitate formed. The mixture was centrifuged at maximum speed (>15,000x g) for 10 minutes at 4°C to pellet the precipitate.

A HiBind DNA Midi Column was inserted into a 15 mL collection tube. The column was equilibrated for optimal plasmid yields by adding 1 mL 3 M NaOH to the HiBind DNA Midi Column and incubating for 4 minutes at room temperature. Then, this was centrifuged at 4,000x g for 3 minutes. The filtrate was discarded and the collection tube reused. 3.5 mL cleared supernatant was transferred from the 4 microcentrifuge tubes to the HiBind DNA Midi Column. The 4 microcentrifuge tubes containing identical plasmid DNA were combined back onto the same HiBind DNA Midi Column for purification. This was centrifuged at 4,000x g for 3 minutes, the filtrate discarded, and the collection tube reused. 3.5 mL of cleared supernatant continued to be transferred to the HiBind DNA Midi Column and centrifuged at 4,000x g until all of the cleared supernatant was removed from the 4 microcentrifuge tubes.

3 mL of HBC buffer (must be diluted with isopropanol prior to use) was added to the column, centrifuged at 4,000x g for 3 minutes, the filtrate was discarded, and the collection tube reused. 3.5 mL DNA Wash Buffer (must be diluted with 100% ethanol prior to use) were then added to the column, centrifuged at 4,000x g for 3 minutes. The filtrate was discarded and this process repeated for a second DNA wash step. Then, the empty HiBind DNA Midi Column was centrifuged at 4,000x g for 10 minutes to dry the column matrix. The column was transferred to a nuclease-free 15 mL centrifuge tube, 500 μL elution buffer added directly to the center of the column and left to sit at room temperature for 3 minutes. The column was then spun at 4,000x g for 5 minutes. Eluate was placed back onto column and centrifuged at 4,000x g for 5 minutes to recover additional bound DNA. DNA was stored at -20°C.

2.1.4 Quantification of plasmid DNA

Purified plasmid DNA preps were analyzed using a ThermoScientific NanoDrop2000 UV-vis spectrophotometer to determine concentration and purity. In most cases, 2 μL of elution buffer was used to blank the spectrophotometer. If the plasmid DNA was eluted during the prep using nuclease-free water, then this was used to blank the spectrophotometer. 2 μL purified plasmid DNA from preps was used for measurements. DNA preps that

showed a concentration of at least 100 ng/μL and an absorbance ratio at 260 nm to 280 nm of 1.80-1.90 were considered suitable for mammalian cell culture transfections (see section *2.6.1*).

2.1.5 Agarose gel electrophoresis

Isolation of PCR products and DNA fragments from restriction digest reactions were performed using agarose gel electrophoresis. In brief, 0.8% agarose gels were produced by adding 0.4 g molecular grade agarose (Fisher BioReagents Pittsburgh, PA USA) to 50 mL Tris-Acetate EDTA (TAE) (pH 8.1; 40 mM Tris, 20 mM acetate, and 2 mM EDTA) buffer and gently boiling in a lab microwave oven to completely dissolve the agarose. After cooling the molten agarose solution to just above the agarose melting point, ethidum bromide (0.2 μg/mL) was added and the solution was poured into a gel mold with an appropriate comb. Once cooled, the gel was submerged in TAE buffer within an agarose gel tank. DNA samples were combined with 6X Purple Gel Loading Dye (New England Biolabs Ipswich, MA USA) and electrophoresed at 90 V for roughly 30 min. DNA bands were visualized under UV illumination and the size determined by comparison with 1 kb plus ladder (ThermoScientific). The desired DNA fragments were recovered using the method described in section *2.1.6*.

2.1.6 Purification of DNA fragments from agarose gel electrophoresis

Purification of DNA fragments from agarose gel electrophoresis was performed using the Promega (Madison, WI USA) Wizard SV Gel and PCR Clean-up System. Following electrophoresis, the required DNA bands were cut from the gel. Each gel slice was placed in a separate 1.5 mL microcentrifuge tube and the mass of the slice determined using an electronic balance. The slice was completely dissolved by incubating at 50-65°C 10 μL Membrane Binding Solution per 10 mg of gel slice with occasional vortexing.

A SV Minicolumn was inserted into a collection tube. The dissolved gel mixture was transferred to the Minicolumn assembly, incubated at room temperature for 1 minute, and centrifuged at 16,000x g for 1 minute. The flow through was discarded and the Minicolumn reinserted into the collection tube. 700 μL Membrane Wash Solution (with ethanol added) were added to the column, centrifuged at 16,000x g for 1 minute, the flowthrough discarded, and Minicolumn reinserted into the collection tube. The column matirx was washed with 500 μL Membrane Wash Solution and centrifuged at 16,000 x g for 5 minutes. The collection tube was emptied and centrifuged at 16,000 x g to dry column assembly with the microcentrifuge tube lid open, removing residual ethanol. The Minicolumn was transferred to a clean 1.5 mL microcentrifuge tube.

To elute the DNA, 50 μL of nuclease-free water was added to the Minicolumn, incubated at room temperature for 1 minute, and centrifuged at 16,000x g for 1 minute. The eluted DNA is either used immediately or stored at -20°C.

2.2 Generation of fluorescent fusion expression constructs

In order to study PINK1:Parkin mitophagy dynamics in living cells, plasmid constructs to express fluorescent fusions of PINK1 and Parkin were produced using traditional molecular cloning techniques, which made use of polymerase chain reaction (PCR), restriction endonucleases, and DNA ligases. Primers suitable for PCR amplification of PINK1 and Parkin cDNA sequence were ordered from Life Technologies/ThermoScientific. Primer stocks were suspended in diethyl pyrocarbonate-treated (DEPC) water to a concentration of 100 μM and subsequently diluted to 10 μM for working stocks. PCR reactions were performed in a total volume of 50 μL with Vent polymerase (New England Biolabs). The typical composition of a 50 μL PCR reactions was as follows: 5 μL 10x ThermoPol Reaction buffer, 5 μL DNA template (diluted to 10 ng/μL before use), 2 μL of 10 mM deoxynucleotide soultion mix (dNTPs) for a final concentration of 400 μM, 1 μL of both forward and reverse primers (10 μM stock) for a final concentration of 0.2 μM, and 0.5 μL (1 unit) Vent polymerase enzyme. Thermal cycler step settings were 95°C for 5 minutes (initial denaturation),

followed by 25 cycles of 95°C for 20 s, 55°C for 20 s, and 72°C for 90 s (1 minute per kb). The final extension step was performed for 5 min at 72°C and then held at 4°C indefinitely, until collected.

2.2.1 EYFP-Parkin

In order to make EYFP-Parkin, primers were designed to amplify the Parkin coding sequence (Table 1) from an existing pCDNA3 vector containing full-length human Parkin and ligate this into an pEYFP-C1 (Takara/Clontech; Figure 4). For this approach, both the forward and reverse primers were designed to incorporate the restriction enzyme *Bam*HI cut site so that *Bam*HI-digested Parkin PCR product could be directly ligated into the multiple cloning site of pEYFP-C1 that had been cut with the same enzyme.

The EYFP-C1 vector backbone was cut with *Bam*HI-HF (New England Biolabs). The restriction digest reaction was carried out in total volume of 60 μL at 37°C for 1 hour and consisted of 22.5 μL water, 6 μL 10x Cutsmart buffer, 30 μL plasmid DNA (2 μg), and 1.5 μL *Bam*HI-HF. Restriction digest of the Parkin PCR product was also carried out in a total volume of 60 μL at 37°C for 1 hour consisting of 1.5 μL water, 6 μL 10x Cutsmart buffer, 50 μL (entire contents of purified PCR product gel slice) DNA, and 2.5 μL B*am*HI-HF. Contents of the restriction digest reactions were ran on gel electrophoresis to recover purified,

*Bam*HI-cut Parkin PCR product and linearized EYFP-C1 for use in the ligation reaction of EYFP-Parkin.

Ligation of EYFP-Parkin was performed using T4 DNA ligase (New England Biolabs) at room temperature for 30 minutes. The ligation reaction had a total volume of 10 μL and was made up of 1 μL 10x T4 ligase buffer, 3.5 μL EYFP-C1 linearized vector, 5 μL insert (*Bam*HI-cut Parkin PCR product), and 0.5 μL T4 DNA ligase enzyme. A negative control for the ligation reaction was performed to get a rough estimate of the number of transformants that would not truly contain the desired EYFP-Parkin construct. This reaction was setup with 5 μL of water, 1 μL 10x T4 ligase buffer, 3.5 μL EYFP-C1 linearized vector, 0 μL insert, and 0.5 μL T4 DNA ligase enzyme.

As the cloning strategy used raised the possibility of the Parkin sequence entering the vector during ligation in two different orientations, it was necessary to determine which transformants contained the plasmid with the Parkin sequence in the correct orientation, restriction enzyme cut sites within the Parkin sequence were chosen that would yield a unique banding pattern of the vector during gel electrophoresis. After plasmid clones with the Parkin CDS in the correct orientation were identified, these were sequenced by Eurofins Genomics using the stock sequencing primers EGFPC1F and EGFCP1R (Table 2). While the

Parkin CDS was correct and did not contain any mutations, the natural Parkin stop codon was absent, resulting a short 8 aa C-terminal tag. Experimental validation demonstrated that the fusion was functional in that it was autoinhibited in cells with polarized networks, translocated from the cytosol to the mitochondria post-treatment with mitochondrial ionophores, and was able to direct the formation of ppUb. Additional experiments also demonstrated that the 8 aa tag did not affect the kinetics of mitochondrial relocalization of the protein.

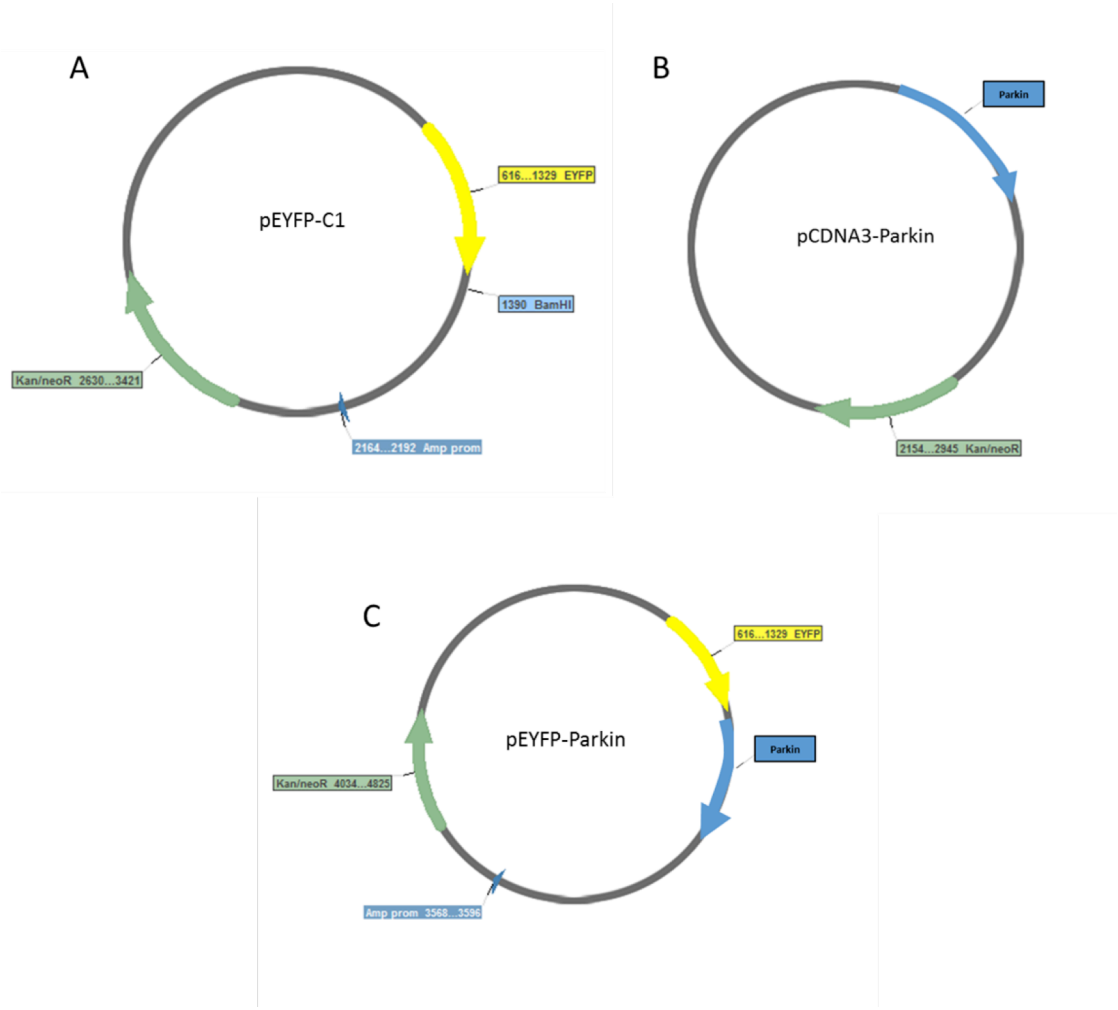

Figure 4: **Cloning of the EYFP-Parkin fusion.** (A) The pEYFP-C1 backbone was digested with BamHI. (B) pCDNA3-Parkin was used as template for amplification of Parkin DNA sequence. (C) The Parkin PCR product was ligated into EYFP-C1 to create EYFP-Parkin.

Table 1: **PCR primers for molecular cloning.** The primers listed here were used for amplifying the Parkin or mCherry CDS for the production of Parkin-Venus, EYFP-Parkin, pShooterMito-mCherry, and mCherry-Parkin plasmid constructs.

Cloning primers (name)	Sequence
*Bam*HI Parkin F	GCATGGATCCATGATAGTGTTTGTCAGG
*Apa*I Parkin R	GCATGGGCCCCTACACGTCGAACCAGTGGTCC
*Bam*HI Parkin R	GCAATGGATCCCTACACGTCGAACCAGTGGTCC
*Xho*I mCherry F	CGTTACTCGAGATGGTGAGCAAGGGCGAGGAGG
*Xho*I mCherry R	CGTTACTCGAGTTACTTGTACAGCTCGTCCATGC

Table 2: **Sequencing primers.** The primers listed here were used for sequencing the Parkin CDS in EYFP-Parkin and mCherry-Parkin.

Sequencing primers (name)	Sequence
EGFPC1F	GATCACTCTCGGCATGGAC
EGFPC1R	CATTTTATGTTTCAGGTTCAGGG
mCherry-F	CCCCGTAATGCAGAAGAAGA
mCherry-R	TTGGTCACCTTCAGCTTGG

2.2.2 pShooterMito-mCherry

In order to visualize mitochondria in living cells and take measurements of Parkin or PINK1 translocation to the mitochondria, a red fluorescent marker of the mitochondria was designed and generated. This was achieved through modification of the pShooter-Mito mammalian expression vector (ThermoScientific), containing a N-terminal mitochondrial targeting sequence that was fused with mCherry. The approach was to PCR amplify the mCherry sequence from the pmCherry-N1 vector and ligate this into the pShooter Mito vector (Figure 5). Both forward and reverse primers (Table 1) were designed to incorporate *Xho*I restriction sites for ligation into the vector. All reactions were performed as described in section *2.2.3* and transformants were screened for orientation of the insert in a similar manner. This construct was not sequenced but was functionally verified via transfection into HeLa cells and imaging using fluorescence microscopy. The mito-mCherry protein was found to associate with both intact, fused mitochondrial networks and highly fragmented mitochondrial networks in the absence and presence of mitochondrial depolarizing agents, respectively.

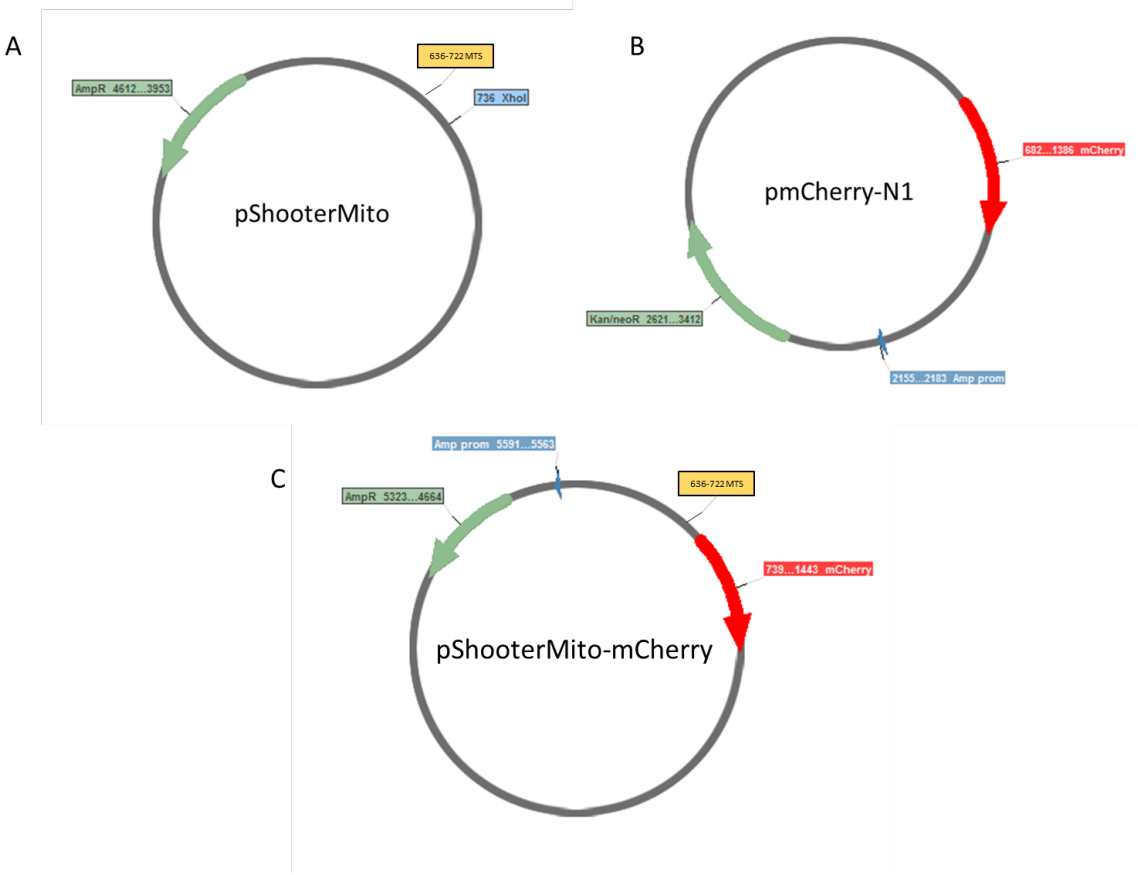

Figure 5: **Cloning of pShooterMito-mCherry.** (A) The pShooterMito vector was digested with XhoI. (B) pmCherry-N1 was used as template for amplification of the mCherry DNA sequence. (C) The mCherry PCR product was ligated into pShooterMito to create pShooterMito-mCherry.

2.2.4 mCherry-Parkin

The mitophagy literature showed that a search for the 'true' mitochondrial autophagy adaptor protein had become increasingly important and timely (Bansal et al., 2018; Moore and Holzbaur, 2016a; Wong and Holzbaur, 2015a). This work convincingly demonstrated that OPTN is currently the best candidate for conjugation of phosphoubiquitin-tagged mitochondria to the autophagosome. As such, we sought to investigate the dynamics of OPTN recruitment to Parkin-positive mitochondria in a manner consistent with our previous experiments at the PINK1 and Parkin level. This necessitated the cloning of an mCherry-Parkin construct.

This was achieved through a 'color swap' of EYFP-Parkin and did not require PCR amplification of DNA sequences. Instead, the approach utilized was to perform a restriction digest of both the previously created EYFP-Parkin and pmCherry-N1 vectors with *Nhe*I and *Bsr*GI (gifted by Dr. Brian Robertson, Middle TN State University). This resulted in excision of EYFP from the Parkin-containing plasmid and mCherry separately. The products of the restriction digest reactions were separated using agarose gel electrophoresis and recovered and purified using the method described in section *1.2.4*. After this, the mCherry fragment was ligated into the Parkin vector to create pmCherry-Parkin (Figure

6). This plasmid was sequenced by Eurofins Genomics using standard mCherry primers (Table 2), and because it was derived from the EYFP-Parkin plasmid, it too was found to contain an additional 8 amino acid (aa) extension beyond the stop codon for Parkin.

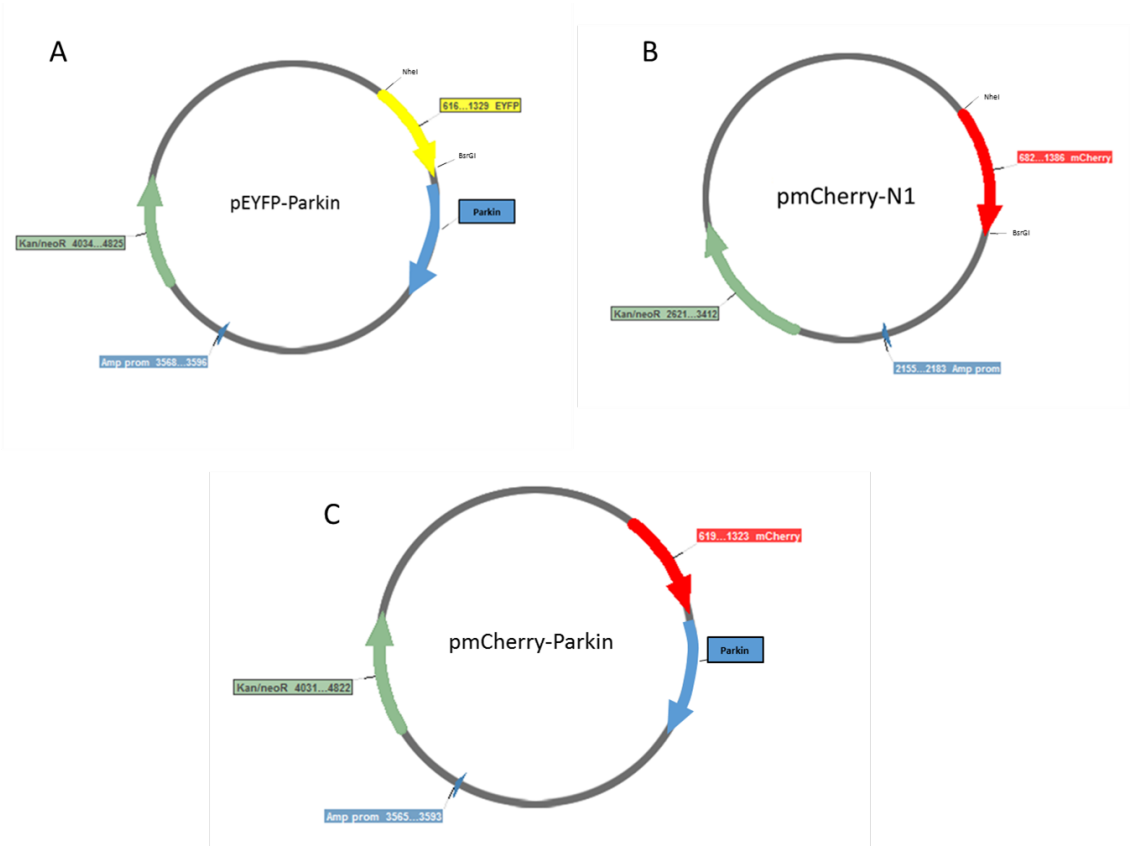

Figure 6: **Production of the pmCherry-Parkin expression construct.** (A) EYFP-Parkin and (B) pmCherry-N1 were both digested with *Nhe*I and *Bsr*GI to remove the EYFP CDS from pEYFP-Parkin and liberate an mCherry-coding fragment from pmCherry-N1. Both the pEYFP-Parkin vector backbone and mCherry fragment were purified. (C) The mCherry DNA fragment was ligated into the linearized Parkin vector to create pmCherry-Parkin.

2.3 Cell lines and tissue culture

HeLa (CCL-2) human cervical adenocarcinoma cells, U2OS (HTB-96) human osteosarcoma cells, and SH-SY5Y (CRL-2266) human neuroblastoma cells were obtained from ATCC (Manassas, VA). HeLa cells were cultured in DMEM supplemented with 10%FBS, 20 mM L-glutamine, and 100 units/mL penicillin and streptomycin. SH-SY5Y cells were cultured in a 1:1 mix of Eagle's minimum essential medium and F12 medium supplemented with 10% FBS and 100 units/mL penicillin and streptomycin. Both cell lines were maintained at 37°C in a humidified 5% CO_2 atmosphere. Cells were plated onto 35 mm glass-bottom dishes (Celvis Mountain View, CA USA) at a density of $1x10^5$ cells/dish for live cell microscopy. Cells were plated onto 60 mm tissue culture treated dishes at a density of $5x10^6$ cells/dish for western blots.

2.4 Immunofluorescence

For immunofluorescence assays (IFA), cells were plated onto 35 mm glass-bottom dishes and paraformaldehyde (PFA)-fixed following any experimental treatments. The protocol for this was performed by collecting and washing the cells 2x with 2 mL PBS, followed by a 10-minute incubation with 1 mL 4% PFA in phosphate buffered saline (PBS). Cells were again washed 2x with 2 mL PBS. Permeabilization of cell membranes was achieved with a 5-minute incubation of

2 mL 0.5% TritonX-100/PBS at 4°C. Following this, cells were incubated with 2 mL 5% goat serum for 30 minutes at room temperature to prevent non-specific binding of the primary antibody. Then, cells were washed 2x with 2 mL PBS, incubated with 500 μL 5% goat serum and appropriately diluted primary antibody, applied directly to the glass-bottom portion of the dish for 45 minutes at room temperature (see Table 3 for a list of antibodies utilized and their dilutions), and washed 2x with 2 mL PBS. Secondary antibodies were also diluted in 5% goat serum and applied directly to the glass-bottom dish in a volume of 500 μL and incubated for 45 minutes at room temperature, washed 2x with 2 mL PBS, and imaged using a Zeiss LSM 700 confocal microscope. In some cases, cells were also stained with NucBlue/Hoechst 33342 or MitoTracker Green FM (both products of ThermoFisher Scientific). MitoTracker green FM was used at a final concentration of 100 mM. Antibodies used throughout this study can be found in Table 3, along with the manufacturer and dilution that was used.

Table 3. Primary and secondary antibodies for IFA. The antibodies listed here were used for IFA experiments in 5% goat serum, following the dilutions listed above.

Name	Manufacturer	Dilution
TOM20 (D8T4N) rabbit mAb	Cell Signaling Technology Danvers, MA USA	1:200
Donkey anti-rabbit AlexaFluor647 IgG H&L AlexaFluor647	Abcam Cambridge, MA USA	1:1000
mCherry Mouse	Novus Biologicals Littleton, CO USA	1:500
Anti-mouse IgG H&L F $(ab')_2$ AlexaFluor647 conjugate	Cell Signaling Technology	1:1000

2.5 Live cell imaging

2.5.1 Transfections

Polyethylenimine (PEI) (Polyscience Inc.), a linear long-chain lipid with a molecular weight of approximately 25 kDa, was used as the transfection reagent for the majority of microscopy experiments where cells were transiently transfected. To prepare the PEI transfection reagent the Cold Springs Harbor protocol was followed (Tom et al., 2008). In brief, 1 g of PEI was dissolved in 1 L of ultra-pure water (1 mg/mL) on a stir plate by first lowering the pH to ~2 with hydrochloric acid and stirring the solution for 2 hours. After the solution was homogenous, sodium hydroxide was added to return the pH to 7, and the solution was filter-sterilized through a 0.22-μM membrane. 15 mL aliquots of PEI were kept at -80°C for long-term storage. 1 mL aliquots were stored at -20°C for up to one year, and working stocks were stored at 4°C for roughly 1 month while in use.

To transfect mammalian cells 1 μg total plasmid DNA per 35mm glass-bottom dish was added to 100 μL opti-MEM (ThermoFisher Scientific) together with 3 μL of PEI (1 mg/mL). The mixture was vortexed, and incubated at room temperature for 10 minutes to form DNA-lipid complexes. Following incubation, the transfection mixture was added dropwise to 35 mm glass-bottom dishes seeded

with cells. The transfection mixture was allowed to remain 6-18 hours before washing and cells were typically visualized 24-48 hours post-transfection.

2.5.2 Fluorophores utilized

Most of the fluorescent fusion proteins used in this study were created in-house but were engineered with widely available and commonly utilized fluorophores (e.g. EYFP and mCherry). Of particular note, many of the live-cell images show Parkin-expressing cells colored green, the fluorophore actually used was EYFP-Parkin. In some cases, AlexaFluor647 conjugates were used to visualize IFA samples.

2.5.3 Wide field Microscopy

Live cells were imaged using a Nikon Ti-eclipse wide field microscope equipped with a CFI Plan 40x oil immersion NA 1.3 objective, Intensilight epifluorescent illuminator, computer controlled stage (Nikon), CoolSNAP MYO camera (Photometrics), and a full environmental enclosure with CO_2, humidity, and temperature control (InVivo Scientifc). The microscope was controlled using Nikon Elements Software (Nikon). Images were acquired at the indicated intervals. EGFP was excited through a 480/40 nm excitation filter and emitted light was detected through a 535/50 nm barrier filter reflected from a 510 nm dichroic mirror. EYFP was excited through a 500/20 nm excitation filter and

emitted light was detected through a 535/30 nm barrier filter reflected from a 515 nm dichroic mirror. TMRM and mCherry were excited through a 570/40 nm excitation filter and emitted light was detected through a 645/75 nm barrier filter reflected from a 600 nm dichroic mirror. For experiments involving the measurement of MMP, cells were incubated with 10 nM TMRM for 15 min at 37 degrees Celsius prior to live imaging. TMRM concentration was kept constant even if CCCP concentration varied during the experiment.

2.5.4 Confocal microscopy

The imaging of immunofluorescent samples and some live cell experiments (where indicated) were performed using a Zeiss LSM700 confocal laser scanning microscope equipped with a Plan-Apochromat 63x NA 1.4 oil DIC M27 objective (Carl Zeiss). Alexa Fluor 647 fluorescence was excited using a 639 nm laser and emitted light was detected through a 645 nm filter. NucBlue (Hoechst 33342; ThermoFisher Scientific) fluorescence was excited using a 405 nm laser and emitted light was detected through a 420 nm filter. EGFP and EYFP fluorescence was excited using a 488 nm laser and detected through appropriate filters.

2.5.5 Image analysis

Image analysis for Figures 7-15 were performed in Fiji (Schindelin et al., 2012) and computed in Microsoft Excel worksheets. All other image analysis was

performed using Zeiss Zen software to calculate Pearson's correlation coefficients (Figure 16) or line scans of fluorophore intensity over a particular distance (Figures 17 and 18). The data generated for Figure 19 was performed by physically counting all the Parkin-positive puncta in an image for not less than 19 HeLa cells co-expressing mCherry-Parkin and OPTN-EGFP.

2.6 Statistical analysis

Statistical tests were performed as indicated in the figure legends. Before a One-way analysis of variance (ANOVA) was performed the data was checked to see if it met the assumptions of the test. In all cases there were three or more categorically independent groups. Furthermore, all treatments were observed independently, and the outcome of one treatment group did not affect the others. The data also showed no significant outliers and met requirements for normal distribution and uniformity of variance across the groups. Because the One-way ANOVA only reported on differences between the means of the groups, and not which groups were different from each other, a Tukey's post-hoc multiple comparisons test was also performed.

In order to measure colocalization of Parkin and OPTN, a Pearson's correlation coefficient was calculated at regular intervals following treatment with 10 μM CCCP. This measurement assumes a liner relationship between Parkin and

OPTN. A value between 0.50 and 1.00 (perfect association), indicate a high degree of association between the two components, while a decrease in PCC would indicate dissociation. This test was performed within the Zeiss Zen software from confocal images.

CHAPTER THREE: TOOL VALIDATION

3.1 Introduction

As stated in section 1.2.12, the primary purpose of this study is to determine how the PINK1:Parkin pathway responds to mitochondrial insults of differing magnitude and how these responses influence mitochondrial fate (i.e. mitophagy). In order to achieve this objective, it was first necessary to establish appropriate methodology to both control MMP in living cells in such a way that it could be completely or partially disrupted for short or longer periods of time and also quantify changes in PINK1 and Parkin levels and localization. At the inception of the study it was decided that best route to achieve this would be the use of live cell fluorescence microscopy as this would enable us to measure changes in the subcellular localization of the proteins being studied and capture changes in mitochondrial network morphology at high temporal resolution as well as detecting any heterogeneity in the response between cells.

There are a variety of existing methods to disrupt or interrupt mitochondrial activity in cells. These include the targeted generation of reactive oxygen species at mitochondria to induce oxidative damage using genetically encoded tools such as KillerRed (Wang et al., 2012), or reversible mitochondrial protonophores such as CCCP (Heo et al., 2015; Narendra et al., 2008, 2010b; Yamano and Youle, 2013) or BAM15 (Kenwood et al., 2013; Tai et al., 2018). Of these, CCCP is

perhaps the most widely used mitochondrial depolarizing agent in the PINK1:Parkin and mitophagy field. In the majority of studies, it is used at high doses sufficient to completely collapse the proton gradient across the inner mitochondrial membrane. While the dose required to achieve this seems to exhibit cell type (and user) variation, it is typically reported to be between 10 μM (Burchell et al., 2013; Kazlauskaite et al., 2014; Matsuda et al., 2010; Okatsu et al., 2010; Sarraf et al., 2013; Vives-Bauza et al., 2010) and 20 μM (Cai et al., 2012). The use of lower CCCP concentrations that would likely cause partial loss of MMP are less frequently reported in the literature. While one group was able to detect stabilization of PINK1 and Parkin at the mitochondria with 3-hour treatments of CCCP concentrations as low as 2 μM (Narendra et al., 2010b) the dynamics of the PINK1:Parkin response to partial loss of MMP and how these differ from the response to a complete loss of MMP have not previously been reported.

In order to measure the changes in PINK1 and Parkin levels and localization in living cells, the use of genetically encoded fluorescent tags is almost unavoidable and would be necessary for this particular study. In the vast majority of cases, fluorescent protein tags are benign and have little effect on the activity, localization, and stability of the tagged protein (Crivat and Taraska, 2012). However, this is by no means certain and although GFP-tagging had been used

to study PINK1 (Lazarou et al., 2012; Matsuda et al., 2010) and Parkin (Cai et al., 2012; Narendra et al., 2008) in prior studies, it was important to rigorously re-explore that at the beginning of this study as tagged proteins would be used for all or almost all of our experiments.

In this chapter, we present data to show that controlled CCCP titration and washout can be used to reproducibly stimulate decreases in MMP of differing magnitude and duration in single living cells and that it is possible to track the responses of PINK1 and Parkin individual but not simultaneously in these cells. In this way, we define a basic methodology that will be used across the following chapters to answer the main questions of this dissertation.

3.2 Manipulation of mitochondrial membrane potential

As described in the chapter introduction, in order to determine whether the PINK1:Parkin pathway responded differently to different levels of mitochondrial stress and depolarization, it was first necessary to establish a protocol for inducing partial and complete depolarization of mitochondria in cultured mammalian cells. Given that prior studies using CCCP indicate that 10 μM dose was sufficient to completely depolarize mitochondria and 2 μM was the minimum to achieve a measurable PINK1:Parkin response, this defined the range for our initial experiments.

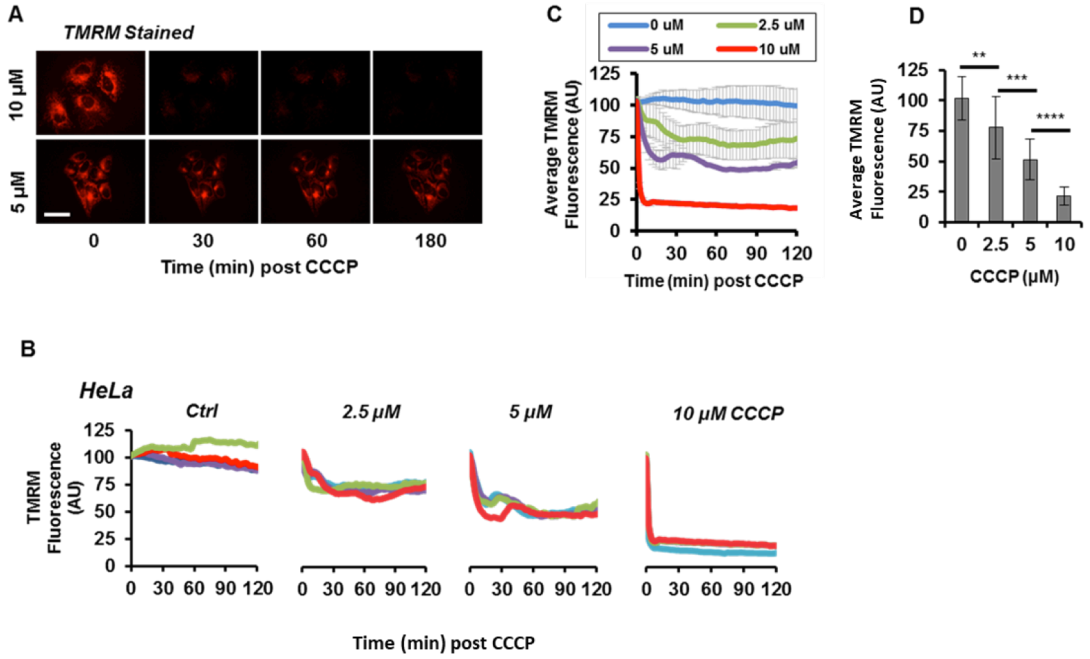

Figure 7: **Dose-dependent depolarization response to CCCP in living cells.** (A) Cells incubated with TMRM and treated with different doses of CCCP show different levels of fluorescence. (B) Individual cell profiles of TMRM fluorescence over time are unique to CCCP dose. (C) Cell population averages of TMRM fluorescence over time display distinctly separate groups. (D) Average difference in fluorescence of cell population at t = 120 min post-CCCP treatment is statistically significant between the groups. Scale bar is 50 µm. Statistical differences in TMRM fluorescence were determined using one-way ANOVA followed by Tukey's multiple comparisons test. **p<.01, ***p<.001, ****p<.0001. Error bars represent the S.E.M.

In order to measure MMP in these experiments, cells were stained with 10 nM TMRM. This mitochondrial marker is specific in that it only labels mitochondria that are actively respiring, allowing for quantification of the magnitude of depolarization in cells treated with CCCP by measuring the fluorescence intensity of the mitochondrial network (Chazotte, 2011; Creed and McKenzie, 2019; Distelmaier et al., 2008; Falchi et al., 2005; Mao and Kisaalita, 2004). Through use of this approach, it was demonstrated that doses of 2.5, 5, and 10 μM CCCP created discrete and discernible levels of MMP loss in HeLa cells. This effect was measurable at both the individual cell (Figure 7 A + B) and averaged population level (Figure 7 C + D). At the single cell level, in cells treated continuously with 2.5 and 5 μM CCCP, fluctuations in MMP could be observed. Surprisingly, these appeared somewhat synchronous in cells incubated with 5 μM CCCP as a prominent but short-lived partial recovery in MMP was observed roughly 30 min after treatment and this can be seen in the population average data (Figure 7 B). As PINK1 is directly responsive to changes in MMP, we hypothesized that these fluctuations could elicit PINK1 and Parkin dynamics in cells with partially depolarized mitochondrial networks. This hypothesis is directly addressed in Chapter 4 and will not be further discussed here.

In order to determine whether the CCCP doses established in these experiments had similar effects in other cell lines, we performed a similar experiment in the dopaminergic neuronal cell line SH-SY5Y, a neuroblastoma-derived cell line that is frequently used in PD and mitophagy research. As a modification to the prior experiment protocol, the concentration of CCCP present in the cell growth medium was increased in a stepwise fashion during live cell imaging before a final wash-out step. The concentration of TMRM was kept constant throughout the imaging period. We observed a similar dose-dependent response in SH-SY5Y to that observed in HeLa cells and this experiment confirmed that the loss in MMP induced by CCCP treatment is reversible (Figure 8 A + B). Individual cells demonstrated partial recovery of TMRM fluorescence when CCCP concentration was decreased from 10 μM to 5 μM at t = 60 min, indicating partial repolarization of mitochondrial networks in these cells (Figure 8 B). When the CCCP concentration was dropped from 5 μM to 0 μM at t = 120 min, a further increase in TMRM was evident that exceeded initial (t=0 min) levels in some cells indicating complete recovery of MMP (Figure 8 B).

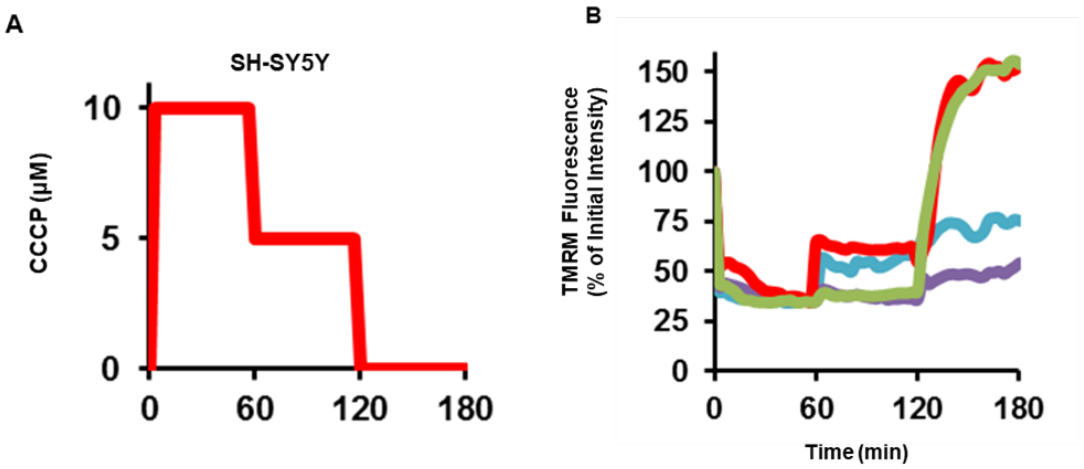

Figure 8: **MMP response to CCCP in SH-SY5Y cells.** (A) Diagram depicts titration of CCCP throughout the experiment. (B) Individual cell profiles of TMRM fluorescence.

3.3 Expression, localization, and sequencing of fluorescent fusion proteins

When the human Parkin CDS was cloned into pEYFP-C1, the entire open reading frame for the cDNA was inserted in-frame with EYFP such that the expressed protein would have an N-terminal EYFP tag. A number of prior studies had successfully utilized N-terminal GFP-tagging of Parkin so we also adopted this strategy, reasoning that the addition of a large, bulky C-terminal tag may interfere with the C-terminal RING domains of Parkin and the E3 ligase activity of the protein. The Parkin cDNA sequence was amplified without a stop codon. This was provided instead by the pEYFP-C1 vector, resulting in a short 8 aa C-terminal tag. The entirety of the Parkin CDS was checked by bi-direction Sanger Sequencing (Eurofins Genomics (KY, USA) and was found to be correct, lacking mutations of any kind. This was also true for the pmCherry-Parkin expression construct, which was produced from pEYFP-Parkin by a simple color-swap. Having successfully generated and sequenced the pEYFP-Parkin construct, functional validation was performed to test whether the fusion protein i) was expressed in mammalian cells, ii) exhibited normal auto-inhibition and cytoplasmic localization prior to mitochondrial depolarization, iii) translocated to mitochondria post-CCCP treatment, and iv) could direct the assembly of ppUb chains.

Western blot analysis performed by other lab members demonstrated that the fusion protein was successfully expressed in HeLa cells, a Parkin-null cell line, in transient transfection experiments and was found to have the predicted molecular weight of 79 kDa (Parkin = 52 kDa, EYFP = 27 kDa). Furthermore, expression of EYFP-Parkin proteins successfully rescued CCCP-stimulated ppUb production in these cells with no ppUb detectable prior to CCCP treatment (Bowling et al., 2019). Collectively, these data confirmed that the fusion protein is expression, was functional, and was capable of auto-inhibition.

In order to test whether the EYFP-Parkin fusion correctly translocated from the cytoplasm to the mitochondria in response to depolarization with CCCP, HeLa cells co-expressing EYFP-Parkin and the fluorescent mitochondrial marker, mito-mCherry were treated continuously with 10 μM CCCP and imaged by live cell microscopy (Figure 9 A). Translocation of EYFP-Parkin was apparent by ~9 min post-CCCP treatment and plateaued by ~60 min. This was consistent with prior live cell imaging studies of Parkin translocation kinetics (Matsuda et al., 2010; Narendra et al., 2008).

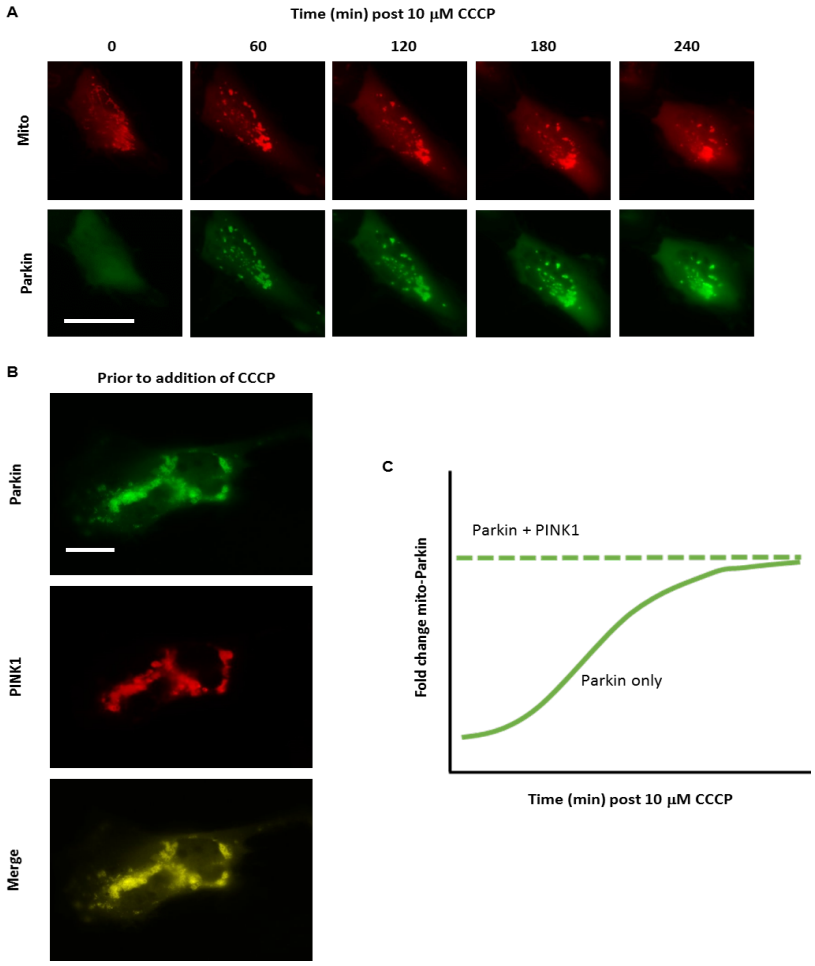

Figure 9: **EYFP-Parkin relocalizes from the cytoplasm to the mitochondria post-CCCP treatment** (A) Single cell time course images showing Parkin translocation to mitochondria when treated with 10 μM CCCP. (B) Representative images of constitutive localization to mitochondria when PINK1 and Parkin are co-expressed. (C) Pictor representation of experiment findings: In HeLa cells expressing exogenous EYFP-Parkin and endogenous PINK1, CCCP treatment induces mitochondrial accumulation of EYFP-Parkin. If PINK1 is overexpressed, EYFP-Parkin is exhibits mitochondrial recruitment in the absence of CCCP treatment. Scale bar in 'A' is 50 μm. Scale bar in 'B' is 20 μm.

As we wanted to investigate the dynamics of the PINK1:Parkin mitophagy pathway to mitochondrial stressors at both the PINK1 and Parkin level, a PINK1-mCherry construct was also produced. As EYFP and mCherry are spectrally separable using the live cell microscopes available to us, we reasoned that this would enable us to observe both proteins simultaneously in live cells. Unlike EYFP-Parkin, which has an N-terminal FP tag, the PINK1 expression construct was produced so that this protein had a C-terminal tag. This was essential as the N-terminal portion of PINK1 is removed as part of normal PINK1 processing (section 1.2.4), which would result in the loss of N-terminal tags. The pmCherry-PINK1 expression construct was successfully produced by other lab members and its validation is described elsewhere (Bowling et al., 2019).

We cotransfected HeLa cells with pEYFP-Parkin and pPINK1-mCherry constructs and attempted to repeat the experiment described in Figure 9A. Surprisingly, we found that this resulted in PINK1-mCherry stabilization and co-localization of both proteins to the mitochondria in the absence of CCCP treatment (Figure 9 B+C). In the absence of exogenous Parkin, PINK1-mCherry is near-undetectable prior to CCCP treatment. Similarly, expression of EYFP-Parkin alone in HeLa cells, which express endogenous PINK1 did not lead to notable mitochondrial accumulation of EYFP-Parkin. These data indicated that the PINK1:Parkin pathway is highly sensitive to the expression level of both proteins and while the expression of exogenous proteins of one type or the other is tolerable, co-expression spontaneously activates the pathway. For this reason, no further experiments using co-expression of exogenous PINK1 and Parkin were attempted.

3.4 ROS-induced mitochondrial accumulation of EYFP-Parkin

Although CCCP titration provided an efficient and reproducible method to manipulate MMP in cultured cells, it may not accurately represent mitochondrial damage and stresses experienced by cells *in vivo*. It is widely known that normal mitochondrial activity produces ROS as a byproduct and this is increased as a result of mitochondrial dysfunction. ROS can result in oxidative damage of the mitochondria resulting in further damage, dysfunction and decreasing MMP. For this reason, we tested the genetically-encoded mitochondrial-targeted photosensitizer, mitoKillerRed as a method to stimulate localized ROS production at specific regions of mitochondrial networks in living cells.

In our hands, mitoKillerRed could be successfully co-expressed in HeLa cells with EYFP-Parkin with both proteins exhibiting the expected localization (mitochondrial and cytoplasmic, respectively) prior to photoactivation. However, after multiple attempts following manufacture-supplied and published protocols (Wang et al., 2012; Yang and Yang, 2013), we were only able to detect measurable mitochondrial Parkin accumulation in a minority of cells (Figure 10).

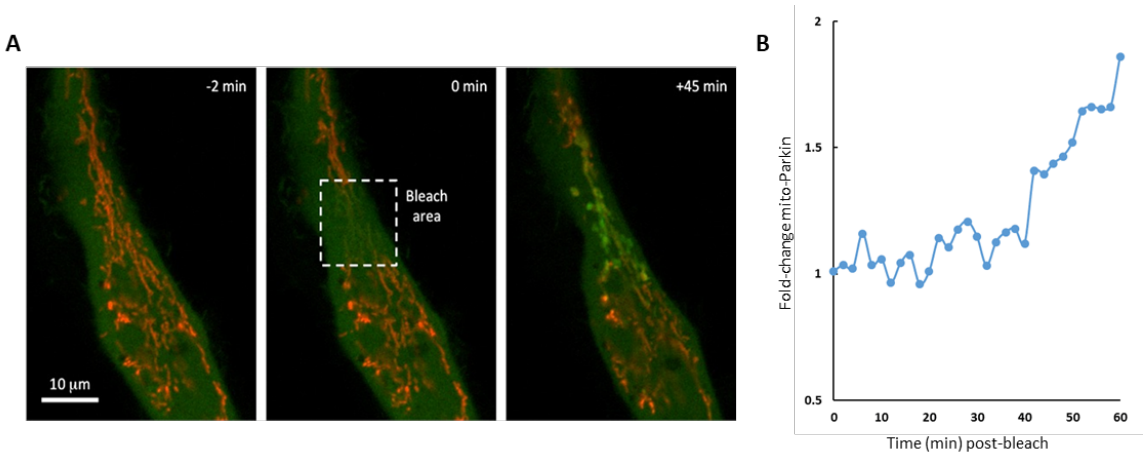

Figure 10: **ROS-induced recruitment of Parkin to mitochondria with mitoKillerRed.** (A) A single HeLa cell co-expressing mitoKillerRed (red) and EYFP-Parkin (green) were photobleached within the indicated area with a 555 nm laser at 100% power within the indicated area and observed for one hour by confocal microscopy. (B) Quantification of the EYFP signal at the mitochondria expressed as a ratio of the EYFP signal in the cytosol within the photobleached region indicates localized recruitment of Parkin.

3.5 Discussion

The focus of this first results chapter is the appraisal of tools for the control of MMP and the visualization of the PINK1:Parkin pathway response to changes in this in living cells. The establishment for a robust methodology for both is essential for the answering of the core questions of this thesis.

The performance of the FP-tagged PINK1 and Parkin proteins was unsurprising as other groups have successfully used tagged exogenous PINK1 and Parkin in prior studies (Matsuda et al., 2010; Narendra et al., 2008, 2010a, 2010b), and all evidence suggests that these tags do not compromise the activity or ability of these proteins to relocalize or accumulate in response to mitochondrial stress. A small number of studies have suggested that the addition of Myc or other small epitope tags to Parkin can compromise the ability of the protein to maintain autoinhibition in the absence of mitochondrial stress and can lead to spurious autoubiquitination. In broader studies performed by our lab, we saw little to no evidence of this as we found that expression of EYFP-Parkin in HeLa cells was not by itself sufficient to induce ppUb formation in these cells (Bowling et al., 2019).

For the control of MMP, we tested two existing methods in the field; the use of the mitochondrial ionophore, CCCP, and the mitochondrially-targetted

photosensitizer, mitoKillerRed. While a small number of publications have successfully used mitoKillerRed to stimulate Parkin-dependent mitophagy in single cells using laser-based photoactivation, the technique is seldom used in the PINK1:Parkin field and we were unable to reliably use this tool to stimulate mitochondrial translocation of EYFP-Parkin in HeLa cells. While the precise reason for this is unclear, it is possible that we did not adequately deplete ROS-quenching molecules from the cell growth medium in our experiments. As the system depends on ROS-induced damaged to essential mitochondrial structures in order to disrupt electron transport and collapse the IMM proton gradient, the presence of antioxidants in the cell growth medium can block its effects. For this reason, these experiments were performed in the absence of glutathione in the medium and phenol red that may have absorbed photons from the laser used to stimulate ROS production by mitoKillerRed. It's worth mentioning that for live cell imaging, particularly the longer experiments presented later in this thesis, the presence of antioxidants in can help to prevent phototoxicity. Additionally, the lack of reproducibility and inability to reverse ROS damage once it had been generated made this method an impractical choice for the later experiments described in this thesis.

In contrast to mitoKillerRed, we found that CCCP titration was an ideal method to control MMP in our experiments. We showed that it had a dose-dependent effect on MMP in both HeLa and SH-SY5Y cells and could be readily washed out, restoring MMP. Furthermore, the effects of CCCP appeared relatively uniform between mitochondria within the same cell and between separate cells. As a small caveat, unlike high doses of CCCP that completely depolarized mitochondria and led to a long-lasting stable loss of TMRM fluorescence, intermediate CCCP doses that partial depolarized mitochondria frequently produced a small but transient recovery in MMP approximately 30 min post-treatment. As CCCP concentration was not varied in these experiments (Figure 7), the cause of these fluctuations is unclear. While distinct from these, natural, stochastic fluctuations in MMP have been described previously and are fairly well documented (Buckman and Reynolds, 2001; Teodoro et al., 2018). Nevertheless, we assert that these data demonstrate that CCCP titration provides an appropriate method to study the responses of the PINK1:Parkin pathway to complete, partial and transient loss of MMP.

CHAPTER FOUR: PINK1/PARKIN DYNAMICS IN RESPONSE TO MITOCHONDRIAL DE- AND REPOLARIZATION

4.1 Introduction

The data in this chapter seeks to determine PINK1 and Parkin dynamics in response to incomplete depolarization or repolarization. Previous experimentation from Chapter 3 demonstrated that we have developed a valid approach to address these questions through measurement of MMP with TMRM and CCCP titration/washout. In order to test PINK1:Parkin dynamics under these circumstances, we determined that we would transfect cells with either PINK1-EGFP or EYFP-Parkin, manipulate the concentration of CCCP throughout the course of imaging, and measure the change in expression or localization of these two mitophagic regulators over time. This would enable us to determine how the PINK1:Parkin axis interprets intermediate mitochondrial depolarization, as well as the response to transient complete depolarization.

An important distinction here is that experiments studying PINK1:Parkin-dependent mitophagy have largely neglected to test how this pathway responds to partial mitochondrial depolarization. While repolarization has been studied by some groups (Lazarou et al., 2012; Narendra et al., 2008), these experiments were performed using biochemical analyses that report on average cell behavior that may mask true cellular responses. These reports suggest that PINK1 is rapidly degraded following repolarization and retention of Parkin at the OMM is lost.

However, it has become necessary to test how PINK1 and Parkin respond to partial depolarization or repolarization at the single cell level in order to understand how this pathway has evolved to interpret more PD-relevant mitochondrial insults, such as those that may differ in magnitude or duration. Our expectation was that we would see dose-dependent responses by PINK1:Parkin to depolarization with CCCP, rather than a thresholded, all-or-nothing response. This was determined with data from Figure 7 that showed discrete levels of losses in MMP with different doses of CCCP and suggests that the PINK1:Parkin response would likely differ markedly.

This chapter will present data to show that the PINK1 response to 5 and 10 μM CCCP results in its differential expression and that this difference is due to a greater loss of MMP in cells treated with 10 μM CCCP. Furthermore, it will be demonstrated that restoration of MMP results in degradation of mitochondrial PINK1 species. In sharp contrast, similar experiments with Parkin do not result in the same behavior. Depolarization with 5 or 10 μM CCCP in this case showed that Parkin displays similar translocation kinetics in response to both doses and remains at the OMM, dissociating slowly when MMP is restored.

4.2 PINK1 response to unique levels of mitochondrial membrane depolarization

The data presented in chapter 3 showed that different levels of MMP loss could be achieved in HeLa cells using CCCP titration. We predicted two possible responses to this at the PINK1 level, i) that the response would be thresholded and that PINK1 accumulation would only be observed after MMP dropped below a certain threshold level or ii) PINK1 would produce a 'stronger' response, accumulating in a dose dependent manner to diminishing MMP. To test this HeLa cells were transfected with PINK1-EGFP and mito-mCherry and treated continuously with either 5 μM (Figure 11 B) or 10 μM CCCP (images not shown). The data showed drastically different responses in terms of PINK1 mitochondrial accumulation between the treatments with the different doses (Figure 11 A). When cells were treated with 5 μM CCCP to partially depolarize the mitochondria, PINK1 accumulated at the mitochondria as expected, peaking within 60 min post-treatment but this was followed by rapid dissociation and degradation, nearly returning to basal levels. While this happened consistently across the cell population, dissociation of PINK1 from the mitochondria occurred at different time points for individual cells.

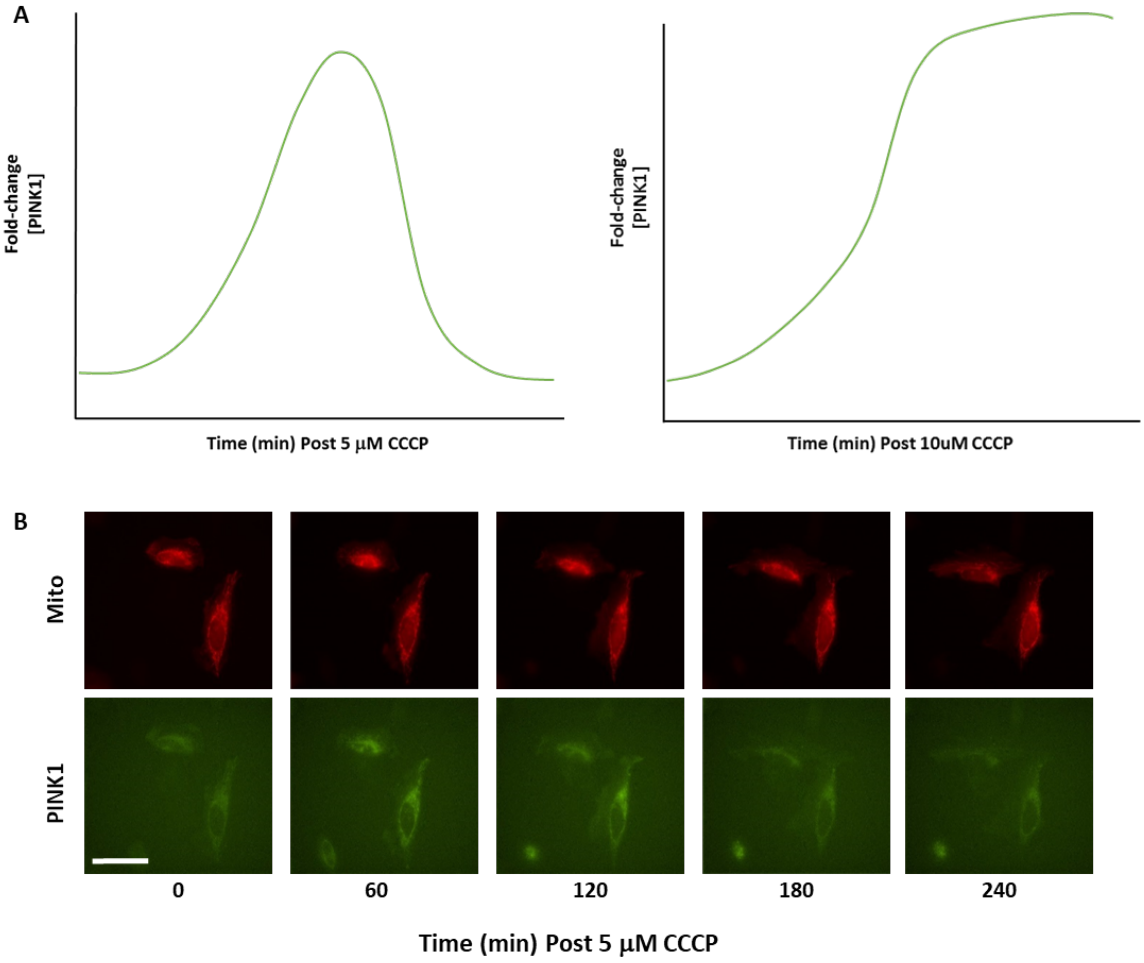

Figure 11: **PINK1 localization response to different magnitudes of mitochondrial depolarization.** (A) Graphical representation of the change in expression and localization of PINK1 within the cell when cells are treated with either 5 or 10 μM CCCP. These representations are informed by data presented in Bowling et al 2019. (B) Cells continuously treated with 5 μM CCCP show transient accumulation of PINK1 at the mitochondria, peaking at ~120 min post-treatment and rapidly declining by 180 min. Scale bar is 50 μm.

In contrast to the PINK1 response observed in cells treated with 5 μM CCCP, treatment with 10 μM CCCP resulted in stable accumulation of PINK1 to levels similar to the peak of the 5 μM response but this was not followed by PINK1-EGFP during the period of observation. This result differed from our initial predictions. Rather than showing a straightforward dose-dependent response or even thresholded response, PINK1 produced a transient response to partial depolarization and continuous response to complete loss of MMP. This result raised the question of what was causing PINK1 to dissociate in partially depolarized cells.

As our prior experiments using TMRM to measure MMP showed small fluctuations in MMP at intermediate CCCP doses (Figure 7 B), we hypothesized that these small increases in MMP might precede the dissociation and degradation of PINK1. PINK1 surveillance of MMP and retention at the OMM under conditions where MMP is lost, has been firmly established (Matsuda et al., 2010). However, it is not known to what extent MMP must be restored for cells to release mitochondrial-bound PINK1. All previous reports had only investigated this under conditions of complete loss of MMP followed by complete restoration. The effects of more subtle changes in MMP had not been explored. To test this, HeLa cells expressing PINK1-EGFP were incubated with TMRM and imaged by

widefield fluorescence microscopy during a 2 h period of continuous treatment with 5 μM CCCP. As expected, in cells that showed mitochondrial accumulation of PINK1-EGFP followed by loss, the decrease in PINK1-EGFP was immediately preceded by an increase in TMRM fluorescence, indicative of a recovery in MMP (Figure 12 A). The magnitude of this recovery and its timing was somewhat asynchronously across the population but, in most cases, still resulted in PINK1 dissociation (Figure 12 B). This was consistent with our earlier finding that the timing of PINK1-EGFP degradation varied between cells (Bowling *et al* 2019). Moreover, it was demonstrated that roughly a 20% restoration in MMP is sufficient to cause PINK1 release from the OMM (Figure 12 B, top-left panel). Remarkably, some cells spontaneously repolarize to pre-CCCP levels during constant 5 μM CCCP treatment (Figure 12 B, top-right panel). These experiments, together with our earlier characterization of MMP changes in response to different CCCP (Figure 7), suggest that this is uncommon and these larger MMP changes are likely transient.

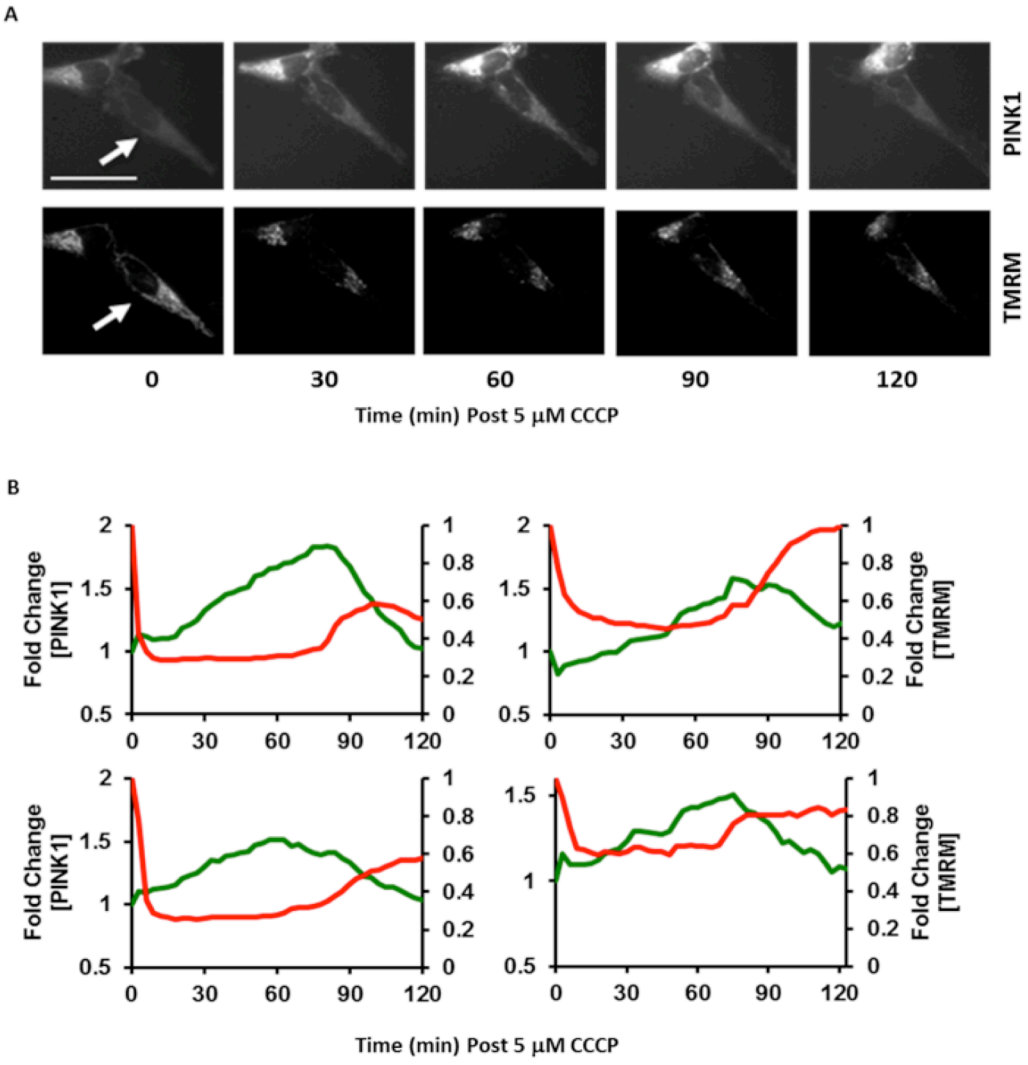

Figure 12: **PINK1 dissociation can be driven by spontaneous restorations in MMP.** (A) Time lapse images displaying PINK1 dissociation with a simultaneous restoration of MMP. Arrow indicates cell that exhibits PINK1 stabilization followed by loss. Levels increase between 0 and 60 minutes post-CCCP treatment. An increase in TMRM fluorescence and therefore MMP is evident at 90 minutes. This is followed by a decline in PINK1-EGFP fluorescence by 120 minutes despite no change in CCCP concentration in cell growth medium. (B) Quantification of 4 representative single cells expression/fluorescence levels of PINK1-EGFP (green) and TMRM (red). Scale bar is 50 µm.

4.3 PINK1 response to synchronous mitochondrial repolarization events

The ability of PINK1 to respond rapidly to mitochondrial depolarization and repolarization has important implications in how cells react to mitochondrial insults and make decisions regarding mitophagy. Though PINK1 dissociation from the OMM upon complete removal of CCCP has been previously demonstrated, many of these experiments were performed using biochemical analyses, such as western blotting, that do not report on single cell behavior (Lazarou et al., 2012; Narendra et al., 2010b).

It is important to note that the experiments described in section 4.2 only show a correlation between small recoveries in MMP and PINK1-EGFP degradation. To explicitly test whether incomplete recovery of MMP can promote loss of PINK1-EGFP from the mitochondria, we repeated our live cell imaging experiments in PINK1-EGFP and mito-mCherry-expressing HeLa cells, this time decreasing the CCCP concentration from 10 μM to 5 μM after one hour after initial treatment to produce a synchronous partial recovery of MMP across the population of cells (Figure 13 A-C). In these experiments, the vast majority of cells now showed synchronous loss of mitochondrial PINK1-EGFP (Figure 13 A, D+E). A small number of cells did not show PINK1-EGFP loss post-CCCP reduction (Figure 13

D and 14 A). This subtlety, while only a minor detail, is lost in the average behavior of the population.

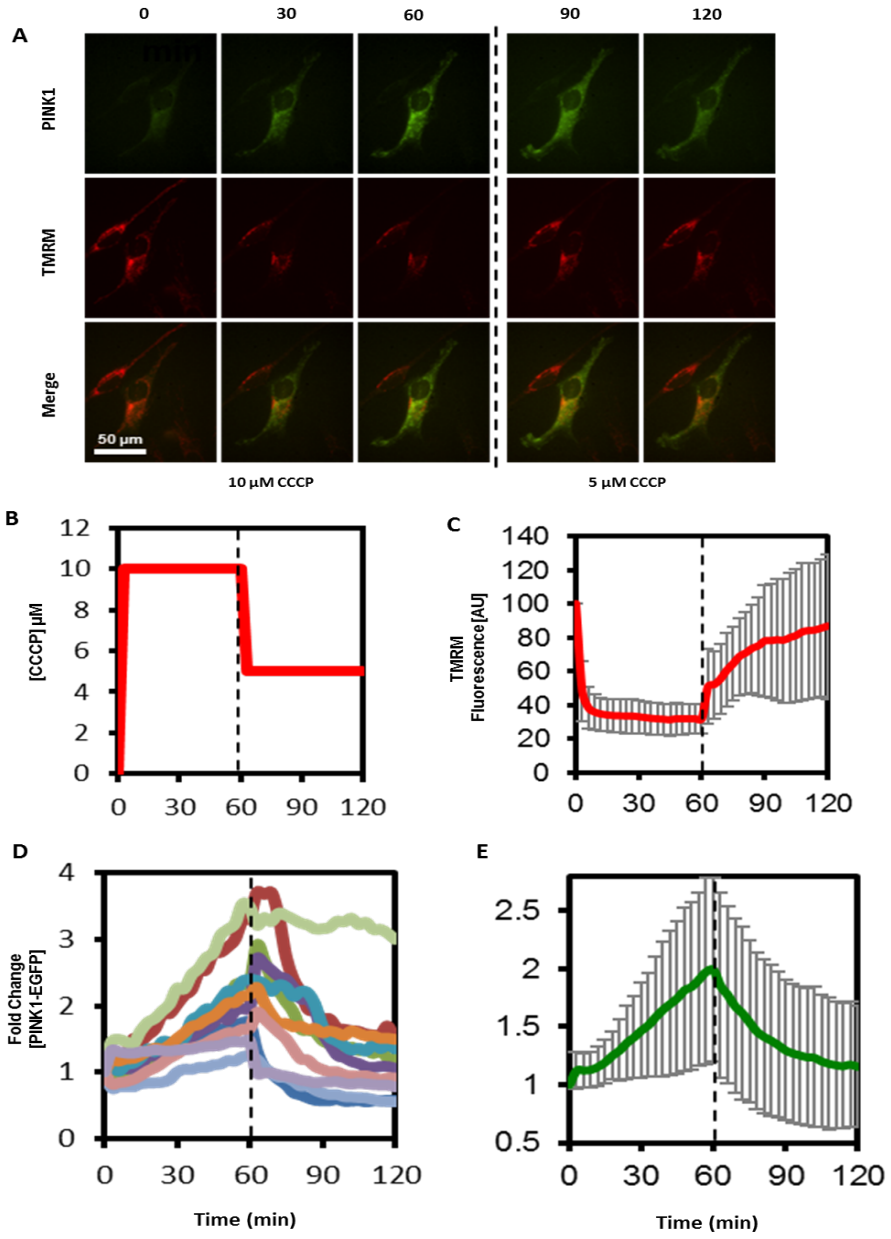

Figure 13: **PINK1 dissociation can be caused by synchronous repolarization events.** (A) Time lapse images displaying PINK1 dissociation and MMP restoration when CCCP concentration is lowered. (B) Depiction of CCCP titration throughout the experiment. (C) Quantification of population average membrane potential. (D) Single cell measurements of PINK1 expression. (E) Population average of PINK1 expression. Dashed lines represent CCCP concentration being lowered from 10 µM to 5 µM. Error bars represent the S.E.M.

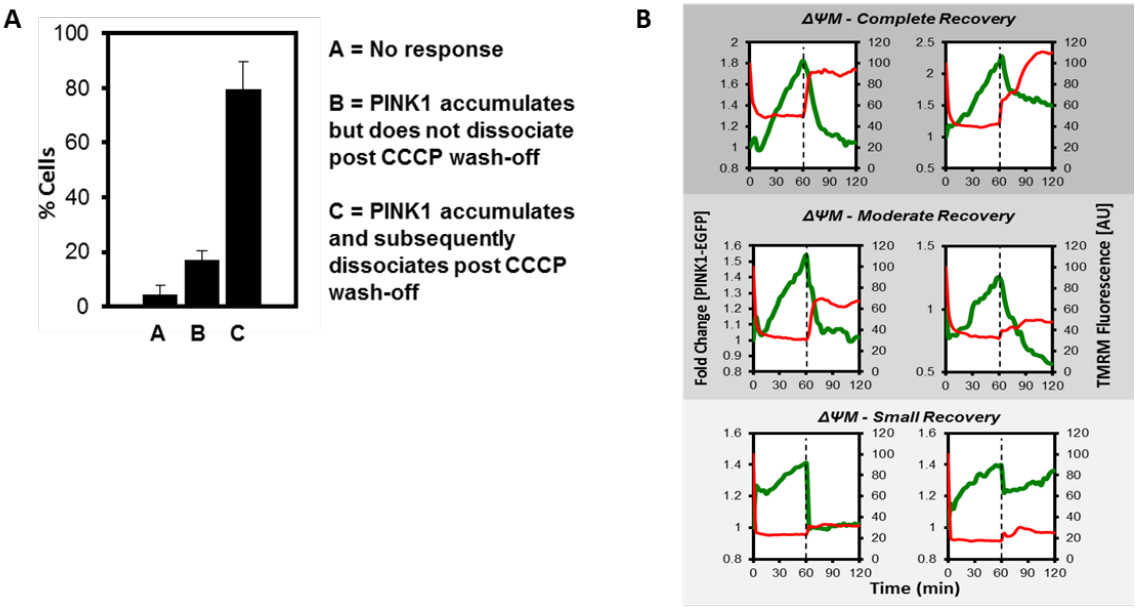

Figure 14: **Complete restoration of MMP is not required for PINK1 dissociation.** (A) Graph shows cell population percentages organized into categories based on PINK1 response. (B) PINK1 dissociation can occur if MMP recovery is small, moderate, or complete (2 cells displayed per group). Dashed lines represent CCCP concentration being lowered from 10 μM to 5 μM. Error bars represent the S.E.M.

Our results are still in agreement with the published literature but further these findings by showing that recovery of MMP need not be complete in order for PINK1 to dissociate from the mitochondria (Figure 13 A, B, C and Figure 14 B). Even small increases in MMP were found to be sufficient to induce PINK1-EGFP degradation.

4.4 Magnitude and duration of depolarization affects Parkin retention

Our discovery that PINK1 is capable of rapidly dissociating (< 1 hour) from the OMM to nearly basal levels in response to restoration of MMP made us question whether similar behavior would be observed at the Parkin-level and whether Parkin loss from the OMM would occur over the same or similar timescales to PINK1 loss. Surprisingly, this question has seldom been addressed in the literature. To the best of our knowledge, this has been previously explored only once using western blot detection of Parkin in mitochondrial fractions after complete repolarization of mitochondrial networks (Lazarou et al., 2012). The authors of this study reported that Parkin, like PINK1 is completely lost from the OMM relatively quickly after repolarization. We felt that this particular assay was flawed. The data itself appeared inconclusive did not provide sufficient temporal resolution to make a clear statement about the rate of Parkin loss as

compared to PINK1. Furthermore, it wasn't obvious whether the experiment had been repeated.

We hypothesized that the rate of Parkin loss from the OMM post-repolarization would be slower than PINK1. Our assumptions for this were as follows. In order for stabilized mitochondrial PINK1 to be lost, it is only necessary that the MMP-dependent TIM resumes function so that PINK1 can be processed by PARL and subsequently shed from the mitochondria. This would likely occur relatively rapidly. For Parkin to be released, the ppUb chains that served as OMM binding site for Parkin (but not PINK1) would need to be removed. At the time these experiments were conducted, the mechanisms of ppUb removal were unclear. A ppUb phosphatase had not been identified and it was only known that mitochondrial deubiquitinases, such as USP30 dissasembled ppUb chains at slow rate as they were essential protected by phosphorylation of the ubiquitin moieties that formed the chains (Bingol et al., 2014; Cunningham et al., 2015).

To test our hypothesis, we repeated the experiment described in figures 13 and 14, this time using HeLa cells co-expressing EYFP-Parkin and mito-mCherry. As predicted, our results showed Parkin dissociation from the mitochondria occurs at a far slower rate that PINK1 loss (Figure 15). Interestingly, the rate of Parkin loss from the mitochondria appeared constant even if mitochondria were

repolarized before Parkin became saturating at the OMM (i.e. CCCP washout at 30 min instead of 60 min post-treatment; Figure 15 A). For the 60 min CCCP washout experiments (Figure 15 B-E), Parkin was still noticeably present one hour post-CCCP washout. By way of contrast, PINK1-EGFP had returned to basal levels in most cells by 30 min post-CCCP washout (Figure 13 D+E). Furthermore, these findings were consistent regardless of whether MMP was partially restored (10 μM to 5 μM) or completely restored (10 μM to 0 μM) (Figure 15 B + C).

This stark difference in PINK1 and Parkin behavior, while somewhat surprising, were consistent with our initial hypothesis and previous studies that demonstrate Parkin is tethered to the OMM in a different manner than PINK1, and that this difference could be responsible for the differences seen in kinetics of dissociation. While other researchers have not seen Parkin retention following CCCP washout (Narendra et al., 2010b; Tanaka et al., 2010), our results demonstrate that Parkin is retained at the mitochondria following CCCP washout and dissociates at a slow rate.

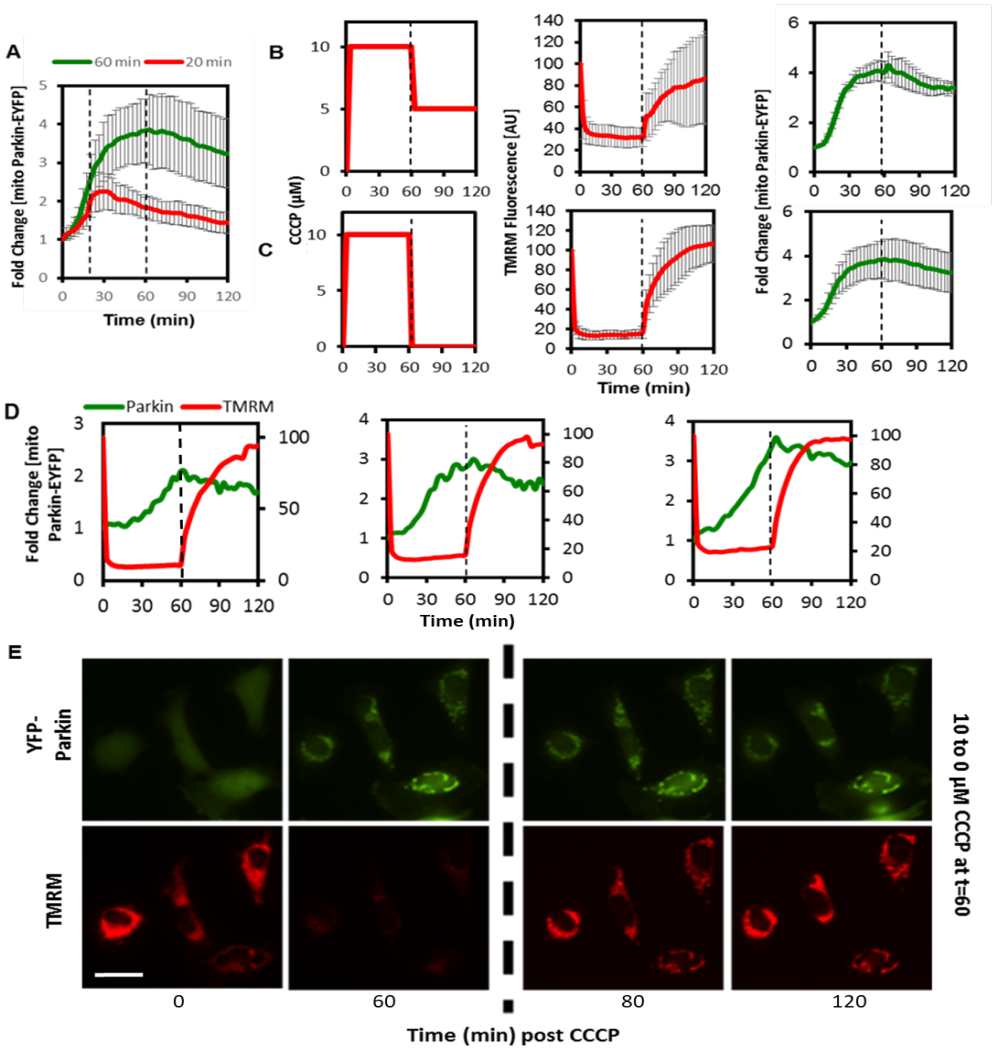

Figure 15: **Parkin exhibits a slow rate of dissociation from the mitochondria after partial or complete recovery of MMP.** (A) Quantification of fold change in mitochondrial Parkin (population average) over time. CCCP concentration was dropped from 10 μM to 5 μM at either 60 min or 20 min. (B) Depiction of CCCP titration to 5 μM (left), quantification of TMRM fluorescence as a measure of MMP (middle), and measurement of mitochondrial Parkin (right). (C) Same as panel B but CCCP titration to 0 μM. (D) Individual cell measurements for both MMP and Parkin localization when CCCP concentration is dropped to 0 μM. (E) Time lapse images of Parkin and MMP measured by TMRM. Dashed lines indicate changes in CCCP concentration. Scale bar is 50 μm. Error bars represent S.E.M.

4.5 Discussion

The data presented in this chapter demonstrate that Parkin and PINK1 operate on different timescales in response to changes in MMP. Despite the great number of prior studies characterizing the response of both proteins to loss of MMP (Cai et al., 2012; Matsuda et al., 2010; Narendra et al., 2008, 2010b), these differences have remained largely unrecognized and have not been explored in any detail. Possible reasons for this include the relatively infrequent use of live cell imaging in the field in favor of fixed-timepoint IFA and biochemical fractionation to investigate PINK1 and Parkin OMM accumulation, as well as the near exclusive use of high doses of CCCP or other depolarizing agents (e.g. BAM15 or AO) to stimulate complete loss of MMP.

Although the most striking result presented in this chapter is the long-lasting retention of Parkin after MMP recovery, the finding that small perturbations in MMP can promote PINK1 loss is also novel and merits discussion. Collectively, our data indicate that under conditions of partial loss of MMP, the PINK1 response is not binary in the sense that it shifts from an 'off' (i.e. destabilized' to a 'on' (stabilized and mitochondrial). Instead, it appears to be highly dynamic, rising and falling in response to small changes in MMP. While this was not observed in these relatively short experiments, we speculate that in cells cultured

for longer periods of time in intermediate concentrations of CCCP, recurrent rounds of PINK1 stabilization and loss at the OMM may be observed driven by stochastic fluctuations in MMP. These fluctuations likely affect the activity of the MMP-dependent TIM, which transports PINK1 into the matrix for processing. If the increase in MMP is sufficient to shift TIM from inactive to an active state, as PINK1 is poised within the TOM:TIM complexes at depolarized mitochondria, it would be rapidly processed on-mass and quickly destroyed, consistent with what was observed in our live imaging experiments (Figure 13).

Overall, our data indicate PINK1 is highly dynamic, changing its concentration rapidly to follow shifts in MMP. This would seem a desirable property for the PINK1:Parkin pathway as it would enable cells to pause ppUb production and Parkin activation if mitochondria show signs of recovery. Given that mitochondria show fluctuations in MMP as part of normal cellular functions (Buckman and Reynolds, 2001), this seems like a reasonable fail-safe to prevent inappropriate mitochondrial destruction.

In comparison to PINK1, Parkin retention and its slow dissociation from the OMM following mitochondrial repolarization events suggest that Parkin is bound to the OMM in a different manner than PINK1 and that this mechanism may impart a means for the cell to determine which mitochondria have faced a

previous (but recent) mitochondrial insult. In this way, Parkin, or more accurately ppUb chains established by PINK1 and Parkin together, can effectively serve as a marker for mitochondria that have been recently depolarized and allow the cell to assess mitochondrial health over time, only committing to mitophagy when ppUb levels achieve a threshold concentration at the OMM sufficient to stably recruit autophagy receptors and the autophagic machinery. Presumably this would correspond to a state where mitochondrial integrity has also reached a critical threshold where it could not be salvaged and risked harming the broader mitochondrial network and health of the cell. It is also worth mentioning that although Parkin can be retained for many minutes after PINK1 loss from the OMM and may still be able to catalyze pUb formation, all ppUb formation would cease in the absence of PINK1 so no near binding sites for Parkin could be formed, essentially placing mitophagy on pause as soon as some recovery in MMP occurs.

The deposition of ppUb chains by PINK1 and Parkin also function as docking sites for the recruit autophagy adaptors, including OPTN, which eventually leads to degradation of the mitochondrion (Bansal et al., 2018; Wong and Holzbaur, 2015a). With this in mind, we wanted to further investigate the dynamics of OPTN downstream of Parkin to determine if OPTN expression or

localization displayed a similar mechanism for labelling mitochondria in a specific manner, dependent upon the length and magnitude of mitochondrial depolarization and repolarization events. Because recruitment of OPTN and the autophagosome would ultimately mark the mitochondrion for degradation, the questions and experiments addressed in Chapter 5 seek to investigate the consequences of PINK:Parkin dynamics on recruitment of OPTN and link this to mitochondrial fate.

CHAPTER FIVE: THE AUTOPHAGY RECEPTOR OPTN & MITOCHONDRIAL FATE

5.1 Introduction

For years, the mitophagy literature has largely focused on the actions of PINK1, Parkin, and modifications to their targets. More recently, however, the field has become increasingly interested in how the activities of PINK1 and Parkin promote autophagosome formation around depolarized mitochondria and their eventual autophagic destruction. Organelle-specific modes of macroautophagy require the action of bivalent autophagy receptors to link the activity of the pathway that recognizes the organelle to be destroyed with the autophagy machinery itself. This was an obvious gap in our basic knowledge of the function of this mitophagy pathway but also had some disease relevance. In addition to the PD associated mutations identified in PD patients, deficiencies in lysosomal function and trafficking, both essential for autophagy, have been tightly linked to neurodegenerative disease (Lie and Nixon, 2019).

The search for an autophagy receptor unique to mitophagy has suggested both NDP52 and OPTN as candidates for this role (Evans and Holzbaur; Heo et al., 2015; Padman et al., 2019; Richter et al., 2016). Within the context of PINK1:Parkin mitophagy, OPTN appears to be more important of the two. Work by the Holzbaur lab and others have provided evidence that OPTN binds ppUb chains at depolarized mitochondria, coating the OMM and serves as an adaptor to the autophagy machinery, binding LC3 and promoting autophagosome

formation. These studies begin to link the actions of PINK1 and Parkin to downstream consequences including how these actions are interpreted to recruit autophagic machinery and ultimately lead to mitochondrial clearance. The data highlight the importance of ppUb chains in mitochondrial fate and suggest that this is the most critical modification present at the OMM to induce mitophagy.

Looked at within the context of the data presented in the prior chapters, we hypothesized that like PINK1 and Parkin, OPTN would also show differing recruitment dynamics in cells exposed to different mitochondrial stresses and that restoration of MMP after a brief period of depolarization may interrupt the coating of mitochondria with OPTN due to the slow decline in ppUb post-repolarization.

5.2 OPTN colocalizes with Parkin and labels mitochondria discretely

In order to investigate the dynamics of OPTN recruitment to depolarized and repolarized mitochondria, HeLa expressing EGFP-tagged full-length human OPTN (OPTN-EGFP) and mCherry-Parkin were treated with 10 μM CCCP for one hour, followed by one hour of 0 μM CCP (Figure 16 A-D) or continuously treated with 10 μM CCCP for two hours (Figure 16 E+F).

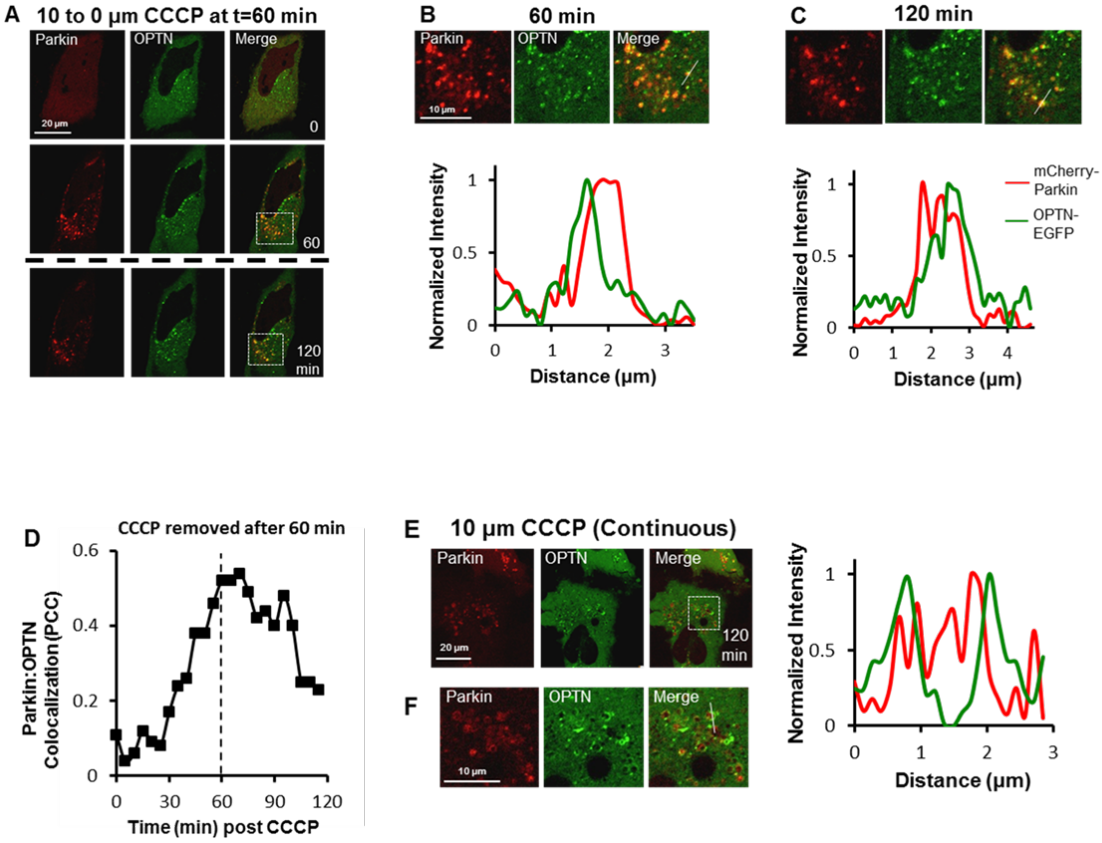

Figure 16: **OPTN labels Parkin-positive substrates uniquely depending on the length of the depolarization event.** (A) One-hour washout images. (B) Zoomed inset (white dashed box) for 60-minute mark of one-hour washout (top) and line intensity scan for that time point (bottom). (C) Inset image at 120-minute time point, one hour post-CCCP washout (top) and line intensity scan for that time point (bottom). (D) Pearson's correlation coefficient for Parkin:OPTN colocalization over time for one-hour washout. (E) 2-hour continuous 10 µM CCCP image at 120-minute mark. (F) Inset image for 2-hour continuous treatment. (G) Line intensity scan for 120-minute time point of 2-hour continuous treatment. Dashed lines represent CCCP washout.

Images were acquired throughout the 2-hour experiment, and Pearson's correlation values were calculated for OPTN and Parkin in the one-hour washout sample (Figure 16 D). Line intensity scans were performed on the 60 and 120-minute images for the one-hour washout sample (Figure 16 B + C) and 120-minute image for the continuously treated sample (Figure 16 E + F). The data show that the different treatments resulted in discrete labelling of OPTN and Parkin-positive puncta (Figure 16 B + C and E + F).

The one-hour washout sample showed strong colocalization between OPTN and Parkin up to the 60-minute mark but steadily declined following removal of CCCP (Figure 16 D). Furthermore, during these experiments OPTN failed to surround and coat Parkin-postive mitochondria at either the 60 or 120-minute time points, suggesting that while OPTN is recruited under these circumstances, it does not proceed to completion (Figure 16 B + C). However, the continuously treated cells showed a marked difference in OPTN labelling. In this case, OPTN fully wrapped around Parkin-positive mitochondria. This can be seen in figure 16E+F where line scans demonstrate OPTN-EGFP labeling is distal to the mCherry-Parkin on either side of mitochondria. This suggests that the mitochondria and surrounded by a layer of mCherry-Parkin and a layer of

OPTN-EGFP surrounds this, as would be expected for successful coating of mitochondria with this autophagy receptor (Figure 3).

In order to verify that OPTN and Parkin were colocalizing at mitochondria, a 3-color imaging experiment was performed by co-transfecting cells with pOPTN-EGFP, pmCherry-Parkin and pShooterMito-CFP constructs (The latter was produced by El Park, Nelson Lab, Middle TN State University) and using the same approach as described in figure 16. These data demonstrate a similar response by OPTN to one-hour washout with 10 μM CCCP and a 2-hour continuous treatment but also verify that Parkin and OPTN are localizing at mitochondria. Again, images from the one-hour washout sample (Figure 17 A) demonstrates colocalization of Parkin, OPTN, and the mitochondria, as determined by line scan intensity profiles at both the 60-min and 120-min mark (Figure 17B + C). The 2-hour continuous treatment in this experiment supported the idea that the length of the depolarization event has an effect on the morphology of OPTN labelling of Parkin-positive mitochondria. These data showed that 2 hours of continuous treatment with 10 μM CCCP results in OPTN fully wrapping around Parkin and the mitochondria. Images acquired from cells exposed to this treatment pattern (Figure 18 A) demonstrate that OPTN labels

these mitochondria by enveloping or completely coating the mitochondria with OPTN.

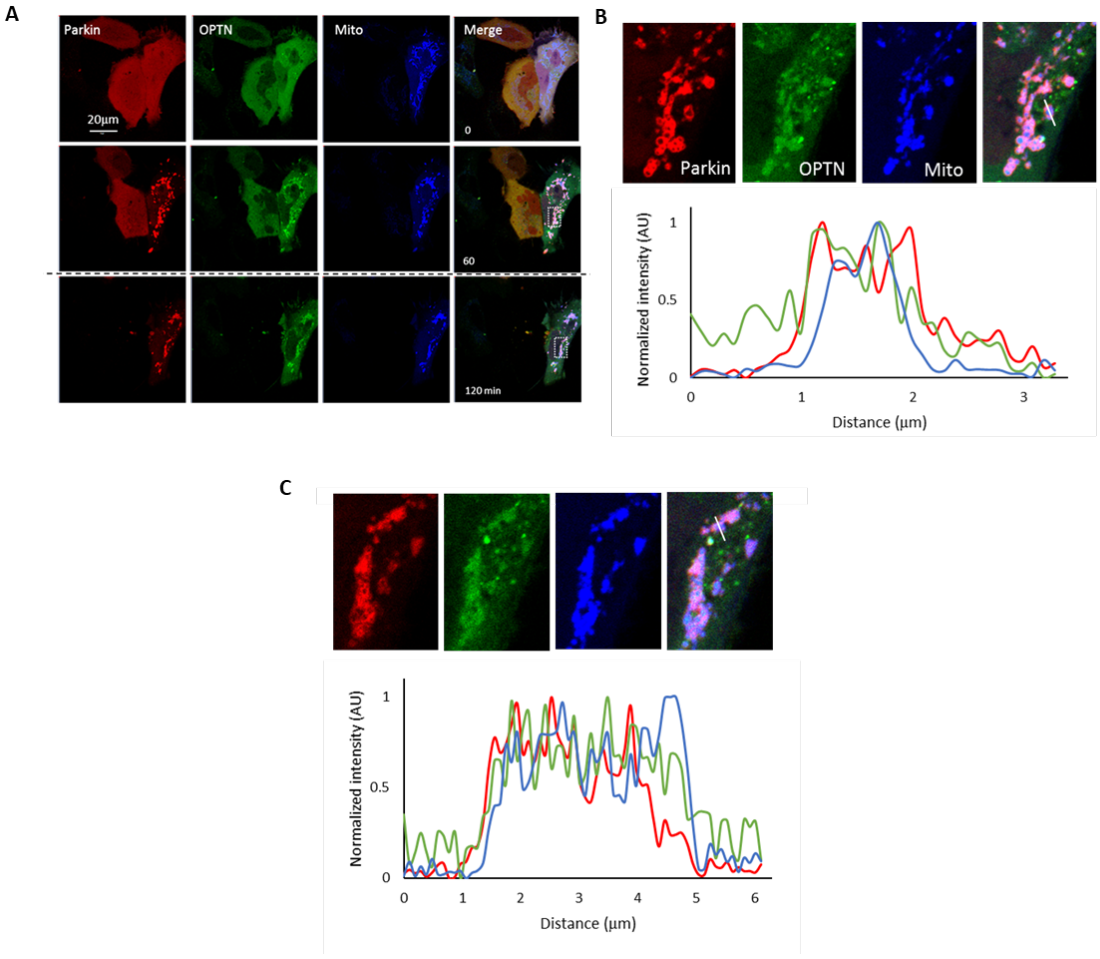

Figure 17: **Localization of OPTN and Parkin at mitochondria in response to one-hour treatment with 10 µM CCCP and washout.** (A) One-hour washout images with additional mitochondrial marker. (B) Inset images of 60-minute time point (top) and line intensity scan (bottom). (C) Inset image of 120-minute time point (top) and line intensity scan (bottom). Scale bar is 20 µm.

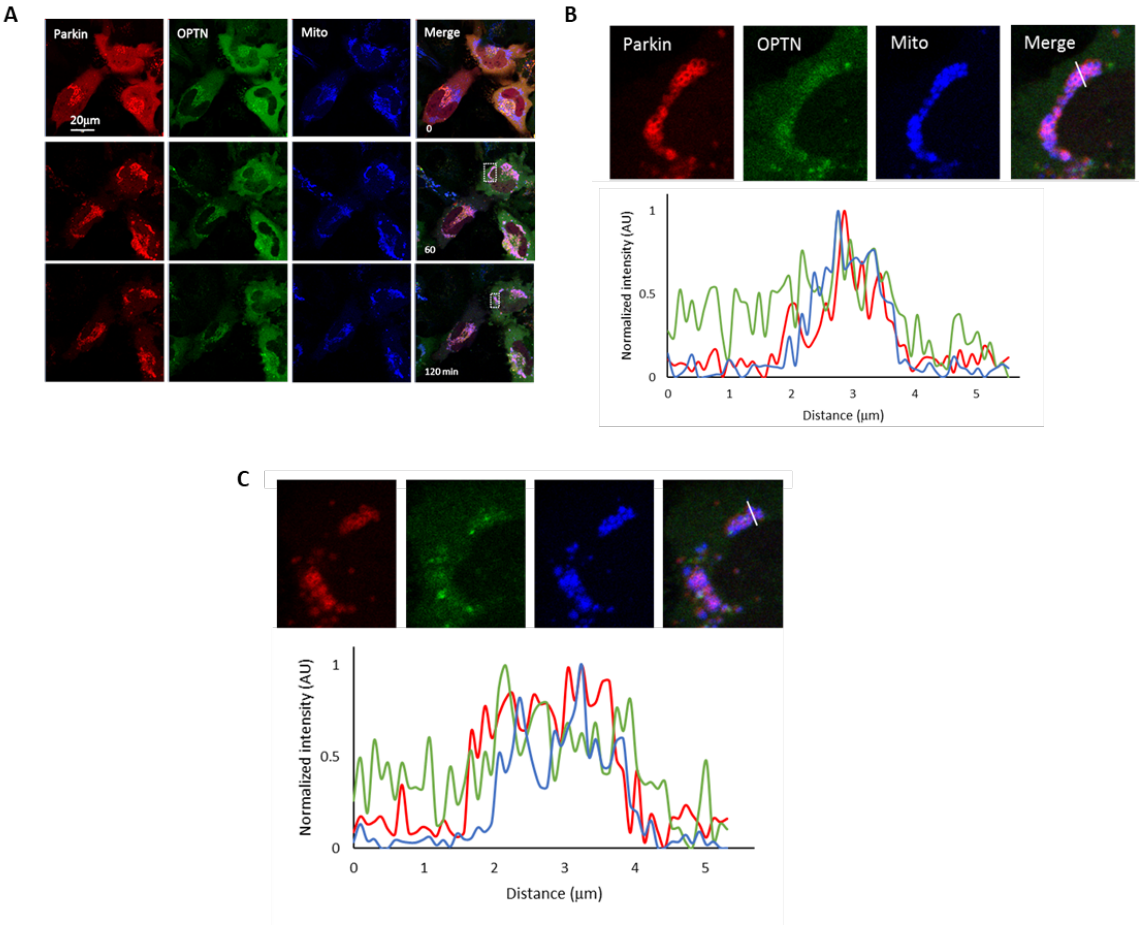

Figure 18: **Localization of OPTN and Parkin at mitochondria in response to two-hour continuous treatment with 10 μM CCCP.** (A) Two-hour washout images with additional mitochondrial marker. (B) Inset images of 60-minute time point (top) and line intensity scan (bottom). (C) Inset images of 120-minute time point (top) and line intensity scan (bottom). Scale bar is 20 μm.

5.3 Using mitochondrial mass and morphology to assess mitophagy

Having shown that like Parkin, OPTN could be retained at mitochondria post-repolarization for an extended period of time albeit as puncta rather than an evenly distributed coat, we speculated that this may prime mitochondria for mitophagy in response to subsequent stresses. In parallel with this work, other members of the Nelson lab had shown that exposure of cells to repeated pulses of CCCP could drive the slow accumulation of Parkin at the OMM to higher levels with each pulse so long as these pulses were spaced no further apart than 30 minutes. These experiments modeled regular fluctuations in MMP that may be somewhat similar to what might be observed in failing mitochondria. \

In support of our central hypothesis that the PINK1:Parkin pathway will produce different responses to mitochondrial insults of differing magnitude, we found that CCCP had a dose-dependent effect on mitochondrial mass, as assayed using a membrane potential-independent dye (Figure 19). We were surprised by the unexpected reduction of mitochondrial mass in cells treated with low-dose CCCP, suggesting that even small but long-lasting decreases in MMP can elicit a decisive and somewhat proportionate response from the PINK1:Parkin pathway.

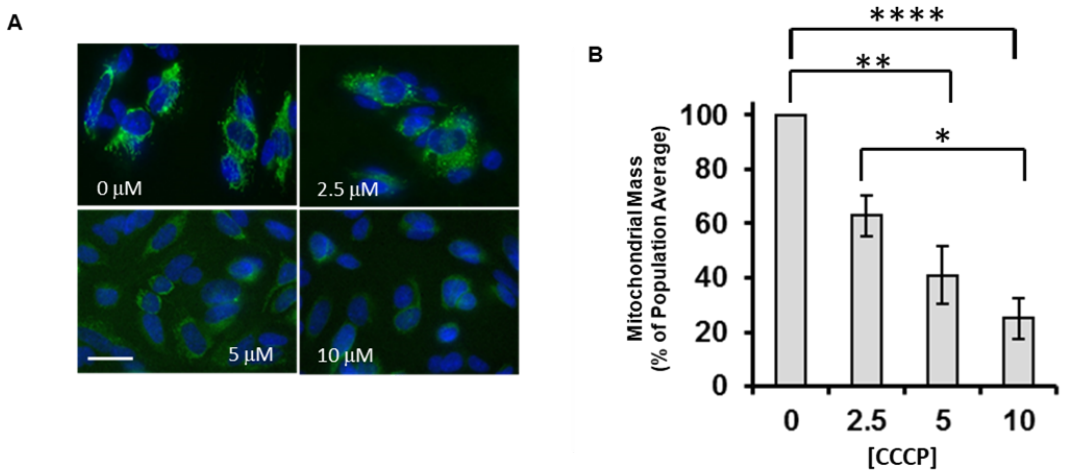

Figure 19: **Mitochondrial mass in SH-SY5Y cells.** (A) SH-SY5Y cells were exposed to different doses of CCCP for 24 hours and stained with MT-Green. (B) Quantitative measurements of fluorescence were made to assess mitochondrial mass.

As a final concluding experiment to link the response of the PINK1:Parkin pathway, OPTN, and mitochondrial fate, an experiment was designed to determine how repeated interruptions in MMP occurring at different frequency affected mitochondrial mass. HeLa cells expressing EYFP-Parkin were exposed to pulsing treatments of 10 μM over a 6-hour time course. An IFA was then performed, probing for TOM20 to determine mitochondrial morphology/mass. Although direct and quantitative mitochondrial mass measurements were not performed (as they were in Figure 7), qualitative assessments of TOM20 immunostaining were done based on mitochondrial morphology and broken into categories (Figure 20 A). This method of appraising the progress of the mitophagic process and mitochondrial clearance is commonly used in the field and is used in numerous publications (Girotra et al., 2019; Lazarou et al., 2012; Narendra et al., 2010a, 2010b; Silva et al., 2013).

As might be expected continuous treatment of the cells with CCCP resulted in mitochondrial clearance from ~20% of the cells with all remaining cells showing perinuclear aggregation of mitochondria, a phase of mitophagy that precedes clearance (Figure 20 B). By way of contrast, a single 30 min CCCP produced either no effect or led to mitochondrial fragmentation, an early but reversible set in mitophagy. Comparing the data from cells treated with 30 min pulses of

CCCP separated at either 30 or 120 min apart, far more aggregation and clearance is observed in the former than the later. This is consistent with our data that suggests regular disruption of MMP occurring at intervals no greater than 30 min is sufficient to drive escalating Parkin accumulation at mitochondria (Bowling et al. 2019) and provide support for the notion that the PINK1:Parkin signaling axis is capable of temporal integration of mitochondrial stress signals. Moreover, these qualitative assessments of mitochondrial morphology provide evidence that the behaviors and dynamics of PINK1:Parkin signaling during the initial 2-4 hours of a mitochondrial depolarization event have consequences on mitochondrial fate and the amount of mitochondrial degradation.

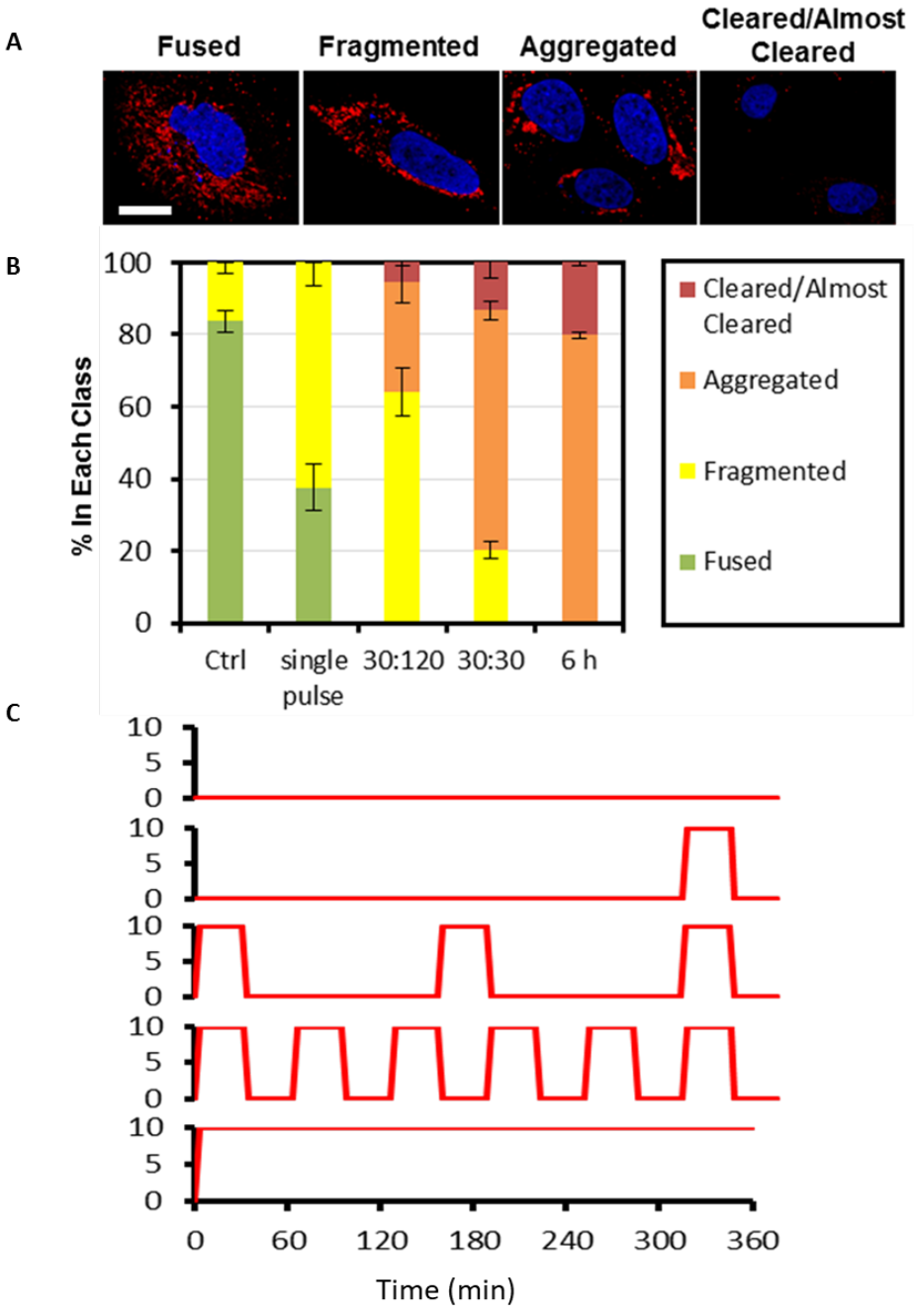

Figure 20: **Mitochondrial mass and morphology measurements for complex depolarization events.** (A) TOM20 immunostaining of mitochondrial networks broken into qualitative categories. (B) Percentage of cells in each category, grouped based on treatment regime. (C) Graphical representation of treatments and CCCP titration over the 6-hour time course. Scale bar is 20 μm. Error bars represent the S.E.M.

5.4 Discussion

The study of autophagy adaptors specific for clearance of mitochondria have suggested that OPTN is a prime candidate for this mechanism (Moore and Holzbaur, 2016b; Wong and Holzbaur, 2015b). Furthermore, these studies also provided evidence that OPTN is dynamically recruited to mitochondria marked with ppUb deposited by PINK1 and Parkin. With this in mind, the experiments presented in this chapter were designed to test how the differing dynamics that we observed at PINK1:Parkin level after short or extended periods of mitochondrial depolarization were propagated downstream to the OPTN level, affecting the recruitment of this autophagy receptor to mitochondria. The hypothesis was that the combined actions of PINK1 and Parkin to generate ppUb chains, and the degree to which the OMM was saturated with ppUb chains, would be interpreted differently by OPTN and lead changes in its recruitment. Several methods were used to assess this, including the measurements of changing colocalization of OPTN with Parkin at the mitochondria, as assessed by PCC analysis (Figure 16 D), and line intensity scans across mitochondria to determine whether OPTN were recruited as discreet puncta (present on one side of a mitochondrion) or fully coating mitochondria (Figure 16 B+C and E+F).

The data demonstrated that a sustained loss of MMP, as caused by continuous incubation of cells with CCCP, lead to a more complete response by OPTN to engulf or coat mitochondrial fragments. In contrast, transient depolarization events, sufficient to trigger a brief period of PINK1 accumulation at mitochondria and Parkin recruitment could still promote OPTN recruitment. In most cases, this was as puncta. The difference between these two outcomes was likely due to the density of ppUb present at the OMM, which would almost certainly be higher after sustained loss of MMP. This surprising result yet again suggests that a short period of depolarization primes a mitochondrion for destruction as this data demonstrates that a quantity of OPTN can be held locally to these mitochondria for an extended period of time and would likely increase the rate at which it could coat the mitochondria and recruit downstream autophagy regulators should MMP decline again.

CHAPTER SIX: FINAL DISCUSSION

6.1 Introduction

Since its initial characterization as a mitochondria-specific autophagy pathway in *Drosophila (Clark et al., 2006)*, the PINK1:Parkin pathway has been an area of intense scientific interest, not just for cell biologists but also for those interested in understanding how dysfuntion in this pathway could result in neurodegenerative disease. One of the longstanding questions in the field that had not been previously addressed to any level of satisfaction was how the pathway 'decided' when a mitochondrion was beyond recovery and had to be destroyed or how it responded to complex temporal inputs, such as fluctuations in MMP or partial loss of MMP. The data presented in this dissertation take the first steps towards exploring these questions and demonstrate that that the pathway demonstrates previously unrecognized complex behaviors. Using primarily a live cell microscopy approach, we show that PINK1 and Parkin operate on different time scales. This is not detectable in experiments following the mitochondrial accumulation of these two proteins after complete loss of MMP, as used in most previous studies, and is only evident under conditions of partial or transient loss of MMP. To be clear, both proteins accumulate at similar rates, peaking within 60 min during mitochondrial depolarization but while PINK1 responds rapidly to even small increases in MMP, being destroyed in

bulk within minutes, Parkin can persist for over an hour at the OMM after repolarization. This difference imparts a fundamental way for the cell to discriminate between mitochondria that have been recently depolarized and those that have not. While the persistence of Parkin is likely important, it almost certainly a consequence of the slow removal of ppUb chains to which Parkin docks to the OMM. It is these chains, not Parkin, that recruits downstream autophagy receptors, connecting PINK1:Parkin activity to the autophagic machinery.

Collectively, this research shows that mitophagy is not an all-or-nothing response – either destroying mitochondria or leaving them untouched - but is rather a signaling system that has properties of molecular 'memory', with responses that are shaped by prior events and can modulate the rate at which mitochondria are irreversibly commented to autophagy. In this chapter, these findings will be discussed within the context of the recent literature of the field, as well as potential pitfalls associated with techniques utilized to study mitophagy with this approach.

6.2 Outcomes and conclusions arising from this work

The experiments and data presented here were designed to address an overarching hypothesis of how the dynamic responses of PINK1 and Parkin to

transient and incomplete mitochondrial insults could be integrated over time to either abort mitophagy or allow it to proceed to completion. This was assessed by exposing cells transiently transfected with either PINK1 or Parkin to different magnitudes and durations of CCCP-dependent mitochondrial depolarization (Figure 7 A-D and 8 A+C). The work shows that PINK1 responds quickly to mitochondrial depolarization, rapidly associating at the OMM within minutes of treatment with 5 μM CCCP (Figure 11 B and 12 A+B). However, when mitochondria are partially or completely repolarized (Figures 13A-E and 14A+B), PINK1 is capable of quickly dissociating from the OMM. Notably, this occurs immediately after a restoration in MMP that need not be complete (Figure 14 B). This suggests that PINK1 acts as an immediate and primary initiator of the mitophagic response, but, perhaps more importantly, functions in a manner that is conducive to rapidly assessing when a damage stimulus is removed in order to abort or at least pause mitophagy of a mitochondrion that can be salvaged.

In contrast, Parkin dissociation from the mitochondria occurs much more slowly, remaining substantially more concentrated at the mitochondria than prior to depolarization and effectively serves as a marker for recently depolarized mitochondria (Figure 15 A-E). It is likely that this difference in dissociation dynamics is driven by the retention of Parkin at phospho-Ser65 polyubiquitin

(ppUb) chains (Bowling et al., 2019; Okatsu et al., 2015). Due to the difference in dissociation rates between PINK1 and Parkin, it is possible for the cell to distinguish mitochondrial insults that arrive closely together from those that are spaced by an extended length of time, where Parkin is permitted to dissociate to basal levels (Bowling et al., 2019).

It has also been established here that PINK1:Parkin dynamics translate to downstream consequences including losses in mitochondrial mass and deviations from a healthy mitochondrial morphology, stemming from varying lengths and degrees of mitochondrial depolarization (Figures 8 B + D and 20 A-C). Moreover, this effect is not restricted to a single cell type or overexpression of exogenous protein (Figure 8 A + C). The data further show that retention of Parkin and, presumably ppUb chains, can recruit autophagy adaptors specific to the mitochondrion in a unique manner dependent upon the length of the depolarization event (Figures 17 A-C and 18 A-C). This suggests that OPTN can serve to interpret the extent to which mitochondrial depolarization was assessed by the combined actions of PINK1 and Parkin and label mitochondria both uniquely and on an individual basis to ensure their degradation. While it is not clear whether OPTN dissociation from repolarized mitochondria is possible (Figure 19 A + B), it is probable that those mitochondria which become entirely

encapsulated by OPTN are more likely to proceed towards fusion with the autophagosome (Figures 17 A-C and 18 A-C).

6.3 General issues associated with techniques used in this research

6.3.1 Single cell imaging, transient transfection, and the overexpression of exogenous proteins

The nature of this work and approaches utilized here were reliant on transient transfection and, thus, the overexpression of exogenous proteins. Though this is not ideal, it is in alignment with many of the approaches used in the mitophagy field for quite some time (Heo et al., 2015; Narendra et al., 2008, 2010a, 2010b; Ordureau et al., 2014; Tanaka et al., 2010) and is commonly used throughout the cell biology and cell signaling field (Burchell et al., 2013; Narendra et al., 2008, 2010b; Ordureau et al., 2018) . Single cell imaging provides a unique perspective for studying signaling dynamics and provides an opportunity to uncover how individual cells may exhibit markedly different behaviors from one another that may go otherwise unnoticed using a biochemical approach (see section *1.2.11*). Still, concerns arise surrounding whether the responses measured truly reflect the behaviors of the endogenous protein or even the behavior of the unmodified signaling pathway being observed. These concerns are largely associated with the often higher than physiological concentrations of protein that result from

transiently transfected plasmid constructs that frequently make use of strong viral promoters to drive the expression of the proteins being studied. While many signaling pathways are likely robust to changes in the expression of some of their components, other pathways will not be. Within the context of this particular study, we found that transfection of plasmids to express either PINK1 or Parkin alone did not appear to compromise the overall behavior of the mitophagy response, as neither protein showed mitochondrial accumulation prior to the treatment of cells with mitochondrial depolarizing agents. However, over-expression of both proteins were overexpressed in the same cells was sufficient to trigger mitophagy in the absence of stimulus (Figure 9 A-C).

Another concern related to the use of live cell imaging to study signaling dynamics is the necessity to use fluorescent tagging. These tags, which are based on jellyfish or coral-derived proteins, are large and bulky, ~27 kDa in size. To put this into perspective, the EYFP tag used in most experiments included in this dissertation is roughly half the size of Parkin itself. As discussed in section *2.2.2* and *2.2.4*, previous studies had raised concerns about the effects of epitope tags on Parkin function. The EYFP-Parkin constructs utilized in this work contained a small 8 aa C-terminal tag in addition to the N-terminal EYFP tag. We found no evidence to suggest that these tags affected the localization or activity of the

protein as the Parkin-fusions were found to be in a cytosolic, auto-inhibited state prior to CCCP (Figures 9 A, 15 E, 17 A, and 18 A). Furthermore, additional experimentation with a newly generated EYFP-Parkin construct (El Park, Middle TN State University Nelson lab) without the 8 aa C-terminal extension showed similar results in Parkin retention and slow dissociation from the OMM (Figure 21). This demonstrates that the data presented throughout this study is valid and the results support the conclusions drawn herein.

The use of live cell imagine requires its own distinct data analysis methods in order to make sense of the results. Our image acquisition and data analysis were performed in a manner consistent established methods in the field (Lazarou et al., 2012; Moore and Holzbaur, 2016a; Narendra et al., 2008, 2010b; Wong and Holzbaur, 2015a). This included how fluorescent fusions of PINK1 and Parkin were generated, as well as quantitative measurements for PINK1:Parkin dynamics and labelling of mitochondria and Parkin-positive substrates by OPTN. Particularly noteworthy is the observation that concentrations of FBS and BSA in the cell imaging medium can have an effect on the ability of CCCP to depolarize mitochondria (Soutar et al., 2019). This was not known throughout the duration of the study but was unintentionally controlled for by replenishing the medium on the cells immediately prior to imaging.

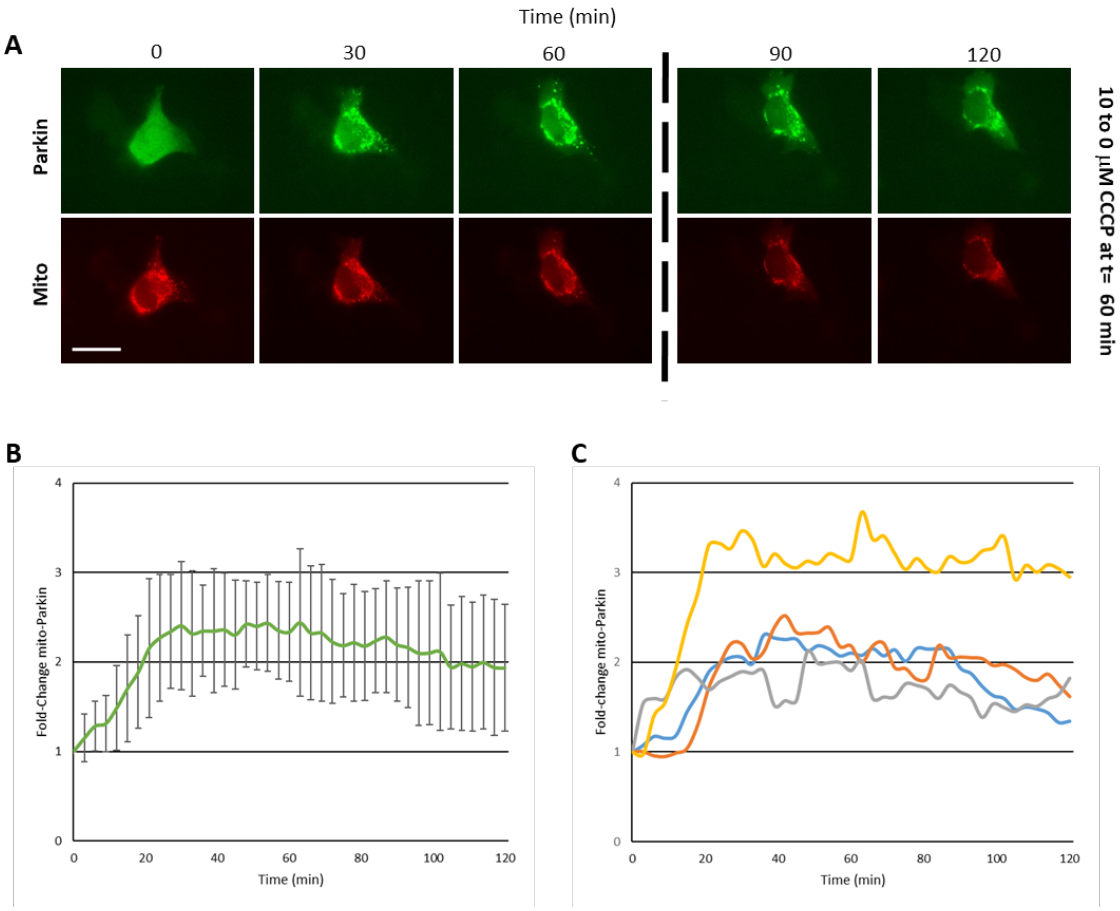

Figure 21: **EYFP-Parkin dynamics are unaffected by 8 amino acid extension** (A) Time lapse images of Parkin and the mitochondria. (B) Population average of fold-change mito-Parkin. (C) Single cell dynamics in fold-change of mito-Parkin shows cell to cell variation but consistent trends in slow dissociation of Parkin from mitochondria. Dashed line represents CCCP washout. Scale bar is 50 μm. Error bars represent the S.D.

6.4 Recently published work on PINK1:Parkin mitophagy

6.4.1 General comments

During the studies carried out in this dissertation, the mitophagy field has begun to show a deeper interest in the substrates of Parkin-dependent ubiquitination, as well as how PINK1 and Parkin work together to establish an interlocking coherent feed-forward loop and generate both polyubiquitin- and phosphopolyubquitin chains that are interpreted differently by the mitophagy pathway (Harper et al., 2018; Heo et al., 2015; Okatsu et al., 2015; Ordureau et al., 2014, 2018). These data show that Parkin targets a plethora of OMM proteins in order to regulate their turnover in addition to signaling mitophagy. Indeed, Parkin is capable of generating at least 4 types of ubiquitin chain linkages (Sarraf et al., 2013), and it is not until PINK1 begins to phosphorylate polyubiquitinated OMM substrates that the full catalytic properties of Parkin are enabled via its binding to the newly modified ppUb chain (Okatsu et al., 2015; Sauvé et al., 2018; Wauer et al., 2015b). Through recruitment of autophagy receptors, these events are now believed to be critical in the regulation of mitophagy, including how the cellular response to intermittent and mild mitochondrial stressors are assessed by the PINK1:Parkin axis (Bowling et al., 2019; Evans and Holzbaur, 2020; Moore and Holzbaur, 2016b; Richter et al., 2016; Wong and Holzbaur, 2015b).

6.4.2 Mitophagy is controlled by the dynamic actions of PINK1 and Parkin, ppUb chain formation, and negative regulators

Recently published data in the field has begun to show a trend that mitophagy is a balancing act between 1) The rate at which PINK1 and Parkin work to establish ppUb chains at the OMM and 2) the phosphatases and deubiquitinases that oppose formation of these chains (Bingol et al., 2014; Marcassa et al., 2019; Wall et al., 2019; Wang et al., 2018a, 2018b) (Figure 22 A-C). In fact, these timely papers support the conclusions drawn in this dissertation by proffering more and more evidence that mitophagy is a highly dynamic and tightly regulated process capable of reversal. While some of the earliest papers concerning mitochondrial deubiquitinases, such as USP30 had started to appear in the literature at the start of this study, the existence of a ppUb phosphatase was purly hypothetical and it was unclear whether or not one existed or whether PINK1:Parkin generated ppUb chains were simply destroyed by the action of a deubiquitinase alone. In the last 2-3 years, it has become clear that the removal of ppUb chains at the OMM is likely a 2-step process, requiring first removal of the phosphate and then disassembly of the ubiquitin chain. This is likely necessary because the S65 phosphorylation of pUb chains by PINK1 to create ppUb appears to protect these chains from the action of deubiquitinases (Bingol et al., 2014; Marcassa et al.,

2019). These results suggest a mechanism for differences in dissociation kinetics seen in this study between PINK1 and Parkin when mitochondria are repolarized as ppUb chain remove is relatively slow and inefficient. Although the exact rate of ppUb chain removal mechanisms remain unknown, at least two phosphatases that act on ppUb chains deposited by PINK1 and Parkin are known as phosphatase and tensin homolog-long (PTEN-L) and protein phosphatase with EF-hand domain 2 (PPEF2) (Wall et al., 2019; Wang et al., 2018a, 2018b), while ubiquitin specific protease 30 (USP30) represents a candidate for the deubiquitination process (Bingol et al., 2014). By providing new insights via novel negative regulators of mitophagy, these data also suggest additional mechanisms that attempt to salvage mitochondria after recruitment of PINK1 and/or Parkin.

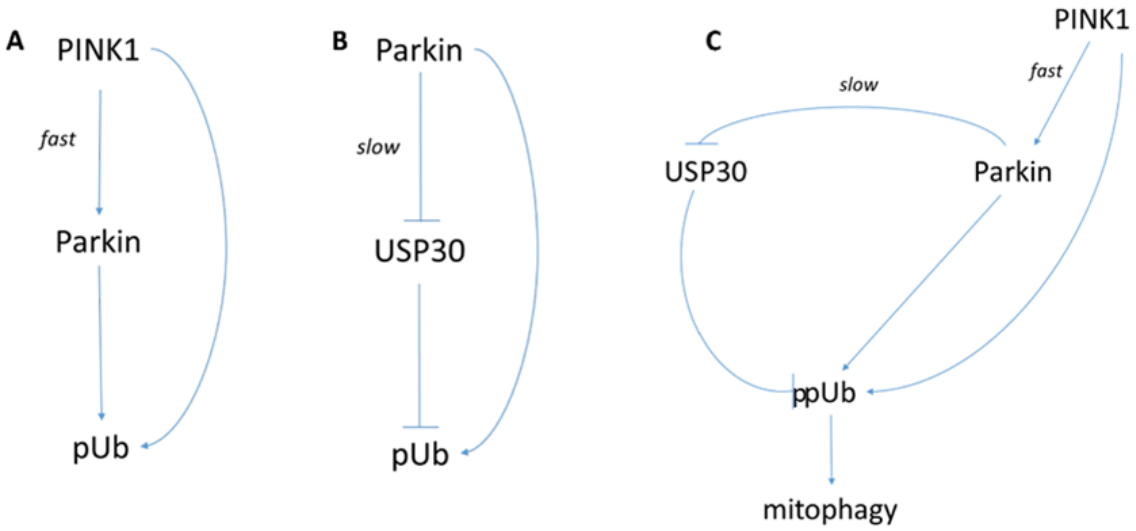

Figure 22: **Network topology of the PINK1:Parkin pathway.** (A) PINK1 activates Parkin quickly and is capable of phosphorylating Ub, but Parkin deposition of Ub chains, later phosphorylated by PINK1, occurs more slowly. (B) Parkin works to degrade the negative regulator of mitophagy, USP30, while being activated further by binding pUb. (C) Together, the actions of PINK1, Parkin and negative regulators, including USP30, are incorporated over time to initiate or abort mitophagy.

6.4.3 Future Research

The data shown here lay a foundation for examination of PINK1:Parkin dynamics as a route for understanding how the pathway interprets stresses, controls the downstream response, and indeed how we could potentially manipulate and control this in the future. These experiments were all performed using wild-type (WT) PINK1 and Parkin in order to more closely study 'natural' PINK1:Parkin signaling and in no way model mitophagy in PD. As, it has been widely reported in the literature (see section 1.1) that there is a genetic, hereditary component to PD that could potentially affect the dynamics of mitophagy as the result of mutated PINK1 or Parkin (Sauvé et al., 2015) (Figure 1), future work could be focused on determining how PD-relevant mutant forms of PINK1 and Parkin affect the dynamics and results seen in this investigation. While many PD-associated Parkin mutants are expressed as completely inactive proteins or are insoluble and do not merit further study, others, such as the R275W mutant remain enigmatic. Parkin R275W, which showing relatively little E3 ligase activity is still capable of translocating to depolarized mitochondria whereas the vast majority of E3 ligase-dead mutant Parkin proteins, such as C431S, cannot. The reasons for this are yet to be resolved and may help to answer fundamental questions about how Parkin is recruited and maintained at

depolarized or previously depolarized mitochondria. While the assumption is that this is purely ppUb-dependent, the behavior of this mutant protein raises the possibility that other factors are involved.

Additionally, experimentation using a hyperactive mutant of Parkin, W403A, may help us to better understand the importance of ppUb for Parkin OMM retention after repolarization. This mutant is recruited to mitochondria with highly similar kinetics to WT Parkin but we expect that it would show dissociation rates that are slower than that of WT-Parkin and may elicit possibly greater losses in mitochondrial mass during a given time frame. These proposed experiments would solidify the results here by demonstrating that the fate of the mitochondrion is decided within hours following mitochondrial depolarization by PINK1:Parkin translocation to the OMM, the establishment of ppUb chains, and recruitment of the autophagic machinery, despite the observation that the downstream effects and final destruction of the mitochondrion operates on a longer time scale.

6.5 Final comments

In recent years, it has become increasingly clear that mitophagy is not a straightforward signaling event but rather operates through the combined actions of many proteins and, importantly, incorporates these actions over time,

adding additional complexities to an already intricate signaling system. This, however, is not unexpected as the mitochondria play an essential role to overall cellular health and are specifically known to create hazardous byproducts in the process. As the causes of PD remain elusive, it may be ROS or improper mitophagic signaling, one undeniable link is that mitochondria are at the core of this disease pathology.

It is my hope that the results here contribute to a greater understanding of the mitophagy response, PINK1:Parkin dynamics, and perhaps even PD development. Additionally, I am optimistic that these results support the notion of how powerful live single-cell imaging and analysis can be in determining how signaling networks operate in response to a range of cellular inputs over time. I believe these approaches offer advantages for biologists across many fields to discover the true nature of signaling networks and uncover not just how but also why signaling networks operate in such a finely tuned, incorporating manner.

Bibliography

Aerbajinai, W., Giattina, M., Lee, Y.T., Raffeld, M., and Miller, J.L. (2003). The proapoptotic factor Nix is coexpressed with Bcl-xL during terminal erythroid differentiation. Blood *102*, 712–717.

Akutsu, M., Dikic, I., and Bremm, A. (2016). Ubiquitin chain diversity at a glance. J. Cell Sci. *129*, 875–880.

Allen, G., Toth, R., James, J., and Ganley, I. (2013). Loss of iron triggers PINK1/Parkin-independent mitophagy. EMBO Rep. *14*.

Alon, U. (2007). Network motifs: theory and experimental approaches. Nat. Rev. Genet. *8*, 450–461.

Bansal, M., Moharir, S.C., Sailasree, S.P., Sirohi, K., Sudhakar, C., Sarathi, D.P., Lakshmi, B.J., Buono, M., Kumar, S., and Swarup, G. (2018). Optineurin promotes autophagosome formation by recruiting the autophagy-related Atg12-5-16L1 complex to phagophores containing the Wipi2 protein. J. Biol. Chem. *293*, 132–147.

Bingol, B., Tea, J.S., Phu, L., Reichelt, M., Bakalarski, C.E., Song, Q., Foreman, O., Kirkpatrick, D.S., and Sheng, M. (2014). The mitochondrial deubiquitinase USP30 opposes parkin-mediated mitophagy. Nature *510*, 370–375.

Bowling, J.L., Skolfield, M.C., Riley, W.A., Nolin, A.P., Wolf, L.C., and Nelson, D.E. (2019). Temporal integration of mitochondrial stress signals by the PINK1:Parkin pathway. BMC Mol. Cell Biol. *20*, 33.

Buckman, J.F., and Reynolds, I.J. (2001). Spontaneous Changes in Mitochondrial Membrane Potential in Cultured Neurons. J. Neurosci. *21*, 5054–5065.

Burchell, L., Chaugule, V.K., and Walden, H. (2012). Small, N-Terminal Tags Activate Parkin E3 Ubiquitin Ligase Activity by Disrupting Its Autoinhibited Conformation. PLOS ONE *7*, e34748.

Burchell, V.S., Nelson, D.E., Sanchez-Martinez, A., Delgado-Camprubi, M., Ivatt, R.M., Pogson, J.H., Randle, S.J., Wray, S., Lewis, P.A., Houlden, H., et al. (2013). The Parkinson's disease genes Fbxo7 and Parkin interact to mediate mitophagy. Nat. Neurosci. *16*.

Cai, Q., Zakaria, H.M., Simone, A., and Sheng, Z.-H. (2012). Spatial Parkin Translocation and Degradation of Damaged Mitochondria via Mitophagy in Live Cortical Neurons. Curr. Biol. *22*, 545–552.

Chai, C., and Lim, K.-L. (2013). Genetic Insights into Sporadic Parkinson's Disease Pathogenesis. Curr. Genomics *14*, 486–501.

Chaugule, V.K., Burchell, L., Barber, K.R., Sidhu, A., Leslie, S.J., Shaw, G.S., and Walden, H. (2011). Autoregulation of Parkin activity through its ubiquitin-like domain. EMBO J. *30*, 2853–2867.

Chazotte, B. (2011). Labeling mitochondria with TMRM or TMRE. Cold Spring Harb. Protoc. *2011*, 895–897.

Chu, C.T., Ji, J., Dagda, R.K., Jiang, J.F., Tyurina, Y.Y., Kapralov, A.A., Tyurin, V.A., Yanamala, N., Shrivastava, I.H., Mohammadyani, D., et al. (2013). Cardiolipin externalization to the outer mitochondrial membrane acts as an elimination signal for mitophagy in neuronal cells. Nat. Cell Biol. *15*, 1197–1205.

Creed, S., and McKenzie, M. (2019). Measurement of Mitochondrial Membrane Potential with the Fluorescent Dye Tetramethylrhodamine Methyl Ester (TMRM). Methods Mol. Biol. Clifton NJ *1928*, 69–76.

Crivat, G., and Taraska, J.W. (2012). Imaging proteins inside cells with fluorescent tags. Trends Biotechnol. *30*, 8–16.

Cunningham, C.N., Baughman, J.M., Phu, L., Tea, J.S., Yu, C., Coons, M., Kirkpatrick, D.S., Bingol, B., and Corn, J.E. (2015). USP30 and parkin homeostatically regulate atypical ubiquitin chains on mitochondria. Nat. Cell Biol. *17*, 160–169.

Daido, S., Kanzawa, T., Yamamoto, A., Takeuchi, H., Kondo, Y., and Kondo, S. (2004). Pivotal role of the cell death factor BNIP3 in ceramide-induced autophagic cell death in malignant glioma cells. Cancer Res. *64*, 4286–4293.

Deas, E., Plun-Favreau, H., Gandhi, S., Desmond, H., Kjaer, S., Loh, S.H.Y., Renton, A.E.M., Harvey, R.J., Whitworth, A.J., Martins, L.M., et al. (2011). PINK1 cleavage at position A103 by the mitochondrial protease PARL. Hum. Mol. Genet. *20*, 867–879.

Di Rita, A., Peschiaroli, A., D' Acunzo, P., Strobbe, D., Hu, Z., Gruber, J., Nygaard, M., Lambrughi, M., Melino, G., Papaleo, E., et al. (2018). HUWE1 E3 ligase promotes PINK1/PARKIN-independent mitophagy by regulating AMBRA1 activation via IKKα. Nat. Commun. *9*, 3755.

Distelmaier, F., Koopman, W.J.H., Testa, E.R., de Jong, A.S., Swarts, H.G., Mayatepek, E., Smeitink, J.A.M., and Willems, P.H.G.M. (2008). Life cell quantification of mitochondrial membrane potential at the single organelle level. Cytom. Part J. Int. Soc. Anal. Cytol. *73*, 129–138.

Diwan, A., Koesters, A.G., Odley, A.M., Pushkaran, S., Baines, C.P., Spike, B.T., Daria, D., Jegga, A.G., Geiger, H., Aronow, B.J., et al. (2007). Unrestrained erythroblast development in Nix-/- mice reveals a mechanism for apoptotic modulation of erythropoiesis. Proc. Natl. Acad. Sci. U. S. A. *104*, 6794–6799.

Evans, C.S., and Holzbaur, E.L. (2020). Degradation of engulfed mitochondria is rate-limiting in Optineurin-mediated mitophagy in neurons. ELife *9*.

Evans, C.S., and Holzbaur, E.L. Degradation of engulfed mitochondria is rate-limiting in Optineurin-mediated mitophagy in neurons. ELife *9*.

Falchi, A.M., Isola, R., Diana, A., Putzolu, M., and Diaz, G. (2005). Characterization of depolarization and repolarization phases of mitochondrial membrane potential fluctuations induced by tetramethylrhodamine methyl ester photoactivation. FEBS J. *272*, 1649–1659.

Ferrari, R., Forabosco, P., Vandrovcova, J., Botía, J.A., Guelfi, S., Warren, J.D., UK Brain Expression Consortium (UKBEC), Momeni, P., Weale, M.E., Ryten, M., et al. (2016). Frontotemporal dementia: insights into the biological underpinnings of disease through gene co-expression network analysis. Mol. Neurodegener. *11*, 21.

Ferrell, J.E., and Machleder, E.M. (1998). The biochemical basis of an all-or-none cell fate switch in Xenopus oocytes. Science *280*, 895–898.

Girotra, M., Thierry, A.-C., Harari, A., Coukos, G., Naveiras, O., and Vannini, N. (2019). Measurement of Mitochondrial Mass and Membrane Potential in Hematopoietic Stem Cells and T-cells by Flow Cytometry. J. Vis. Exp. JoVE.

Gladkova, C., Maslen, S., Skehel, J.M., and Komander, D. (2018). Mechanism of Parkin activation by PINK1. Nature *559*, 410–414.

Greene, A.W., Grenier, K., Aguileta, M.A., Muise, S., Farazifard, R., Haque, M.E., McBride, H.M., Park, D.S., and Fon, E.A. (2012). Mitochondrial processing peptidase regulates PINK1 processing, import and Parkin recruitment. EMBO Rep. *13*, 378–385.

Guardia-Laguarta, C., Liu, Y., Lauritzen, K.H., Erdjument-Bromage, H., Martin, B., Swayne, T.C., Jiang, X., and Przedborski, S. (2019). PINK1 Content in Mitochondria is Regulated by ER-Associated Degradation. J. Neurosci. *39*, 7074–7085.

Harper, J.W., Ordureau, A., and Heo, J.-M. (2018). Building and decoding ubiquitin chains for mitophagy. Nat. Rev. Mol. Cell Biol. *19*, 93–108.

Hattori, N., Kitada, T., Matsumine, H., Asakawa, S., Yamamura, Y., Yoshino, H., Kobayashi, T., Yokochi, M., Wang, M., Yoritaka, A., et al. (1998). Molecular genetic analysis of a novel Parkin gene in Japanese families with autosomal recessive juvenile parkinsonism: evidence for variable homozygous deletions in the Parkin gene in affected individuals. Ann. Neurol. *44*, 935–941.

Heo, J.-M., Ordureau, A., Paulo, J.A., Rinehart, J., and Harper, J.W. (2015). The PINK1-PARKIN mitochondrial ubiquitylation pathway drives a program of TBK1 activation and recruitment of OPTN and NDP52 to promote mitophagy. Mol. Cell *60*, 7–20.

Imazu, T., Shimizu, S., Tagami, S., Matsushima, M., Nakamura, Y., Miki, T., Okuyama, A., and Tsujimoto, Y. (1999). Bcl-2/E1B 19 kDa-interacting protein 3-like protein (Bnip3L) interacts with bcl-2/Bcl-xL and induces apoptosis by altering mitochondrial membrane permeability. Oncogene *18*, 4523–4529.

Itakura, E., Kishi-Itakura, C., Koyama-Honda, I., and Mizushima, N. (2012). Structures containing Atg9A and the ULK1 complex independently target depolarized mitochondria at initial stages of Parkin-mediated mitophagy. J. Cell Sci. *125*, 1488–1499.

Kazlauskaite, A., Kondapalli, C., Gourlay, R., Campbell, D.G., Ritorto, M.S., Hofmann, K., Alessi, D.R., Knebel, A., Trost, M., and Muqit, M.M.K. (2014). Parkin is activated by PINK1-dependent phosphorylation of ubiquitin at Ser65. Biochem. J. *460*, 127–139.

Kenwood, B.M., Weaver, J.L., Bajwa, A., Poon, I.K., Byrne, F.L., Murrow, B.A., Calderone, J.A., Huang, L., Divakaruni, A.S., Tomsig, J.L., et al. (2013). Identification of a novel mitochondrial uncoupler that does not depolarize the plasma membrane. Mol. Metab. *3*, 114–123.

Kitada, T., Asakawa, S., Hattori, N., Matsumine, H., Yamamura, Y., Minoshima, S., Yokochi, M., Mizuno, Y., and Shimizu, N. (1998). Mutations in the parkin gene cause autosomal recessive juvenile parkinsonism. Nature *392*, 605–608.

Klein, C., and Westenberger, A. (2012). Genetics of Parkinson's Disease. Cold Spring Harb. Perspect. Med. *2*.

Kundu, M., Lindsten, T., Yang, C.-Y., Wu, J., Zhao, F., Zhang, J., Selak, M.A., Ney, P.A., and Thompson, C.B. (2008). Ulk1 plays a critical role in the autophagic clearance of mitochondria and ribosomes during reticulocyte maturation. Blood *112*, 1493–1502.

Lazarou, M., Jin, S.M., Kane, L.A., and Youle, R.J. (2012). Role of PINK1 binding to the TOM complex and alternate intracellular membranes in recruitment and activation of the E3 ligase Parkin. Dev. Cell *22*, 320–333.

Levsky, J.M., and Singer, R.H. (2003). Gene expression and the myth of the average cell. Trends Cell Biol. *13*, 4–6.

Lie, P.P.Y., and Nixon, R.A. (2019). Lysosome trafficking and signaling in health and neurodegenerative diseases. Neurobiol. Dis. *122*, 94–105.

Liu, Y., Guardia-Laguarta, C., Yin, J., Erdjument-Bromage, H., Martin, B., James, M., Jiang, X., and Przedborski, S. (2017). The Ubiquitination of PINK1 Is Restricted to Its Mature 52-kDa Form. Cell Rep. *20*, 30–39.

Lücking, C.B., Abbas, N., Dürr, A., Bonifati, V., Bonnet, A.M., de Broucker, T., De Michele, G., Wood, N.W., Agid, Y., and Brice, A. (1998). Homozygous deletions in parkin gene in European and North African families with autosomal recessive juvenile parkinsonism. The European Consortium on Genetic Susceptibility in Parkinson's Disease and the French Parkinson's Disease Genetics Study Group. Lancet Lond. Engl. *352*, 1355–1356.

Mao, C., and Kisaalita, W.S. (2004). Determination of resting membrane potential of individual neuroblastoma cells (IMR-32) using a potentiometric dye (TMRM) and confocal microscopy. J. Fluoresc. *14*, 739–743.

Marcassa, E., Kallinos, A., Jardine, J., Rusilowicz-Jones, E.V., Clague, M.J., and Urbé, S. (2019). New aspects of USP30 biology in the regulation of pexophagy. Autophagy *15*, 1634–1637.

Martinez, A., Lectez, B., Ramirez, J., Popp, O., Sutherland, J.D., Urbé, S., Dittmar, G., Clague, M.J., and Mayor, U. (2017). Quantitative proteomic analysis of Parkin substrates in Drosophila neurons. Mol. Neurodegener. *12*, 29.

Matsuda, N., Sato, S., Shiba, K., Okatsu, K., Saisho, K., Gautier, C.A., Sou, Y., Saiki, S., Kawajiri, S., Sato, F., et al. (2010). PINK1 stabilized by mitochondrial depolarization recruits Parkin to damaged mitochondria and activates latent Parkin for mitophagy. J. Cell Biol. *189*, 211–221.

Matsumine, H., Saito, M., Shimoda-Matsubayashi, S., Tanaka, H., Ishikawa, A., Nakagawa-Hattori, Y., Yokochi, M., Kobayashi, T., Igarashi, S., Takano, H., et al. (1997). Localization of a gene for an autosomal recessive form of juvenile Parkinsonism to chromosome 6q25.2-27. Am. J. Hum. Genet. *60*, 588–596.

Matsushima, M., Fujiwara, T., Takahashi, E., Minaguchi, T., Eguchi, Y., Tsujimoto, Y., Suzumori, K., and Nakamura, Y. (1998). Isolation, mapping, and functional analysis of a novel human cDNA (BNIP3L) encoding a protein homologous to human NIP3. Genes. Chromosomes Cancer *21*, 230–235.

Mehta, S.H., Dickson, D.W., Morgan, J.C., Singleton, A.B., Majounie, E., and Sethi, K.D. (2016). Juvenile onset Parkinsonism with “pure nigral” degeneration and POLG1 mutation. Parkinsonism Relat. Disord. *30*, 83–85.

Miller, S., and Muqit, M.M.K. (2019). Therapeutic approaches to enhance PINK1/Parkin mediated mitophagy for the treatment of Parkinson’s disease. Neurosci. Lett. *705*, 7–13.

Moore, A.S., and Holzbaur, E.L.F. (2016a). Dynamic recruitment and activation of ALS-associated TBK1 with its target optineurin are required for efficient mitophagy. Proc. Natl. Acad. Sci. U. S. A. *113*, E3349-3358.

Moore, A.S., and Holzbaur, E.L.F. (2016b). Dynamic recruitment and activation of ALS-associated TBK1 with its target optineurin are required for efficient mitophagy. Proc. Natl. Acad. Sci. U. S. A. *113*, E3349-3358.

Murakawa, T., Yamaguchi, O., Hashimoto, A., Hikoso, S., Takeda, T., Oka, T., Yasui, H., Ueda, H., Akazawa, Y., Nakayama, H., et al. (2015). Bcl-2-like protein 13 is a mammalian Atg32 homologue that mediates mitophagy and mitochondrial fragmentation. Nat. Commun. *6*, 7527.

Murphy, M.P. (2009). How mitochondria produce reactive oxygen species. Biochem. J. *417*, 1–13.

Narendra, D., Tanaka, A., Suen, D.-F., and Youle, R.J. (2008). Parkin is recruited selectively to impaired mitochondria and promotes their autophagy. J. Cell Biol. *183*, 795–803.

Narendra, D., Kane, L.A., Hauser, D.N., Fearnley, I.M., and Youle, R.J. (2010a). p62/SQSTM1 is required for Parkin-induced mitochondrial clustering but not mitophagy; VDAC1 is dispensable for both. Autophagy *6*, 1090–1106.

Narendra, D.P., Jin, S.M., Tanaka, A., Suen, D.-F., Gautier, C.A., Shen, J., Cookson, M.R., and Youle, R.J. (2010b). PINK1 is selectively stabilized on impaired mitochondria to activate Parkin. PLoS Biol. *8*, e1000298.

Okatsu, K., Saisho, K., Shimanuki, M., Nakada, K., Shitara, H., Sou, Y., Kimura, M., Sato, S., Hattori, N., Komatsu, M., et al. (2010). p62/SQSTM1 cooperates with Parkin for perinuclear clustering of depolarized mitochondria. Genes Cells *15*, 887–900.

Okatsu, K., Koyano, F., Kimura, M., Kosako, H., Saeki, Y., Tanaka, K., and Matsuda, N. (2015). Phosphorylated ubiquitin chain is the genuine Parkin receptor. J. Cell Biol. *209*, 111–128.

Okatsu, K., Sato, Y., Yamano, K., Matsuda, N., Negishi, L., Takahashi, A., Yamagata, A., Goto-Ito, S., Mishima, M., Ito, Y., et al. (2018). Structural insights into ubiquitin phosphorylation by PINK1. Sci. Rep. *8*, 10382.

Olgiati, S., Quadri, M., Fang, M., Rood, J.P.M.A., Saute, J.A., Chien, H.F., Bouwkamp, C.G., Graafland, J., Minneboo, M., Breedveld, G.J., et al. (2016). DNAJC6 Mutations Associated With Early-Onset Parkinson's Disease. Ann. Neurol. *79*, 244–256.

Ordureau, A., Sarraf, S.A., Duda, D.M., Heo, J.-M., Jedrychowski, M.P., Sviderskiy, V.O., Olszewski, J.L., Koerber, J.T., Xie, T., Beausoleil, S.A., et al. (2014). Quantitative proteomics reveal a feedforward mechanism for mitochondrial PARKIN translocation and ubiquitin chain synthesis. Mol. Cell *56*, 360–375.

Ordureau, A., Paulo, J.A., Zhang, W., Ahfeldt, T., Zhang, J., Cohn, E.F., Hou, Z., Heo, J.-M., Rubin, L.L., Sidhu, S.S., et al. (2018). Dynamics of PARKIN-Dependent Mitochondrial Ubiquitylation in Induced Neurons and Model Systems Revealed by Digital Snapshot Proteomics. Mol. Cell *70*, 211-227.e8.

Ott, M., Robertson, J.D., Gogvadze, V., Zhivotovsky, B., and Orrenius, S. (2002). Cytochrome c release from mitochondria proceeds by a two-step process. Proc. Natl. Acad. Sci. *99*, 1259–1263.

Padman, B.S., Nguyen, T.N., Uoselis, L., Skulsuppaisarn, M., Nguyen, L.K., and Lazarou, M. (2019). LC3/GABARAPs drive ubiquitin-independent recruitment of Optineurin and NDP52 to amplify mitophagy. Nat. Commun. *10*.

Peng, Y., Fang, Z., Liu, M., Wang, Z., Li, L., Ming, S., Lu, C., Dong, H., Zhang, W., Wang, Q., et al. (2019). Testosterone induces renal tubular epithelial cell death through the HIF-1α/BNIP3 pathway. J. Transl. Med. *17*, 62.

Rasool, S., Soya, N., Truong, L., Croteau, N., Lukacs, G.L., and Trempe, J.-F. (2018). PINK1 autophosphorylation is required for ubiquitin recognition. EMBO Rep. *19*.

Richter, B., Sliter, D.A., Herhaus, L., Stolz, A., Wang, C., Beli, P., Zaffagnini, G., Wild, P., Martens, S., Wagner, S.A., et al. (2016). Phosphorylation of OPTN by TBK1 enhances its binding to Ub chains and promotes selective autophagy of damaged mitochondria. Proc. Natl. Acad. Sci. U. S. A. *113*, 4039–4044.

Rojansky, R., Cha, M.-Y., and Chan, D.C. (2016). Elimination of paternal mitochondria in mouse embryos occurs through autophagic degradation dependent on PARKIN and MUL1. ELife *5*, e17896.

Sandoval, H., Thiagarajan, P., Dasgupta, S.K., Schumacher, A., Prchal, J.T., Chen, M., and Wang, J. (2008). Essential role for Nix in autophagic maturation of erythroid cells. Nature *454*, 232–235.

Sarraf, S.A., Raman, M., Guarani-Pereira, V., Sowa, M.E., Huttlin, E.L., Gygi, S.P., and Harper, J.W. (2013). Landscape of the PARKIN-dependent ubiquitylome in response to mitochondrial depolarization. Nature *496*, 372–376.

Sauvé, V., Lilov, A., Seirafi, M., Vranas, M., Rasool, S., Kozlov, G., Sprules, T., Wang, J., Trempe, J.-F., and Gehring, K. (2015). A Ubl/ubiquitin switch in the activation of Parkin. EMBO J. *34*, 2492–2505.

Sauvé, V., Sung, G., Soya, N., Kozlov, G., Blaimschein, N., Miotto, L.S., Trempe, J.-F., Lukacs, G.L., and Gehring, K. (2018). Mechanism of parkin activation by phosphorylation. Nat. Struct. Mol. Biol. *25*, 623–630.

Schindelin, J., Arganda-Carreras, I., Frise, E., Kaynig, V., Longair, M., Pietzsch, T., Preibisch, S., Rueden, C., Saalfeld, S., Schmid, B., et al. (2012). Fiji: an open-source platform for biological-image analysis. Nat. Methods *9*, 676–682.

Schubert, A.F., Gladkova, C., Pardon, E., Wagstaff, J.L., Freund, S.M.V., Steyaert, J., Maslen, S.L., and Komander, D. (2017). Structure of PINK1 in complex with its substrate ubiquitin. Nature *552*, 51–56.

Schweers, R.L., Zhang, J., Randall, M.S., Loyd, M.R., Li, W., Dorsey, F.C., Kundu, M., Opferman, J.T., Cleveland, J.L., Miller, J.L., et al. (2007). NIX is required for programmed mitochondrial clearance during reticulocyte maturation. Proc. Natl. Acad. Sci. U. S. A. *104*, 19500–19505.

Seibenhener, M.L., Du, Y., Diaz-Meco, M.-T., Moscat, J., Wooten, M.C., and Wooten, M.W. (2013). A Role for Sequestosome1/p62 in Mitochondrial Dynamics, Import and Genome Integrity. Biochim. Biophys. Acta *1833*, 452–459.

Seirafi, M., Kozlov, G., and Gehring, K. (2015). Parkin structure and function. Febs J. *282*, 2076–2088.

Sekine, S., and Youle, R.J. (2018). PINK1 import regulation; a fine system to convey mitochondrial stress to the cytosol. BMC Biol. *16*, 2.

Shen, Q., Yamano, K., Head, B.P., Kawajiri, S., Cheung, J.T.M., Wang, C., Cho, J.-H., Hattori, N., Youle, R.J., and van der Bliek, A.M. (2014). Mutations in Fis1 disrupt orderly disposal of defective mitochondria. Mol. Biol. Cell *25*, 145–159.

Silva, D.F., Selfridge, J.E., Lu, J., E, L., Roy, N., Hutfles, L., Burns, J.M., Michaelis, E.K., Yan, S., Cardoso, S.M., et al. (2013). Bioenergetic flux, mitochondrial mass and mitochondrial morphology dynamics in AD and MCI cybrid cell lines. Hum. Mol. Genet. *22*, 3931–3946.

Soutar, M.P.M., Kempthorne, L., Annuario, E., Luft, C., Wray, S., Ketteler, R., Ludtmann, M.H.R., and Plun-Favreau, H. (2019). FBS/BSA media concentration determines CCCP's ability to depolarize mitochondria and activate PINK1-PRKN mitophagy. Autophagy *15*, 2002–2011.

von Stockum, S., Marchesan, E., and Ziviani, E. (2018). Mitochondrial quality control beyond PINK1/Parkin. Oncotarget *9*, 12550–12551.

Strappazzon, F., Nazio, F., Corrado, M., Cianfanelli, V., Romagnoli, A., Fimia, G.M., Campello, S., Nardacci, R., Piacentini, M., Campanella, M., et al. (2015). AMBRA1 is able to induce mitophagy via LC3 binding, regardless of PARKIN and p62/SQSTM1. Cell Death Differ. *22*, 419–432.

Tai, Y., Li, L., Peng, X., Zhu, J., Mao, X., Qin, N., Ma, M., Huo, R., Bai, Y., and Dong, D. (2018). Mitochondrial uncoupler BAM15 inhibits artery constriction and potently activates AMPK in vascular smooth muscle cells. Acta Pharm. Sin. B *8*, 909–918.

Tanaka, A., Cleland, M.M., Xu, S., Narendra, D.P., Suen, D.-F., Karbowski, M., and Youle, R.J. (2010). Proteasome and p97 mediate mitophagy and degradation of mitofusins induced by Parkin. J. Cell Biol. *191*, 1367–1380.

Tang, M.Y., Vranas, M., Krahn, A.I., Pundlik, S., Trempe, J.-F., and Fon, E.A. (2017). Structure-guided mutagenesis reveals a hierarchical mechanism of Parkin activation. Nat. Commun. *8*, 14697.

Teodoro, J.S., Palmeira, C.M., and Rolo, A.P. (2018). Mitochondrial Membrane Potential (ΔΨ) Fluctuations Associated with the Metabolic States of Mitochondria. Methods Mol. Biol. Clifton NJ *1782*, 109–119.

Thomas, B., and Beal, M.F. (2007). Parkinson's disease. Hum. Mol. Genet. *16 Spec No. 2*, R183-194.

Tom, R., Bisson, L., and Durocher, Y. (2008). Transfection of Adherent HEK293-EBNA1 Cells in a Six-Well Plate with Branched PEI for Production of Recombinant Proteins. CSH Protoc. *2008*, pdb.prot4978.

Trempe, J.-F., Sauvé, V., Grenier, K., Seirafi, M., Tang, M.Y., Ménade, M., Al-Abdul-Wahid, S., Krett, J., Wong, K., Kozlov, G., et al. (2013). Structure of parkin reveals mechanisms for ubiquitin ligase activation. Science *340*, 1451–1455.

Tsukada, M., and Ohsumi, Y. (1993). Isolation and characterization of autophagy-defective mutants of Saccharomyces cerevisiae. FEBS Lett. *333*, 169–174.

Vande Velde, C., Cizeau, J., Dubik, D., Alimonti, J., Brown, T., Israels, S., Hakem, R., and Greenberg, A.H. (2000). BNIP3 and genetic control of necrosis-like cell death through the mitochondrial permeability transition pore. Mol. Cell. Biol. *20*, 5454–5468.

Vives-Bauza, C., Zhou, C., Huang, Y., Cui, M., de Vries, R.L.A., Kim, J., May, J., Tocilescu, M.A., Liu, W., Ko, H.S., et al. (2010). PINK1-dependent recruitment of Parkin to mitochondria in mitophagy. Proc. Natl. Acad. Sci. U. S. A. *107*, 378–383.

Wall, C.E., Rose, C.M., Adrian, M., Zeng, Y.J., Kirkpatrick, D.S., and Bingol, B. (2019). PPEF2 Opposes PINK1-Mediated Mitochondrial Quality Control by Dephosphorylating Ubiquitin. Cell Rep. *29*, 3280-3292.e7.

Wang, L., Cho, Y.-L., Tang, Y., Wang, J., Park, J.-E., Wu, Y., Wang, C., Tong, Y., Chawla, R., Zhang, J., et al. (2018a). PTEN-L is a novel protein phosphatase for ubiquitin dephosphorylation to inhibit PINK1–Parkin-mediated mitophagy. Cell Res. *28*, 787–802.

Wang, L., Wang, J., Tang, Y., and Shen, H.-M. (2018b). PTEN-L puts a brake on mitophagy. Autophagy *14*, 2023–2025.

Wang, Y., Nartiss, Y., Steipe, B., McQuibban, G.A., and Kim, P.K. (2012). ROS-induced mitochondrial depolarization initiates PARK2/PARKIN-dependent mitochondrial degradation by autophagy. Autophagy *8*, 1462–1476.

Wauer, T., Simicek, M., Schubert, A., and Komander, D. (2015a). Mechanism of phospho-ubiquitin-induced PARKIN activation. Nature *524*, 370–374.

Wauer, T., Swatek, K.N., Wagstaff, J.L., Gladkova, C., Pruneda, J.N., Michel, M.A., Gersch, M., Johnson, C.M., Freund, S.M.V., and Komander, D. (2015b). Ubiquitin Ser65 phosphorylation affects ubiquitin structure, chain assembly and hydrolysis. EMBO J. *34*, 307–325.

Whitworth, A.J., and Pallanck, L.J. (2009). The PINK1/Parkin pathway: a mitochondrial quality control system? J. Bioenerg. Biomembr. *41*, 499–503.

Wong, Y.C., and Holzbaur, E.L.F. (2015a). Temporal dynamics of PARK2/parkin and OPTN/optineurin recruitment during the mitophagy of damaged mitochondria. Autophagy *11*, 422–424.

Wong, Y.C., and Holzbaur, E.L.F. (2015b). Temporal dynamics of PARK2/parkin and OPTN/optineurin recruitment during the mitophagy of damaged mitochondria. Autophagy *11*, 422–424.

Yamano, K., and Youle, R.J. (2013). PINK1 is degraded through the N-end rule pathway. Autophagy *9*, 1758–1769.

Yamano, K., Fogel, A.I., Wang, C., van der Bliek, A.M., and Youle, R.J. (2014). Mitochondrial Rab GAPs govern autophagosome biogenesis during mitophagy. ELife *3*, e01612.

Yang, J.-Y., and Yang, W.Y. (2013). Bit-by-bit autophagic removal of parkin-labelled mitochondria. Nat. Commun. *4*, 1–8.

Yi, W., MacDougall, E.J., Tang, M.Y., Krahn, A.I., Gan-Or, Z., Trempe, J.-F., and Fon, E.A. (2019). The Landscape of Parkin Variants Reveals Pathogenic Mechanisms and Therapeutic Targets in Parkinson's Disease. Hum. Mol. Genet.

Yoshii, S.R., and Mizushima, N. (2015). Autophagy machinery in the context of mammalian mitophagy. Biochim. Biophys. Acta BBA - Mol. Cell Res. *1853*, 2797–2801.

Yun, J., Puri, R., Yang, H., Lizzio, M.A., Wu, C., Sheng, Z.-H., and Guo, M. (2014). MUL1 acts in parallel to the PINK1/parkin pathway in regulating mitofusin and compensates for loss of PINK1/parkin. ELife *3*.

Zhang, J., and Ney, P.A. (2009). Role of BNIP3 and NIX in cell death, autophagy, and mitophagy. Cell Death Differ. *16*, 939–946.

Zhang, J., Zhang, C., Jiang, X., Li, L., Zhang, D., Tang, D., Yan, T., Zhang, Q., Yuan, H., Jia, J., et al. (2019a). Involvement of autophagy in hypoxia-BNIP3 signaling to promote epidermal keratinocyte migration. Cell Death Dis. *10*, 234.

Zhang, M., Liu, Q., Li, L., Ning, J., Tu, J., Lei, X., Mo, Z., and Tang, S. (2019b). Cytoplasmic M□CSF facilitates apoptosis resistance by inhibiting the HIF□1α/BNIP3/Bax signalling pathway in MCF□7 cells. Oncol. Rep. *41*, 1807–1816.

Zhang, T., Xue, L., Li, L., Tang, C., Wan, Z., Wang, R., Tan, J., Tan, Y., Han, H., Tian, R., et al. (2016). BNIP3 Suppresses PINK1 Proteolytic Cleavage to Promote Mitophagy. J. Biol. Chem. jbc.M116.733410.

Zhong, Z., Umemura, A., Sanchez-Lopez, E., Liang, S., Shalapour, S., Wong, J., He, F., Boassa, D., Perkins, G., Ali, S.R., et al. (2016). NF-κB Restricts Inflammasome Activation via Elimination of Damaged Mitochondria. Cell *164*, 896–910.

Zhou, C., Huang, Y., Shao, Y., May, J., Prou, D., Perier, C., Dauer, W., Schon, E.A., and Przedborski, S. (2008). The kinase domain of mitochondrial PINK1 faces the cytoplasm. Proc. Natl. Acad. Sci. *105*, 12022–12027.